Characterization of Rad52 protein function during DNA double-strand break repair in G2 phase mammalian cells

TECHNISCHE UNIVERSITÄT DARMSTADT

Vom Fachbereich Biologie der Technischen Universität Darmstadt

zur Erlangung des akademischen Grades eines

Doctor rerum naturalium (Dr. rer. nat.) genehmigte Dissertation von

M.Sc. Anugrah Gawai

aus Padhar (Indien)

1. Referent: Prof. Dr. Markus Löbrich

2. Referentin: Prof. Dr. M. Cristina Cardoso

Tag der Einreichung: 27.10.2017

Tag der mündlichen Prüfung: 20.12.2017

Darmstadt 2018

D 17

Table of contents

Figures

Tables

Abbreviations

53BP1	p53 binding protein 1
A	Alanine
aa	Amino acid
alt-NHEJ	Alternative non-homologous end-joining
APS	Ammonium persulfate
ATM	Ataxia telangiectasia mutated
ATR	ATM-and Rad-3 related
ATRIP	ATR interacting protein
BIR	Break-induced replication
BLM	Bloom syndrome mutated protein
bp	base pair
BRC	Breast cancer
BRCA1/2	Breast cancer type 1/2 susceptibility protein
BrdU	5-bromo-2'-deoxyuridine
BSA	Bovine serum albumin
CDKs	Cyclin-dependent kinases
Chk1/2	Checkpoint kinases
c-NHEJ	Classical non-homologous end joining
CPT	Camptothecin
CtIP	C-terminal binding protein-interacting protein
DAPI	4',6-diamidino-2-phenylindole
DDR	DNA damage response
DHJ	Double Holliday-Junction
D-loop	Displacement loop
DMEM	Dulbecco's Modified Eagle Medium
DNA	Deoxyribonucleic acid
DNA2	DNA replication nuclease 2
DNA-PK	DNA-dependent protein kinase
DNA-PKcs	DNA-dependent protein kinase catalytic subunit
DSBs	Double-strand breaks
dsDNA	Double stranded DNA
EdU	5-ethynyl-2'-deoxyuridine
Eme1	Essential meiotic endonuclease 1
Exo1	Exonuclease 1
FCS	Fetal calf serum
GAPDH	Glyceraldehyde-3-phosphate-Dehydrogenase
Gen1	flap endonuclease GEN homolog 1
GFP	Green fluorescent protein
Gy	Gray
h	Hour
H2AX	Histone 2AX
HR	Homologous recombination
HRP	Horseradish peroxidase
hTert	Human telomerase reverse transcriptase
IF	Immunofluorescence

IR	Ionizing radiation
kDA	Kilo Dalton
keV	Kiloelectron volt
kV	Kilo volt
LET	Linear energy transfer
Lig1	Ligase I
Lig3	Ligase III
Lig4	Ligase IV
mA	Milli Ampere
MEF	Mouse embryonic fibroblasts
MEM	Minimum Essential Medium Eagle
MeV	Megaelectron volt
MilliQ	Purified water
min	Minutes
Mre11	Meiotic recombination 11
MRN	Mre11-Rad50-Nbs1
MUS81	MMS and UV sensitive 81
Nbs1	Nijmegen breakage syndrome 1
NEA	Non-essential amino acids
Nek1	NIMA-related kinase 1
NLS	Nuclear localization signal
OH	Hydroxyl
PALB2	Partner and localizer of BRCA2
PARP	Poly(ADP-ribose) polymerase
PAXX	Paralog of XRCC4 and XLF
PBS	Phosphate buffered saline
PCC	Premature Chromosome Condensation
PCNA	Proliferating cell nuclear antigen
PFA	Paraformaldehyde
Plk3	Polo-like kinase 3
PVDF	Polyvinyldifluoride
Rad	Radiation repair protein
RecA	Recombinase A
RNA	Ribonucleic acid
RNase	Ribonuclease
RPA	Replication protein A
RT	Room temperature
S	Serine
SCE	Sister chromatid exchange
SDS	Sodium dodecyl sulfate
sec	Seconds
shRNA	Short hairpin RNA
siRNA	Small interfering RNA
SSB	Single-strand break
ssDNA	Single stranded DNA
T	Threonine
TBS	Tris buffered saline

V	Volt
V(D)J	Variable (Diversity) joining
WB	Western blot
WRN	Werner syndrome ATP-dependent helicase
wt	Wild type
XLF	XRCC4-like factor
XRCC1/4	X-ray cross complementing protein

1. Summary

DNA double-strand breaks (DSBs) are the most deleterious damage which cells can encounter. Unrepaired or mis-repaired DSBs can result in genomic instability and cell death. Therefore, DSBs pose a serious threat to genome integrity. Two main repair pathways, canonical non-homologous end-joining (c-NHEJ) and homologous recombination (HR), are known to play a primary role in the repair of DSBs. Cell cycle-specific studies have revealed that c-NHEJ is active throughout the cell cycle, whereas, HR is active in the late-S and G2 phase where a sister chromatid is available as a template for repair. Molecular characterization of these pathways has discovered various key players, such as Ku70/80 and DNA-PKcs of c-NHEJ and Rad51, BRCA2 and Rad54 of HR. Recent findings have made it evident that when c-NHEJ or HR is impaired, alternative end-joining (alt-EJ) pathway operates to remove the DSBs. While alt-EJ acts as a global rescuing mechanism, the removal of DSBs by alt-EJ comes at a cost of elevated chromosomal translocations and sequence alteration at the break ends. Factors implicated in alt-EJ are Mre11, CtIP, DNA ligase 1/3 and PARP1. Recently, DNA polymerase theta (Polθ) was shown to promote alt-EJ by annealing the micro-homologies (MHs), present internal to the resected break ends. Therefore, this pathway is also referred to as DNA polymerase theta-mediated end-joining (TMEJ).

Most of the knowledge about the mechanistic details and the factors involved in HR comes from the studies performed with yeast (*S. cerevisiase*). In *S. cerevisiase*, Rad52 was discovered as the key HR player whose absence results in defects in DNA repair, increased sensitivity to IR and cell death. Surprisingly, loss of Rad52 in vertebrate cells has no effect on DNA repair and Rad52 knock-out mice are fertile and viable. However, increasing evidences suggest that Rad52 is involved in HR in mammalian cells. Earlier work performed in the laboratory of Prof. Löbrich showed that Rad52-GFP foci peak in the late G2 phase and persist in the consequent M phase. A study published by Feng et al. (2011) showed that, in BRCA2-deficient mammalian cells, inactivation of Rad52 is synthetically lethal for the cells. However, the exact function of Rad52 in BRCA2-proficient as well as deficient cells is not yet clearly understood.

In this study the function of Rad52 during DSB repair in G2 phase mammalian cells was characterized. In contrast to earlier speculations, in HeLa cells it was shown that Rad52 is not involved in the loading of Rad51 on to the resected 3'-ssDNA overhangs in G2 phase cells and, thus, cannot compensate for the loss of BRCA2. A synthetically lethal relationship was observed between BRCA2 and Rad52, indicating an important role for Rad52 in BRCA2-depleted HeLa and 82-6 (fibroblast) cells. Importantly, by using HeLa-Rad52-GFP cells, it was shown for the first time that BRCA2-depleted cells show significantly increased amounts of Rad52-GFP foci in G2 phase cells. γH2AX foci analysis, however, showed that the increased numbers of Rad52-GFP foci do not imply activation of a Rad52-dependent alternative repair pathway. Interestingly, co-depletion of BRCA2 and Rad52 rescued the BRCA2 repair defect. Furthermore, it was observed that the rescue of the BRCA2 repair defect was due to the activation of the Polθ-mediated TMEJ repair pathway, which gave rise to increased numbers of chromosomal fusions. These results were true for both Hela and fibroblast (82-6 & HSC-62) cells.

Notably, in HeLa cells, it was shown that the two resection-dependent pathways, HR & TMEJ, are active simultaneously in G2 phase. Nevertheless, rescue of the BRCA2-repair defect after depleting Rad52 was still observed in HeLa cells.

In conclusion, the results suggest that due to its ss-DNA binding activity, Rad52 binds to the resected 3'-ssDNA overhangs in BRCA2-deficient cells. This binding of Rad52 prevents TMEJ from repairing the resected DSB ends as repair by TMEJ can result in increased chromosomal fusions. Thus, by preventing the action of TMEJ pathway, Rad52 suppresses the formation of chromosomal fusions and maintains genomic stability in BRCA2-deficient cells. In context to cancer therapy, inactivation of Rad52 in BRCA2-deficient tumors can prove to be a potential therapeutic strategy. Furthermore, in this study it was shown that inactivation of Polθ and BRCA2 results in significantly increased numbers of chromosomal fusions in HeLa cells. This result is consistent with earlier published data where it was shown that inactivation of Polθ in BRCA2-deficient tumors increases chromosomal aberrations and enhances cell killing. Therefore, combined inactivation of Rad52 and Polθ might prove to be more potent and, thus, provide an alternative strategy to specifically kill BRCA2-deficient cancer cells.

Zusammenfassung

DNA-Doppelstrangbrüche (DSBs) zählen zu den schwerwiegendsten DNA Schäden, da sie die Integrität des Genoms gefährden. Für die Reparatur von DSBs, stehen zwei Hauptreparaturwege zur Verfügung: die klassiche nicht-homologe Endverknüpfung (c-NHEJ) und die homologe Rekombination (HR). Zellzyklus spezifische Studien haben gezeigt, dass c-NHEJ in allen Zellzyklus phasen aktive ist, wohingegen HR nur in der späten-S und G2 Phase aktive ist wenn ein Schwesterchromatid zur Verfügung steht. Es würden bereits viele Schlüsselfaktoren der beiden Reparaturwege durch molekulare Charakterisierung entdeckt, z.B., Ku70/80 und DNA-PKcs, die am c-NHEJ beteiligt sind und die HR Proteine Rad51, BRCA2 und Rad54.Neue Studien haben erwiesen, dass DSBs in c-NHEJ oder HR-defizienten Zellen, durch alternative Endverknüpfung (alt-EJ) reparierte werden. Jedoch ist Reparatur durch alt-EJ fehleranfällig, und kann zu chromosomalen Translokationen führen sowie Sequenzänderungen an der Bruchstelle. Die Faktoren Mre11, CtIP, DNA ligase 1/3 und PARP1 spielen die Hauptrolle während dem alt-EJ. Vor kurzem Zeit haben Forscher entdeckt, dass DNA polymerase-theta (Polθ) auch im alt-EJ beteiligt ist. Polθ übernimmt hierbei die Aufgabe mikrohomologie Sequenzen, die in resektierten DNA Brüchen versteckt sind, zusammen zu bringen. Daher wird alt-EJ auch theta-vermittelte Endverknüpfung (TMEJ) genannt.

Das meiste Wissen über den Mechanismus der Reparatur durch HR ist von Studien bekannt, die in Hefe (*S. cerevisiae*) durchgeführt wurden. Rad52 wurde in *S. cerevisiae* als HR Schlüsselfaktor entdeckt. Die Abwesenheit von Rad52 in *S. cerevisiae* führt zu Defekten in der DNA Reparatur, erhöhter Strahlensensitivität und zu Zelltod. Erstaunlicherweise, hat die Abwesenheit von Rad52 in Säugerzellen aber keinen Phänotyp gezeigt. In den letzten Jahren gab es Jedoch mehrere Studien, die Hinweise geliefert haben, dass Rad52 eine Rolle bei der HR in Säugerezellen spielt.

Frühere Studien der Arbeitsgruppe Löbrich haben gezeigt, nach ionisierender Strahlung (IR) Rad52-GFP Foci in der G2 Phase langsam rekrutiert werden, ein Maximum zu späten Zeitpunkten nach Bestrahlung erreichen und, bis in die M Phase persistieren. Eine Veroffentlichung von Feng et al. (2011) hat außerdem gezeigt, dass die Inaktivierung von Rad52 in BRCA2-defizienten Zellen zu einer synthetischen Lethalität führt. Allerdings, sind die Funktionen von Rad52 in wild type (WT) sowie in BRCA2-defizienten Zellen unbekannt.

In dieser Arbeit wurden die Funktionen von Rad52 in Säugerzellen charakterisiert. Im Gegensatz zu früheren Spekulationen, konnte gezeigt werden, dass Rad52 in HeLa Zellen nicht die Funktion übernimmt Rad51 auf resektierte DNA aufzuladen. Im Rahmen dieser Arbeit konnte zum ersten Mal gezeigt werden, dass in BRCA2-deplietierten Zellen eine signifikant höhere Zahl von Rad52-GFP Foci in der G2 Phase sind. Durch *γ*H2AX Foci analyse wurde verdeutlicht, dass die höhere Zahl an Rad52-GFPFoci allerdings nicht bedeutet dass, ein Rad52-abhängiger alternativer Reparaturweg aktiv ist. Erstaunlicherweise wurde beobachtet, dass eine Doppeldepletion von Rad52 und BRCA2 den BRCA2-Reparaturdefekt aufhebt. Weiterhin, es wurde beobachtet, dass die Reparatur in Rad52 und BRCA2 doppeldepletierten Zellen Polθ-vermitteltes TMEJ darstellt. Es konnte gezeigt werden, dass dieser Reparaturweg zur vermehrtern Entstehung von chromosomalen Fusionen führt. Dieser ergebnisse wurden in HeLa Zellen als auch in humanen Fibroblastzelllinien (82-6 hTert & HSC-62 hTert) gezeigt. In HeLa Zellen es wurde außerdem gezeigt, dass zwei resektions-abhängige Reparaturwege (HR & TMEJ) gleichzeitig in G2 aktiv sind.

Abschließend konnte gezeigt werden, dass in BRCA2-defizienten Zellen Rad52 aufgrund der ss-DNA Bindungsaktivität resektierte DNA Brüche binden kann. Diese bindung verhindert eine Reparatur durch TMEJ und daher auch die Entstehung chromosomalen Fusionen. Daher wird Rad52 für die Erhaltung der genomischen Integrität in BRCA2-defizienten Zellen benötigt. Im Rahmen der Krebs therapie bietet die Inaktivierung von Rad52 daher in BRCA2-defizienten Tumorzellen einen vielversprechenden Therapieansatz. Weiterhin konnte in dieser Arbeit gezeigt werden, dass in HeLa Zellen die Abwesenheit von BRCA2 und Polθ zur Ausbildung von chromosomalen Fusionen führt. Dieses Ergebnis ist im Einklang mit anderen Studien, in denen gezeigt wurde, dass die Inaktivierung von Polθ in BRCA2-defizienten Tumorzellen zum Zelltod führt. Daher konnte die kombinierte Inaktivierung von Rad52 und Polθ in BRCA2-defizienten Tumorzellen sich als eine alternative Strategie in der Krebstherapie erweisen.

2. Introduction

The primary objective of living organisms (single-celled to multi-cellular) is the flawless transfer of its genetic material to the next generation. The deoxyribonucleic acid (DNA) is the repository of genetic material and performs the essential task of carrying the genetic information from one generation to the next. To perform such an important biological task, the integrity of DNA is highly essential. Nevertheless, DNA is constantly exposed to various endogenous and exogenous damaging agents. In fact, each of the approximate 10^{13} cells in the human body receives tens of thousands of DNA lesions per day (Jackson & Bartek, 2009). There are numerous lines of evidence which link DNA damage and human diseases. One of the best known examples is skin cancer which can be caused by exogenously-induced DNA damage from exposure to ultraviolet (UV) radiation present in the spectrum of sunlight. DNA damage caused by tobacco smoke (cigarette smoking) is another example which can lead to lung cancer by causing DNA damages in lung cells. Apart from exogenously-induced DNA damage, endogenous damaging agents, such as byproducts of the cell metabolism (free radicals), can cause oxidative damages to the DNA. To combat these various threats to DNA integrity, cells have evolved different mechanisms to detect DNA damage, signal its presence and mediate its repair. These mechanisms play an important role in maintaining and stabilizing the genomic integrity and also prevent diverse human diseases. If the damages are not repaired, or are repaired incorrectly, they can lead to mutations or wider-scale genome aberrations that threaten cell viability and/or result in the on-set of life-threatening diseases, such as cancer (Jackson & Bartek, 2009). In recent years, deficiencies in DNA repair genes have been linked to a number of hereditary diseases, severe developmental problems and predisposition to cancer (Wiesmüller, Ford, & Schiestl, 2002).

2.1. Ionizing radiation and its effects on biological targets

Ionizing radiation (IR) has the energy to liberate an electron from the outer electron shell of an atom or molecule, thereby ionizing them. IR comprises all types of radiation which can cause the ionization of atoms or molecules and can be distinguished as particulate or electromagnetic radiation. Sub-atomic particles, such as electrons, neutrons, alpha and beta particles, have a mass and belong to particulate radiation. On the other hand, electromagnetic radiation includes X-rays and gamma rays which have no mass and charge and carry energy in the form of electromagnetic waves. Human beings are exposed to radiation due to natural or man-made sources (summarized in Table 2.1). Occupational exposure (nuclear power plant), medical diagnostic exposure (X-rays) and exposure due to air travel (cosmic rays) are some of the common sources of radiation exposure (Environmental Sciences Training Center, 1996).

Natural sources	Man-made sources
External Sources • Cosmic rays • Terrestrial radiation (radioactive material in rocks, such as potassium-40)	Medical Occupational Nuclear power Nuclear explosions

	Nuclear accidents
Internal sources • Inhalation (Radon gas) • Ingestion	

Table 2.1: **Various natural and man-made sources of exposure to IR**. Modified from the Fact sheet (1996), Environmental Sciences Training Center, the State University of New Jersey.

The effects of exposure to IR on biological matter can be exerted through two major mechanisms: direct effect and indirect effect. Based on the direct effect theory, IR hits the target directly, thereby causing ionizations and damage. DNA is the principle target in which IR can induce base damages, single-strand breaks (SSBs) and double-strand breaks (DSBs). Cellular membranes, organelles, proteins, RNA etc., are also vulnerable to the direct effects of IR. Based on the indirect effect theory, the effect of IR is exerted indirectly by the formation of free radicals. IR can interact with the water molecules (major constituent of cells) causing their radiolysis and forming free radicals (hydroxyl OH●). These free radicals can interact with cellular organelles, particularly DNA, and cause severe damages (Desouky, Ding, & Zhou, 2015). The majority of DNA damages after X-ray irradiation are due to the indirect effect.

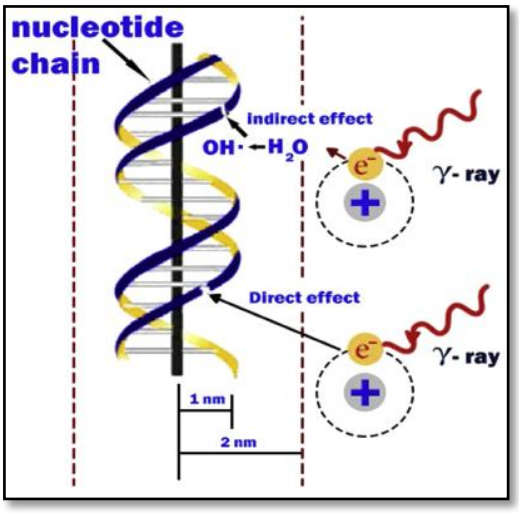

Figure 2.1. **Direct and indirect effects of ionizing radiation on DNA**. IR can hit the DNA directly and damage the sugar-phosphate backbone. Alternatively, IR can hit the DNA indirectly by the formation of free radicals via radiolysis of water and result in the induction of base damages, single-strand and/or double-strand breaks (Desouky et al., 2015).

As mentioned earlier, DNA is the primary target of IR and its damage can lead to lethal cellular consequences. Direct or indirect (free radicals) interactions with DNA can result in the breakage of the sugar-phosphate backbone of DNA, thereby causing SSBs and DSBs (Figure 2.1). SSBs are known to be readily repaired by the cells using the opposite strand as a template, however, base pair substitutions and frameshift mutations can still occur. DSBs, on the other hand, are the most detrimental and lethal lesions produced in cells due to IR exposure. Unrepaired or mis-repaired DSBs can result in chromosomal aberrations, loss of genetic information, initiation of carcinogenesis and cell death. In

order to sense the damage, signal their presence and promote their repair, cells have developed highly coordinated mechanisms, such as, cell cycle checkpoints, repair pathways and apoptosis – collectively termed as DNA damage response (DDR) mechanisms. The proper functioning and interplay of these mechanisms is highly essential for cell viability, whereas, cells with defects in DDR mechanisms are prone to numerous hereditary diseases and predisposed to cancer (Jackson & Bartek, 2009).

2.2. DNA damage response mechanisms

The DNA damage response is a network of cellular pathways which are activated when a cell experiences DNA damage. These cellular pathways comprises of cell cycle checkpoints and DNA repair pathways. The DDR mechanisms work in coordination in order to prevent deleterious consequences for a cell (Jackson & Bartek, 2009).

2.2.1. Cell cycle checkpoints

Upon induction of DNA damage, particularly IR-induced DSBs, cell cycle checkpoints are activated in order to prevent cells from progressing in to the next cell cycle phase and to provide an appropriate amount of time for the cells to repair the damages. A eukaryotic cell cycle consists of four phases: namely G1, S, G2 and M phase. Cyclins and cyclin-dependent kinases (Cdk) control and regulate the traversal of cell from one phase to the other. The cell cycle checkpoints exist at G1/S and G2/M boundary and inhibit cells from replicating their DNA and from undergoing mitosis, respectively. The protein complexes CyclinD/Cdk4/6 and CyclinE/Cdk2 together regulate the S phase entry. In order to prevent the progression of cells in S phase, ATM-dependent phosphorylation of p53 and Mdm2 (negative regulator of p53) occurs which leads to the stabilization and activation of p53. As a result, p53 transcriptionally upregulates a Cdk inhibitor - p21 - and thereby inhibits G1/S entry. Progression to M phase is driven by the protein complex CyclinB1/Cdk1 where dephosphorylation of Cdk1 by the Cdc25 phosphatases is required. In the presence of DNA damage, ATM-dependent phosphorylation of Cdc25 results in the cytoplasmic translocation of Cdc25. Thus, the CyclinB1/Cdk1 protein complex is maintained inactivated and the cells are arrested in G2 phase (Deckbar, Jeggo, & Löbrich, 2011).

2.2.2. DSB repair pathways

In order to recognize and repair the break sites, a plethora of genes and protein complexes are activated. The MRN (MRE11/RAD50/NBS1) complex binds to the DSBs and facilitates the activation of ATM (Vignard, Mirey, & Salles, 2013). ATM is autophosphorylated at the break site resulting in its own activation and, additionally, it phosphorylates its substrates in the surrounding chromatin. One of the numerous ATM substrates is H2AX – an H2A histone variant – which, upon phosphorylation, is called *γ*H2AX. This is considered as one of the earliest DSB signaling markers (Rogakou, Pilch, Orr, Ivanova, & Bonner, 1998). MDC1 recruitment amplifies the H2AX phosphorylation reaction and this signal amplification results in the recruitment of multiple other DDR members, such as RAP-80, 53BP1, KAP-1 and BRCA1 (Vignard et al., 2013). Upon recognition and signaling of the break site, mammalian

cells can employ two major repair pathways to repair DSBs: canonical non-homologous end-joining (c-NHEJ) and homologous recombination (HR).

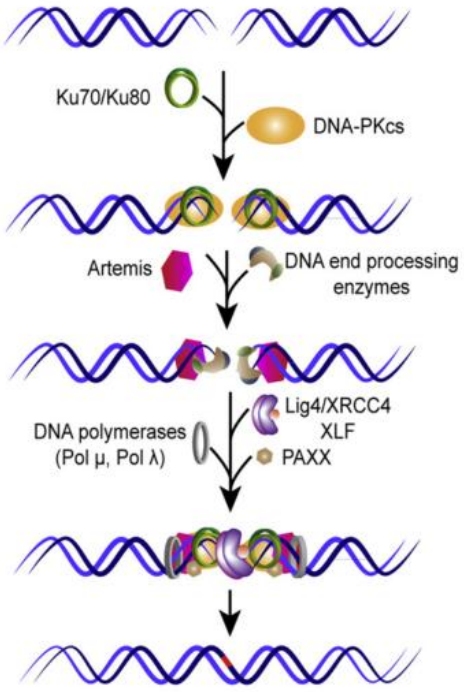

Figure 2.2. **Schematic representation of c-NHEJ.** The DSB ends are immediately bound by the Ku70/80 heterodimer which recruits DNA-PKcs. After minimal end processing steps, the DSB ends are ligated by LigIV, XRCC4 and XLF. Modified from Iliakis et al. 2015.

c-NHEJ is an error-prone repair pathway which rejoins DSBs with little or no end processing and functions throughout the cell cycle (Mao, Bozzella, Seluanov, & Gorbunova, 2008). The key players of NHEJ are the Ku70/80 heterodimer and the DNA-dependent protein kinase catalytic subunit (DNA-PKcs). The Ku70/80 heterodimer binds to the DSB ends and recruits other downstream factors of NHEJ. DNA-PKcs is recruited to the DNA-bound Ku70/80 heterodimer generating the DNA-PK holoenzyme (Jette & Lees-Miller, 2015). After minimal end processing steps by Artemis, DNA ligase IV (LigIV), X-ray cross-complementing protein 4 (XRCC4), XRCC4-like factor (XLF; also called Cernunnos) and paralog of XRCC4 and XLF (PAXX) operate to ligate the DSB ends (Ochi et al., 2015). A schematic representation of c-NHEJ is shown in figure 2.2. It has been shown that the DSB repair kinetics shows a biphasic component – a fast and a slow component – and that c-NHEJ represents the fast component of repair (Riballo et al., 2004).

2.3. Homologous recombination

A model for HR was first proposed by Robin Holliday in 1964. This model introduced the concept of exchange of genetic material between two homologous chromosomes through the formation of a Holliday junction (McCarthy, 2004). The current understanding of HR is based on data obtained from various model organisms and emphasizes the role of HR during meiosis and mitosis (San Filippo, Sung, & Klein, 2008). During DSB repair, the ultimate goal of HR is to faithfully retrieve the lost

sequence information at the DSB site from an undamaged homologous DNA sequence. To achieve this goal, HR uses the undamaged sister chromatid as a template for repair, and therefore, the damaged DNA molecule and the sister chromatid interact directly and undergo synapsis (Figure 2.3). This prerequisite (usage of a sister chromatid) restricts HR to the S and G2 phase of the cell cycle (San Filippo et al., 2008).

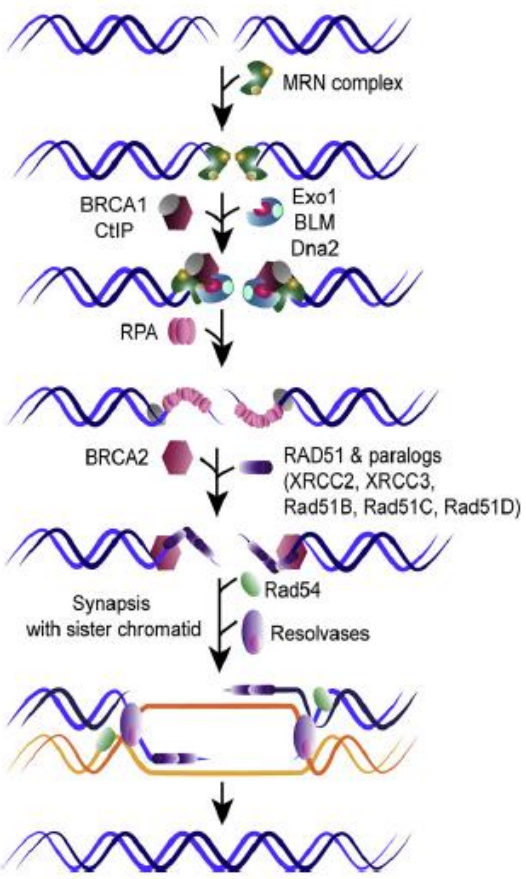

Figure 2.3. **Schematic representation of HR**. DSB end resection is initiated by the MRN complex along with CtIP to generate a 3'-ssDNA overhang, which is immediately bound by RPA molecules. BRCA2-mediated loading of Rad51 on the 3'-ssDNA forms the Rad51 nucleoprotein filaments, required for the strand invasion in the sister chromatid and the formation of D-loop and double-Holliday junctions. Following homology search and DNA repair synthesis, the HR-intermediate structures are processed by the BTR or the MUS81-EME1 complex to finalize HR repair events. Modified from Iliakis et al., 2015.

According to the double Holliday-junction (DHJ) model, the defining steps of HR are the nucleolytic degradation of 5'-DSB ends (resection), strand invasion, formation of HR-intermediate structures (D-loops, Holliday junctions), homology search, DNA repair synthesis and processing of the HR-intermediate structures. Depending on the pathway (dissolution or resolution) used for the processing of the D-loops and/or DHJ, a DNA-crossover structure could be formed (Heyer, Ehmsen, & Liu, 2010). Due to the possibility of formation of a DNA-crossover structure, the DHJ model is also known as gene conversion (GC). A schematic representation of HR is shown in figure 2.3.

Apart from the classical DHJ model, other sub-pathways of HR have also been described: namely, synthesis-dependent strand annealing (SDSA) and break-induced replication (BIR). All the sub-pathways of HR (DHJ, SDSA and BIR) share the similar principles of HR – DSB-end resection, formation of a D-loop and recombination-associated DNA synthesis (figure 2.4). During SDSA, after the strand invasion and DNA repair synthesis steps, the invading strand is displaced back to its original position and anneals with the second end of the DSB. As there is no formation of DHJs during SDSA, no DNA-crossover structures are formed (Heyer et al., 2010). BIR is involved in the repair of one-ended DSBs which are replication-associated and form during S phase (Cells et al., 2014). Previously, BIR was thought to be a dedicated repair pathway for collapsed DNA replication forks. However, it recently became evident that BIR is also involved in DNA replication repair in prophase and in alternative lengthening of telomeres (Dilley et al., 2016; Minocherhomji et al., 2015). A distinct characteristic of BIR is the establishment of a replication fork after D-loop formation. Notably, the D-loop moves together with the replication fork and, thus, results in conservative DNA replication (Donnianni& Symington, 2013). The DHJ-sub-pathway is known to be the most complex HR mechanism and the different steps of this pathway are explained in detail in the next paragraphs.

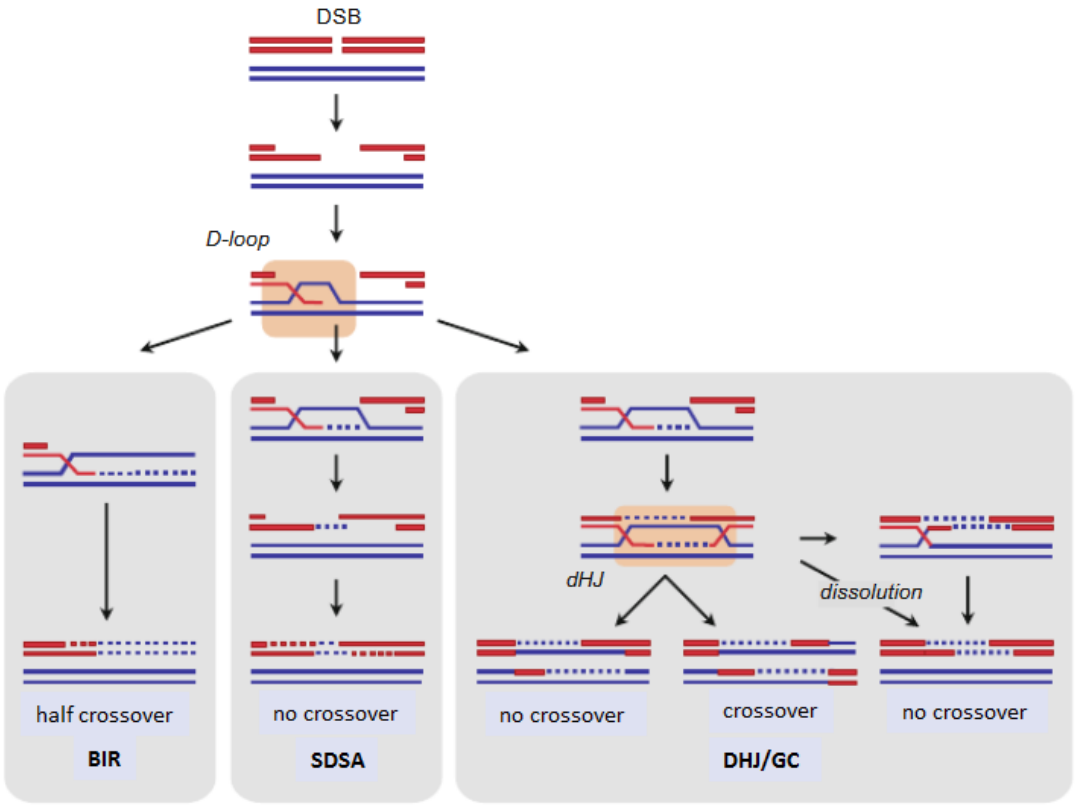

Figure 2.4. **Different sub-pathways of HR**. All the sub-pathways of HR share the common steps of DSB-end resection, formation of D-loop and recombination associated DNA synthesis. Modified from Sebesta and Krejci et al. 2016.

DSB-end resection

DSB-end resection defines the initial step of HR, including all the sub-pathways of HR. Notably, DSB end resection commits the repair to HR and avoids repair by NHEJ pathway (Shibata et al., 2014). Thus, resection plays an important role in the repair pathway choice. The initiation of resection in mammalian cells is carried out by the Mre11-Rad50-Nbs1 (MRN) complex together with CtIP. The endonuclease activity of Mre11 creates an incision on one of the strands of the DNA approximately 300 nucleotides away from the break site. CtIP mediates resection by physically and functionally interacting with the MRN complex (Sartori et al., 2007). In G2 phase, CtIP is phosphorylated by ATM and ATM and Rad3 related (ATR) in a damage-dependent manner and, importantly, two Cdk sites, S327 and T847, have been identified to regulate resection (Huertas & Jackson, 2009). Upon formation of an incision away from the break end, the resection occurs bi-directionally. The exonuclease activity of Mre11 resects the DNA in 3' - 5' direction, towards the break end. The exonucleases Exonuclease1 (Exo1), DNA2 and Blooms syndrome helicase (BLM) carry out long range resection in 5' - 3' direction (away from the break end) which results in the formation of a 3' single strand DNA (3'-ssDNA) (San Filippo et al., 2008). The formed 3'-ssDNA is quickly covered by a single-strand binding protein called Replication Protein A (RPA) and is later used for the function of strand invasion and homology search mediated by a recombinase Rad51. A schematic representation of DSB-end resection is shown in figure 2.5.

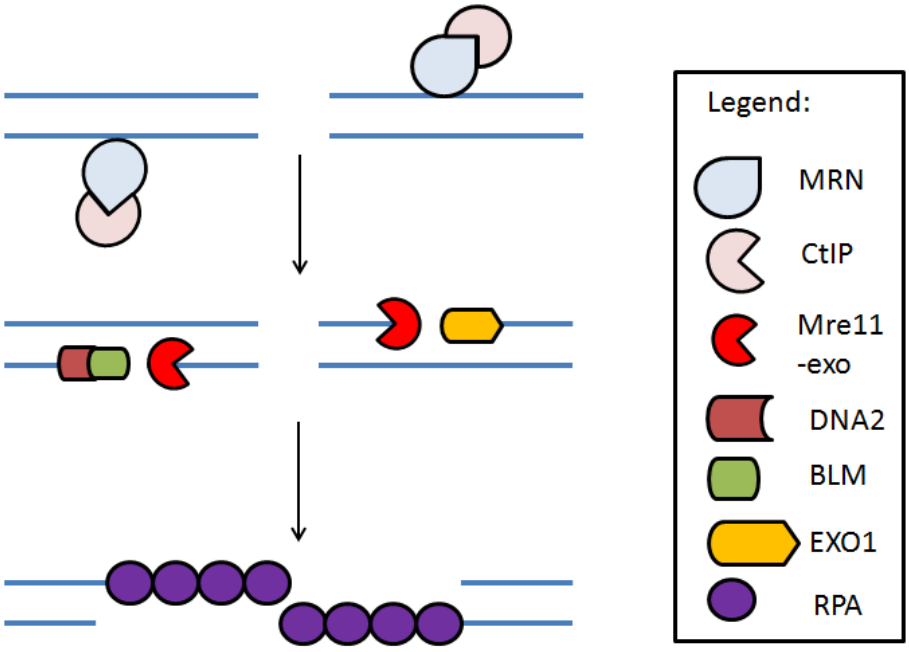

Figure 2.5. **Schematic representation of DSB-end resection**. Initially, the MRN complex together with CtIP creates an incision internal to the break end. Next, the 5'-3' activity of nucleases such as EXO1, DNA2 and BLM carry out the long range resection to create a 3'-ssDNA. The 3'-ssDNA is covered by RPA and performs strand invasion and homology search.

Formation of Rad51 nucleoprotein filaments

The 3'-ssDNA generated as a result of resection, acts as the binding substrate for RPA (figure 2.5). The ssDNA-RPA complex protects the ssDNA from being degraded by nucleases and activates the sensor kinase ATR (Binz, Sheehan, & Wold, 2004). ATR promotes the activity of Checkpoint kinase 1(Chk1) (Shiotani & Zou, 2009), which further activates tumor suppressor BRCA2 (Breast cancer type 2 susceptibility protein) and promotes the loading of Rad51 on the resected ssDNA (Sørensen et al., 2005). BRCA2 interacts with Rad51 through its eight BRC (Breast Cancer) repeats (San Filippo et al., 2008) and actively mediates the loading of Rad51 on to the RPA-coated 3'-ssDNA (Heyer et al., 2010). However, unlike yeast Rad52, human BRCA2 cannot bind to RPA (Jensen, Carreira, & Kowalczykowski, 2010). Recently, a BRCA2 partner, DSS1, has been shown to mimic ssDNA and to reduce the binding affinity of RPA to ssDNA (Zhao et al., 2015). Thus, BRCA2 together with DSS1 promotes the exchange of RPA-Rad51 and facilitates the loading of Rad51 on the resected 3'-ssDNA.

Strand invasion, homology search & DNA repair synthesis

Strand invasion and homology search are the defining steps of HR; however, they are also the least understood steps of the entire HR repair pathway (Renkawitz, Lademann, & Jentsch, 2014). In mammalian cells, Rad51 binds to DNA and promotes ATP-dependent homologous pairing and strand transfer reactions in vitro (Baumann, Benson, & West, 1996). Rad51 harbors two DNA-binding sites: the primary binding site is required and sufficient for binding to the resected ssDNA, whereas the secondary binding site is necessary for homology probing (Renkawitz et al., 2014). Further on, ATP and Mg^{2+}-dependent structural changes in the Rad51 protein induces proper binding to the two DNA substrates and mediate strand invasion (Namsaraev& Berg, 1998). The homology search is facilitated by holding the sister chromatids in close proximity via cohesion complexes (Nasmyth & Haering, 2009).

Studies performed with the Rad51-homolog, RecA from E.coli, have revealed that a minimum of 8 homologous base pairs are required for the initiation of strand invasion. Only upon further pairing of more homologous bases (500-1000 complementary bases in mammalian cells), a stabile HR-intermediate structure – the D-loop – is formed (Renkawitz et al., 2014). Upon strand invasion and homology search, Rad51 nucleoprotein filaments are required to dissociate from the chromatin for the final steps of HR to take place. This function is known to be carried out by the motor protein Rad54. An important function of Rad54 during HR is to transform the synaptic complex (ssDNA:Rad51:dsDNA) in to heteroduplex DNA. During this process, Rad54's ATPase activity promotes the removal of Rad51 from dsDNA. This makes the 3'-ssDNA available to the DNA polymerases and subsequent repair synthesis takes place to enable completion of HR.

Proliferating cell nuclear antigen (PCNA) is known to recruit DNA polymerases at the D-loop to initiate DNA synthesis (Li, Stith, Burgers, & Heyer, 2009a). In vitro studies performed with yeast revealed that DNA Polymerase δ was efficiently recruited to the D-loop by PCNA resulting in DNA repair synthesis

(Li, Stith, Burgers, & Heyer, 2009b). In humans, biochemical screens have identified DNA polymerase η (Polη) as a factor that catalyzes DNA synthesis primed at a synthetic D-loop, whereas, DNA polymerase δ (Polδ) failed at doing so (Mcllwraith et al., 2005).

Processing of Holliday-structures

The timely processing and removal of DHJs is essential for efficient DSB repair as well as for faithful chromosome segregation and genome stability. In mammals, two enzyme complexes: the BTR complex (BLM-topoisomerase IIIα-RMI1-RMI2) and the SLX-MUS complex (SLX1-SLX4-MUS81-EME1) and GEN1 resolvase are known to process the Holliday-junctions. Furthermore, these complexes process DHJs differently – dissolution by the BTR complex and resolution by the SLX-MUS complex and GEN1 resolvase (Sarbajna, Davies, & West, 2014). A schematic representation of dissolution and resolution pathways is shown in figure 2.6.

For dissolution, BLM together with RMI1 and RMI2 recruits and simulates the activity of topoisomerase IIIα on DNA. The BTR complex collectively mediates the convergent branch migration of DHJs and forms a hemicatenane. The formed hemicatenane structure is then dissociated by the activity of topoisomerase IIIα (Sarbajna & West, 2014). The dissolution reaction carried out by the BTR complex yields only non-crossover (NCO) products and is therefore an important pathway to avoid crossover formations in somatic cells. Thus, individuals with mutations in the gene coding for BLM suffer from Bloom syndrome disorder and exhibit dwarfism, sunlight hypersensitivity, increased chromosomal instability, increased frequency of sister chromatid exchange (SCE) and predisposition to cancer (Chaganti, Schonberg, & German, 1974).

The SLX-MUS complex and GEN1 comprise distinct structure-selective endonucleases. MUS81 and EME1 belong to the XPF endonuclease family and GEN1 is an XPG family nuclease which cleaves DHJs by introducing symmetrical nicks across the junction (Sarbajna& West, 2014). In contrast to GEN1, SLX-MUS complex cleaves the DHJs poorly as their preferred DNA substrates are nicked DHJs, 3'-flaps and replication fork structures (H. D. M. Wyatt, Sarbajna, Matos, & West, 2013). The SLX-MUS complex is presumably responsible for processing single Holliday junctions (HJs) that cannot act as the substrate for the BTR complex. During resolution, SLX1-SLX4 introduces a cut to generate a nicked DHJ which can be further processed by the MUS81-EME1. Unlike GEN1, the SLX-MUS complex cleaves the DHJs asymmetrically. Resolution of DHJs results in the formation of crossover products and SCEs and, therefore, is not the preferred pathway to process DHJs (Sarbajna& West, 2014).

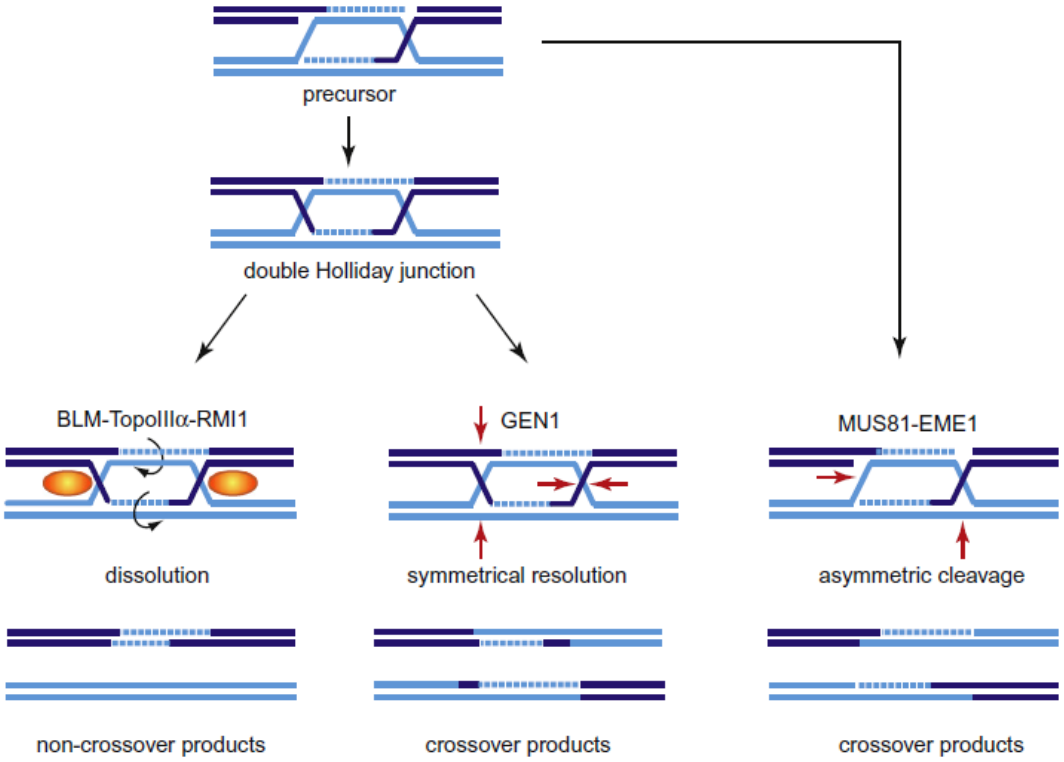

Figure 2.6. **Dissolution and resolution of DHJs**. Dissolution of DHJs is carried out by the BTR complex, whereas, resolution is performed by the MUS81-EME1 complex. For the processing of the DHJs, dissolution is the preferred pathway as no cross-over products are formed. Modified from Symington and Holloman et al. 2008.

2.4. DNA polymerase theta-mediated end joining

During the course of evolution, eukaryotic cells have evolved various repair pathways to repair DSBs. Resected DSBs can be repaired by three possible repair pathways, namely HR, SSA and alt-EJ. Early evidence for alt-EJ came from studies with c-NHEJ deficient cells where an alternative error prone mechanism of end joining was identified. Efficient repair of DSBs and increased formation of chromosomal translocations in c-NHEJ mutants or in cells treated with c-NHEJ inhibitors collectively suggest that additional mechanisms of DSB repair exist (Iliakis, Murmann, & Soni, 2015). Further evidence for the alt-EJ repair pathway came from mice studies where it was observed that c-NHEJ deficient mice exhibit chromosomal translocations (Corneo et al., 2007). The use of alt-EJ, thus, has harmful consequences on the genome integrity because of its tendency to join DSBs present on different chromosomes and thereby forming chromosomal aberrations and mutational rearrangements (Mateos-Gomez et al., 2015).

The mechanistic details of the alt-EJ repair pathway remain unclear, however, molecular characterization of this pathway has revealed that the XRCC1/DNA ligase III complex, PARP and polymerase-theta (Polθ, encoded by *POLQ*) are involved (Sfeir & Symington, 2015). As DSB repair by Polθ relies on the microhomologies (MHs) present internal to the resected break ends, where Polθ mediates annealing of MHs, alt-EJ is also referred to as theta-mediated end joining (TMEJ) (D. W. Wyatt et al., 2016). In this thesis, the term TMEJ is used throughout to represent a Polθ-dependent alt-EJ DSB repair pathway involving MHs. Studies using mammalian cells deficient for the MRN complex,

Mre11 or CtIP have shown that DSB end resection is required for TMEJ. Furthermore, it was shown that TMEJ and HR share the initial step of DSB end resection to repair DSBs in mammalian cells (Truong et al., 2013). In vitro experiments indicate that Polθ promotes TMEJ by using the resected 3'-ssDNA overhang as a primer for DNA synthesis and anneals it to the second-end of the DSB at a short tract of MHs (Kent, Chandramouly, McDevitt, Ozdemir, & Pomerantz, 2015). The various steps of the proposed mechanism for TMEJ are DSB end resection, annealing of microhomologies (MHs) removal of heterologous flaps, gap filling DNA synthesis and ligation. A schematic representation of TMEJ is shown in figure 2.7.

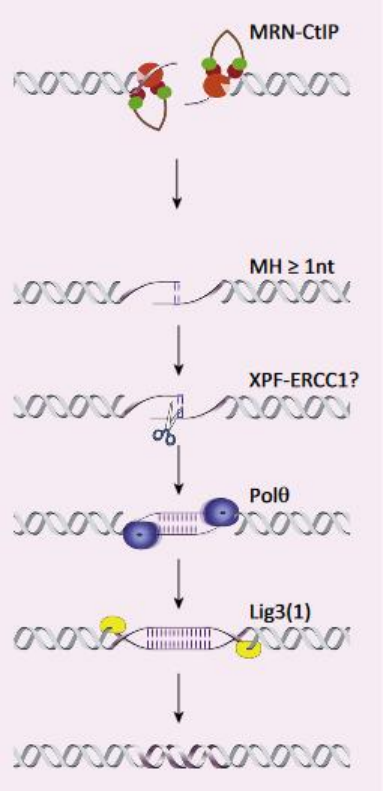

Figure 2.7. **Schematic representation of TMEJ**. DSB-end is mediated by the MRN complex and CtIP together to reveal the micro homologies present within the resected ends. The flaps are cut by structure-specific nucleases followed by DNA repair synthesis promoted by DNA polymerase theta (Polθ). DSBs are ligated by Ligase 3. Modified from Sfeir et al. 2015.

Interplay between HR and TMEJ

HR and TMEJ share the initial step of resection mediated by the MRN complex and CtIP. In HR, however, Rad51 promotes HR by driving strand exchange reaction, whereas, PARP1 mediates TMEJ by recruiting repair factors (such as Polθ) to MHs flanking the break (Audebert, Salles, & Calsou, 2008). Recently, a competitive relationship has been demonstrated between HR and TMEJ. Ceccaldi et al. showed that Polθ, which functions in TMEJ, binds to Rad51 and prevents the formation of Rad51 nucleoprotein filaments and, thus, inhibits HR (Ceccaldi, Liu, et al., 2015). Furthermore, HR-defective tumors were shown to be dependent on Polθ-mediated repair as knockdown of Polθ in HR-deficient cancer cells enhanced cell death. Moreover, it was observed that inactivation of *Fancd2* (an HR gene) and *Polq* in mice resulted in embryonic lethality (Ceccaldi, Liu, et al., 2015). In context of fidelity,

TMEJ is considered to be a mutagenic repair pathway. Chromosomal analysis of Ku80-/- cells have shown that Polθ-dependent chromosome end fusions are formed at the shelterin-free telomeric regions (Mateos-Gomez et al., 2015).

2.5. Rad52

2.5.1. Characterization of the Rad52 protein

Most of the knowledge about the molecular mechanisms of HR and the plethora of genes and proteins involved in this repair pathway comes from studies performed with yeast (*Saccharomyces cerevisiae*). A number of HR genes, such as Rad50, Rad51, Rad52, Rad54, Rad55, Rad57, Rad59, Mre11 and Xrs2, were identified in *S. cerevisiae* during a genetic screening (Game & Mortimer, 1974; Symington, 2002). Moreover, it was shown that these genes belong to the RAD52 epistasis group. Homologues of the RAD52 epistasis group of genes have been identified in eukaryotes and, in some cases, in prokaryotes and archaea too. This indicates a high level of conservation of the RAD52 group from single-celled to multi-cellular organisms. Indeed, mutations in these genes lead to abnormal meiotic and/or mitotic recombination. However, mutations in the Rad52 gene show the most severe effect on HR and DNA repair in *S. Cerevisiae*. Rad52 mutants are most IR-sensitive among all single mutants and additionally exhibit defects in mating-type switching, meiosis, spore viability and homologous DNA integration into genome (Malone & Esposito, 1980; Schiestl, Dominska, & Petes, 1993). Involvement of Rad52 in all the sub-pathways of HR (DSBR/GC, SDSA, BIR) in *S. Cerevisiae* explains why mutation or depletion of Rad52 exhibits the most severe phenotype.

Unlike yeast Rad52 mutants, Rad52 knock-out ($Rad52^{-/-}$) mice are viable, fertile without abnormalities, show no DNA damage sensitivity and are not predisposed to cancer. Furthermore, Rad52-deficient embryonic stem cells are not hypersensitive to agents that induce either simple or complex DSBs (Rijkers et al., 1998; Yamaguchi-Iwai, 1998). Given the important role of Rad52 in yeast, it came as a surprise that $Rad52^{-/-}$ mice exhibit almost normal DNA repair and HR phenotype (Rijkers et al., 1998). Nevertheless, there is increasing evidence supporting the involvement of Rad52 in HR in mammalian cells. Human Rad52 has been shown to interact with other HR factors such as RPA, XPF/ERCC1 and Rad51 (Motycka, Bessho, Post, Sung, & Tomkinson, 2004; Park, Ludwig, Stigger, & Lee, 1996; Shen, Cloud, David, Park, & Chen, 1996). Park et al. (1996) showed that direct physical contact between Rad52 and RPA is essential for HR in mammalian cells (Park et al., 1996). Additionally, in vitro data suggests that Rad52 catalyzes D-loop formation in superhelical DNA as well as mediates capturing and annealing of the second end of a resected DSB post DNA repair synthesis (Kumar & Gupta, 2004; McIlwraith & West, 2008).

Structural studies have revealed that the Rad52 protein consists of two domains – the N terminal domain (NTD) and the C terminal domain (CTD) (figure 2.8). The NTD is known to be well conserved among eukaryotes, whereas, the CTD is poorly conserved (Adzuma, Ogawa, & Ogawa, 1984; Bezzubova, Schmidt, Ostermann, Heyer, & Buerstedde, 1993). Distinct functions have been defined for the NTD and the CTD. The NTD consists of domains for ssDNA and dsDNA-binding and a self-

associating region which is responsible for the multimerization of Rad52 (Lloyd, Forget, & Knight, 2002; Lloyd, McGrew, & Knight, 2005). The CTD, on the other hand, is responsible for the interaction with RPA and Rad51 (Park et al., 1996; Shen et al., 1996).

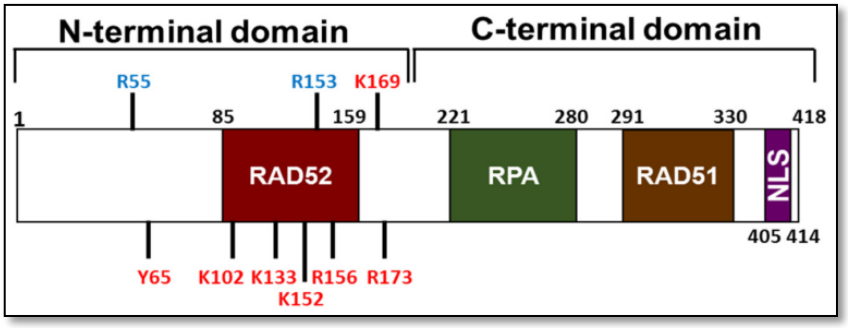

Figure 2.8.**The NTD and CTD domains of Rad52 protein**. The NTD contains a ssDNA-binding domain and the self-associating domain responsible for the formation of the higher order structure (heptameric rings) of the Rad52 protein. The CTD contains the RPA and Rad51-interacting domains. Modified from Hanamshet et al. 2016.

Human Rad52 consists of 418 amino acids (504 amino acids in *S. cerevisiae* Rad52) and eight amino acids (411-418) located in the CTD are responsible for the nuclear and nucleolar localization and for the accumulation of Rad52 at the DSB sites (Koike, Yutoku, & Koike, 2013). Electron microscopy studies have revealed that Rad52 forms a heptameric ring structure with a large central channel (Van Dyck, Hajibagheri, Stasiak, & West, 1998). The self-associating region of NTD is responsible for retaining the ring structure and, in the presence of ssDNA, a filamentous complex is formed by Rad52 comprising of stacks of hepatmeric rings (Kagawa, Kurumizaka, Ikawa, Yokoyama, & Shibata, 2001).

2.5.2. Regulation of the Rad52 protein

Several species-specific post-translational modifications for Rad52 have been described. In *S.cerevisiae*, Rad52 is constitutively phosphorylated at serine and/or threonine residues throughout the cell cycle (de Mayolo et al., 2006). In *S. pombe*, only certain conditions, such as oxidative stress or deficiency of Rad51 and/or Mus81, were able to induce Rad52 phosphorylation (Bellini et al., 2012). In response to DNA damage, Rad52 is phosphorylated at Tyr104 by c-ABL tyrosine kinase in a DNA-PKcs and ATM-dependent manner in mammalian cells (Kitao & Yuan, 2002).

Additionally, post-translational modification of Rad52 by addition of small ubiquitin-like modifiers (SUMO) takes place in *S. cerevisiae*, *S. pombe*, and mammalian cells. Rad52 sumoylation in *S. cerevisiae* is triggered by the formation of the MRX complex and the residues involved in sumoylation are located at the NTD (Sacher, Pfander, Hoege, & Jentsch, 2006a). In mammalian cells (HEK293T), the site of sumoylation of Rad52 was mapped at the nuclear localization site at the CTD suggesting that sumoylation might be playing an important role in the nuclear transport of Rad52 (Saito et al., 2010). Cells carrying sumoylation-defective Rad52 are proficient in HR. However, it has been shown that sumoylation stimulates the function of Rad52 by protecting it against degradation by proteasomes

(Sacher, Pfander, Hoege, & Jentsch, 2006b). An important tumor suppressor, PTEN, was recently reported to physically interact with Rad52 and regulate sumoylation of Rad52 in response to DNA damage (Choi, Chen, & Dai, 2013).

2.5.3. Activities of the Rad52 protein

In *S. cerevisiae*, Rad52 performs the critical step of mediating the assembly of Rad51 filaments on the resected ssDNA, whereas, in mammalian cells, this step is carried out by BRCA2 (Feng et al., 2011). Rad52-mediated annealing of complementary ssDNA strands has been observed for both yeast and human Rad52. Most proteins involved in HR are thought to mediate the annealing of ssDNA strands, but the annealing activity is abolished in the presence of RPA bound to the ssDNA strands. In contrast, the annealing activity mediated by Rad52 takes place in the presence of RPA (Sugiyama, New, & Kowalczykowski, 1998). In mammalian cells, the involvement of Rad52 in SSA repair pathway has been attributed to its ssDNA annealing activity. By using a chromosomally integrated DSB repair reporter containing repeated sequences of the *GFP* gene, it became evident that Rad52 is involved in the SSA repair pathway and functions independent of Rad51 (Stark, Pierce, Oh, Pastink, & Jasin, 2004).

Apart from ssDNA strand annealing during SSA, a role for Rad52 to capture the second DSB end during HR has been proposed. In vitro studies performed with purified Rad52 have revealed that Rad52 is able to bind to the displaced ssDNA strand within the D-loop and anneals it to the resected second-end of the DSB resulting in the formation of a double Holliday-junction (McIlwraith & West, 2008). Rad52's involvement in RNA-mediated DSB repair has also been shown recently in a study where Rad52-mediated annealing between complementary ssDNA and ssRNA was observed (Keskin et al., 2014). Furthermore, a function of inverse strand invasion between dsDNA and RNA or ssDNA has been described for Rad52. It was shown that Rad52 can use non-resected duplex DNA to promote inverse strand exchange and that RPA stimulates this activity of Rad52 (Mazina, Keskin, Hanamshet, Storici, & Mazin, 2017).

2.5.4. BRCA2 and synthetically lethal relationship with Rad52

BRCA2 is an essential tumor suppressor gene and necessary for normal cellular development. The importance of *BRCA2* is underlined by the fact that, individuals with mutations in *BRCA2* exhibit genomic instability and are predisposed to breast, ovarian and other cancers (Simon A. Gayther, Jonathan Mangion, 1997). Genetic studies have revealed that *BRCA2* is one of the key DNA repair genes and an indispensable factor, specifically for the HR repair pathway (Rahman & Stratton, 1998). A direct interaction between the BRCA2 protein and Rad51 is one of the critical steps of HR, leading to strand exchange activity between the damaged DNA molecule and the undamaged sister chromatid (Baumann & West, 1998). As mentioned in section 2.3, the interaction between BRCA2 and Rad51 takes place through the eight BRC repeats located on the C-terminal of BRCA2 (San Filippo et al., 2008). This interaction actively mediates the loading of Rad51 on to the RPA-coated 3'-ssDNA (Heyer et al., 2010). Recently, a BRCA2 partner, DSS1 has been shown to mimic ssDNA to reduce the binding

affinity of RPA to ssDNA and thereby promote the exchange of RPA-Rad51 and facilitate the loading of Rad51 on the resected 3'-ssDNA (Zhao et al., 2015).

In mammalian cells, no comparable function (mediating the assembly of Rad51 nucleoprotein filaments) has been described for Rad52. Nevertheless, in response to IR exposure, BRCA2-independent Rad52 and Rad51 foci formation has been observed in S phase cells (Feng et al., 2011). Importantly, inactivation of Rad52 in BRCA2-deficient mammalian cancer cells leads to increased chromosomal aberrations, decreased clonogenic survival and reduced frequency of HR. Additionally, these effects are also observed upon inactivation of Rad52 in cells deficient for other BRCA2-associated proteins, such as BRCA1 and PALB2 (Lok& Powell, 2012). These observations clearly indicate that loss of Rad52 and BRCA2/BRCA1/PALB2 is synthetically lethal for cells. Interestingly, the Rad52 synthetically lethal phenotype has also been seen in other organisms. For example, in chicken DT40 cells, depletion of Rad52 is lethal with a defect in XRCC3 (a Rad51 paralog) (Fujimori et al., 2001). In *U. maydis*, loss of Rad52 demonstrates synthetic lethality with a mutant rec2 (a Rad51 paralog) (Kojic, Mao, Zhou, Lisby, & Holloman, 2008). It has been proposed that in case of mutant DNA repair genes, such as BRCA2, Rad52 might mediate an alternative repair pathway (Lok & Powell, 2012). However, the function of Rad52 in cells with mutant forms of BRCA2/BRCA1/PALB2 is not fully understood. Nevertheless, it has become evident that in the absence of key DNA repair genes, Rad52 becomes an essential candidate and is responsible for the survival of cells (Feng et al., 2011).

2.5.5. Rad52 – a potential cancer therapeutic target

Inactivation of Rad52 in healthy wild type cells has no impact on DNA repair and cell survival. On the other hand, as mentioned in section 2.4.4, loss of Rad52 in BRCA2-deficient cancer cells is synthetically lethal and boosts cell killing. This observation makes Rad52 an interesting potential therapeutic candidate to treat BRCA2-deficient cancers. Additionally, this approach provides an alternative to other strategies to kill BRCA2-deficient tumor cells, namely poly-(ADP-ribose) polymerase 1 (PARP1) inhibition (Lok & Powell, 2012). The search for inhibitors/chemicals which can potentially disrupt or inhibit the activity of Rad52 has already begun. A 13-amino acid peptide aptamer containing the Rad52 sequence surrounding Phe79 has been shown to prevent the binding of Rad52 to ssDNA by disrupting the Rad52 heptameric ring structure. Furthermore, this aptamer was shown to induce synthetic lethality in selective leukemia patient cells which expressed low levels of BRCA1 or Rad51C (Cramer-Morales et al., 2013). A virtual computer screening of drug libraries, performed by Sullivan et al. (2016), yielded nine small molecule inhibitors of Rad52. Out of these nine inhibitors, adenosine 5-monophosphate (A5MP) and 5-Aminoimidazole-4-carboxamide ribonucleotide (AICAR) were shown to disrupt the Rad52-ssDNA binding and selectively inhibit growth of BRCA1-deficient HCC1937 breast carcinoma cells, BRCA1-deficient leukemia cells and BRCA2-deficient Capan1 pancreatic adenocarcinoma cells (Sullivan et al., 2016). In another study, a high throughput screening assay identified 6-hydroxy-DL-dopa (6-OH-DOPA) as a small molecule Rad52 inhibitor. In mammalian cells, 6-OH-DOPA was shown to work by inhibiting Rad52-ssDNA binding by disrupting the Rad52 heptameric ring structure. 6-OH-DOPA was also shown to inhibit the formation of Rad52 foci in

response to DNA damage by cisplatin and this inhibitor selectively killed BRCA1 and BRCA2-deficient human cancer cells (Chandramouly et al., 2015).

2.6. Aim

HR constitutes a key repair pathway dedicated to faithfully repair DNA damages. It is active mainly in the late S and G2 phases of the cell cycle when a sister chromatid is available as a template for repair (Heyer et al., 2010). The importance of HR in the maintenance of genomic integrity as well as in cancer avoidance is highlighted by the discovery that several human cancer-prone syndromes, such as Nijmegen breakage syndrome (NBS) and ataxia-telangiectasia-like disorder (A-TLD), are caused by defects in HR (Symington, 2002).

In *S. cerevisiae*, Rad52 is the key HR factor and its absence is lethal. Biochemical analysis of *S. Cerevisiae* Rad52 has revealed that, apart from its annealing function, Rad52 interacts with Rad51 and performs the critical step of mediating the assembly of Rad51 nucleoprotein filaments on to the resected DSB ends (Sugiyama et al., 1998). In mammalian cells, the loading of Rad51 on RPA-coated ssDNA is performed by BRCA2. Inactivation of BRCA2 in mammalian cells confers a DSB repair defect in G2 phase cells and, importantly, mutations in the *BRCA2* gene accounts for the majority of familial breast and ovarian cancers (Simon A. Gayther, Jonathan Mangion, 1997; Wooster et al., 1995). Inactivation of Rad52 in organisms containing BRCA2 or a BRCA2 homolog (such as *U. maydis*, chicken and mice), however, causes minimal or no HR and DNA repair defects (Kojic et al., 2008; Rijkers et al., 1998; Yamaguchi-Iwai, 1998). These observations suggest that, in humans, BRCA2 might have overtaken the function of Rad52 and that Rad52 is a dispensable HR factor. Therefore, new research on Rad52 declined for a long time. A recent study published by Feng et al. in 2011 evoked a new interest to understand the function of Rad52 in mammalian cells. This group showed that the absence of BRCA2 and Rad52 results in extensive chromosomal aberrations and is synthetically lethal for cells (Feng et al., 2011). However, the exact physiological function of Rad52 in mammalian cells is unclear. More importantly, the specific mechanisms underlying the Rad52 and BRCA2 synthetic lethal relationship are still not determined. Therefore, the aim of this study was to characterize the function of Rad52 in the context of DSB repair in wild type as well as in BRCA2-deficient cells. Investigating the function of Rad52, especially in BRCA2-deficient cells, is of particular importance because targeting Rad52 can prove to be a potential future strategy to treat BRCA2-mutant tumors.

3. Materials and Methods

3.1. Materials

3.1.1. Laboratory consumables

Table 3.1: Laboratory Consumables

Consumables	Vendor
Blotting Paper, 703	VWR
Cell culture dishes (35x10 mm, 60x15 mm)	nunc™ VWR
Cell culture flasks (25 cm^2, 75 cm^2)	TPP
Cover slips	Roth
Centrifuge tubes (15 ml, 50 ml)	Greiner
Immersion oil	Zeiss
Kim Wipes	NeoLab
Micro tubes (eppis)	Roth
Microscope slides, superfrost	Roth
Parafilm	Bemis
Pasteur pipettes, glass	Roth
Pasteur pipettes, plastic	Roth
Pipette tips	Sarstedt
Pipette tips, filtered	Roth
PVDF membrane	Thermo Scientific

3.1.2. Instruments and Devices

Table 3.2: Instruments & Devices

Instruments & Devices	Version	Vendor
Centrifuge	5415 R/5804 R	Eppendorf
Centrifuge	Biofugepico	Heraeus
Cell counting chamber	Neubauer	Marienfeld Superior
Chemiluminescence detection	ChemiSmart 5000	VilberLourmat
Chemiluminescence detection	Fusion FX	VilberLourmat
Microscope	Axiovert 200M	Zeiss
Microscope	Imager.Z2	Zeiss
Microscope (cell culture)	Eclipse TS 100	Nikon
Nanophotometer	P-Class	Implen
pH Meter	pMX2000	WTW
Power Supply	PowerPac™ HC	BIO-RAD
Scale	TE 1502S/TE 153S-DS	Sartorius
Thermomix	Comfort	Eppendorf
Ultrasound bath	1083	GFL
Vortex	Vortex genie2	Scientific Industries

Water bath	1083	GFL
Western blotting system	Mini Trans-blot® Cell	BIO-RAD
X-Ray tube	MCN 165/796704	Philips

3.1.3. Software

Table 3.3: Software

Software	Manufacturer
Axiovision V4.6.3.0	Zeiss Imaging Solutions
ChemiCapt	Vilber Lourmat
FusionCaptAdvance FX7	Vilber Lourmat
ImageJ	Open Source
Metafer	MetaSystems

3.1.4. Chemicals and Reagents

Table 3.4: Chemicals & Reagents

Chemicals & Reagents	Manufacturer
Agar	Roth
APS	Roth
Bromophenolblue	Roth
BSA	AppliChem
BrdU	BD Bioscience
DAPI	Sigma-Aldrich
DMSO	Sigma-Aldrich
EDTA	Roth
EdU	Invitrogen
Ethanol	Roth
Formaldehyde	Roth
Glycine	Roth
HCl	Roth
Isopropanol	Roth
KCl	Roth
KH_2PO_4	Roth
Methanol	Roth
$MgCl_2$	Roth
Mounting medium	Vectashield® Axxora Alexis
Nonfat-dried milk	Reformhaus
Na_2HPO_4	Roth
NaCl	Roth
NaOH	Roth
PageRuler Plus Prestained Protein Ladder	Fermentas

PFA	Roth
PhosStop 10x	Roche
PIPES	Roth
Protease inhibitor 25x Complete	Roche
RNase A	Sigma-Aldrich
SDS	Roth
Sodiumdeoxycholate	Roth
Sucrose	Roth
TEMED	Roth
Tris	Roth
TritonX-100	Roth
Trypsin	Roth
Tween®20	Roth
β-Mercaptoethanol	Sigma-Aldrich

3.1.5. siRNA

Table 3.5: siRNA

siRNA	Sequence	Concentration	Vendor
Negative control	5'AATTCTCCGAACGTGTCACGT 3'	25 nM	Qiagen
BRCA2	5' TTGGAGGAATATCGTAGGTAA 3'	25 nM	Qiagen
CtIP	5' TCCACAACATAATCCTAATTT3'	50 nM	Qiagen
Rad51	5' AAGGGAATTAGTGAAGCCAAA 3'	10 nM	Qiagen
Rad52	5' CCAACGCACAACAGGAAACTT 3'	50 nM	Dharmacon
Rad54	5' GAACTCCCATCCAGAATGATT 3'	25 nM	Qiagen
PolQ	5' AAGGATCTTAGGCATTCTTAA 3'	20 nM	Qiagen

3.1.6. Transfection reagents and kits

Table 3.6: Transfection reagents & Kits

siRNA transfection	Vendor
HiPerFect	Qiagen
Lipofectamine®RNAiMAX	Thermo Fisher Scientific
Kits	**Vendor**
EdU-Click-IT Kit	baseclick

3.1.7. Inhibitors

Table 3.7: Inhibitors

Inhibitor	Concentration	Vendor
Mre11 exonuclease (Mirin)	100 µM	(Shibata et al., 2014)
PARP (Olaparib)	1 nM	Calbiochem

3.1.8. Antibodies

Table 3.8: Primary antibodies

Antibody	Species	Dilution	Order Number	Vendor	Application
GAPDH	Rabbit	1:1000	SC-25778	Santa Cruz	WB
GFP	Mouse	1:2000	11814460001	Roche	IF
pRPA (pT21)	Rabbit	1:10000	Ab109394	Abcam	IF
Rad51	Mouse	1:10000	Ab63801	Abcam	IF
*γ*H2AX	Mouse	1:2000	05-636	Merck	IF
*γ*H2AX	Rabbit	1:2000	2212-1	Epitomics	IF

Table 3.9: Secondary antibodies

Antibody	Dilution	Order Number	Vendor	Application
Goat anti-mouse AlexaFluor 488	1:1000	A11001	Molecular Probes	IF
Goat anti-mouse AlexaFluor 594	1:1000	A11005	Molecular Probes	IF
Goat anti-rabbit AlexaFluor 488	1:1000	A11008	Molecular Probes	IF
Goat anti-rabbit AlexaFluor 594	1:1000	A11012	Molecular Probes	IF
Goat anti-mouse IgG-HRP	1:10000	Sc-2031	Santa Cruz	WB
Goat anti-rabbit IgG-HRP	1:30000	Sc-2030	Santa Cruz	WB

3.1.9. Solutions, buffers and media

Table 3.10: Solutions, buffers and media

Buffers		
PBS	137 mMNaCl 2.7 mMKCl 8 mM Na_2HPO_4 1.5 mM KH_4PO_4	pH 7.4
TBS	20 mMTris/HCl	pH 7.6

	137 mMNaCl	

Cell culture		
Dulbeccos Modified Eagles Medium (DMEM)	Sigma-Aldrich	
Minimum Essential Medium Eagle (MEM)	Sigma-Aldrich	
Fetal Calf Serum (FCS)	Biochrom	
Non-essential amino acids (NEA)	Biochrom	
Trypsin/EDTA	0.5 M EDTA 2.5% (v/v) Trypsin	pH 8 in PBS
Immunofluorescence		
Fixation	2.5% Formaldehyde	in PBS
Washing 1	1% FCS	in PBS
Permeabilization	0.2% triton-100	in PBS/1%FCS
Blocking	5% BSA	in PBS/1%FCS
Washing 2	0.1% Tween	in PBS/1%FCS
DAPI	0.4 µg/ml	in PBS
Western Blot		
Transfer buffer	20 mMTrisHCl 150 mM Glycine	pH 8.3
Washing	0.1% Tween20	in TBS
Blocking	5% non-fat milk 0.1% Tween20	in TBS
Antibody solution	1% non-fat milk 0.1% Tween20	in TBS
Lumi-Light Western Blot	Roche	
WeternBright™ Quantum/Sirius	Advansta	

3.1.10. Cell lines

Table 3.11: Cell lines

Cell line	Charateristics & Culture method
HeLa-S3	human cancer cell line derived from cervical cancer cells isolated from Henrietta Lacks in 1951, cultivated in DMEM supplemented with 10% FCS and 1% NEA and passaged twice a week (1:8 to 1:10)
HeLaRad52GFP	HeLa-S3 cells stably transfected with pEGFP-Rad52 (L60) plasmid, size – 5973 bp, Resistance to Kanamycin and G418, Dissertation, Dr. Andreas Taubmann (2015)
82-6 hTert	hTert-immortalized wt human fibroblast cell line, cultivated in MEM supplemented with 20% FCS and 1% NEA and passaged weekly (1:10)
HSC-62 hTert	hTert-immortalized BRCA2-deficient human fibroblast cell line, cultivated in MEM

supplemented with 20% FCS and 1% NEA and passaged weekly (1:10)

3.2. Methods

3.2.1. Cell culture

All cell lines used in this study were cultivated at 37°C with 5% atmospheric CO_2. For cell culture only sterile media, buffers and cell culture flasks were used.

Thawing of cells

The correct position (Tower number, box number and position in box) of the cryotube containing the frozen cells in the liquid nitrogen tank was searched in the cryo-databank. The cryotube was removed from the liquid nitrogen tank and placed in a 37°C waterbath for approximately 2-3 minutes. The cell suspension was mixed with 5 ml medium and centrifuged for 5 min at 4°C and 1000 rpm. After centrifugation, the supernatant was discarded and the cell pellet was resuspended in 5 ml of fresh medium and transferred to a 25 cm^2 cell culture flask. After 24 h, depending on the confluency, the cells were transferred to a 75 cm^2 cell culture flask.

Cell passaging

In order to passage cells, the medium was removed and the cells were washed gently twice with PBS. 2 ml of Trypsin/EDTA was added and the cells were incubated at 37°C and 5% CO_2 for approximately 5 min to ensure complete detachment of cells from the surface of the flask. The trypsinization reaction was stopped by adding 8 ml of medium and the cells were resuspended. After resuspending, the cells were passaged at a ratio of 1:8 to 1:10 depending on the cell line and confluency. All cell lines, appropriate media and passaging frequencies are listed in section 3.1.10.

Cell seeding

For cell seeding, the cell number was determined using a Neubauer cell counting chamber. Appropriate numbers of cells were seeded depending on the size of the cell culture dish (Table 3.12).

Table 3.12 Cell seeding

Cell number	Size of cell culture dish	Medium
3.5×10^4	24-well plate	1 ml / well
2.5×10^5	35 mm	2.2 ml / dish
5.0×10^5	60 mm	5.5 ml / dish

3.2.2. Transfections and treatment with inhibitors

siRNA transfection

Cells were transfected with small interfering RNA (siRNA) (see Table 3.5) either using HiPerFect or Lipofectamine® RNAiMAX. For transfection with HiPerFect, cells were transfected immediately after cell seeding, followed by a second transfection 24 h later. For the transfection solution, medium without serum was combined with siRNA and HiPerFect (Table 3.13). The mixture was then vortexed for 1 min, incubated at RT for 10 min and added dropwise to the cells under constant and slow rotation of the dish. Cells were incubated at 37°C with 5% atmospheric $CO_2$for 72 h after the first siRNA transfection until irradiation to ensure efficient depletion of the target protein.

Table 3.13: siRNA transfection solutions with HiPerFect

Cell culture dish	Medium without serum	HiPerFect	siRNA
24 well (1 ml medium)	44.4 µl	4.44 µl	0.53 – 2.5 µl
35 mm (2.2 ml medium)	100 µl	12 µl	1.2 – 3 µl
60 mm (5.5 ml medium)	240 µl	28.8 µl	2.88 – 7.2 µl

For transfection with Lipofectamine® RNAiMAX, the cells were transfected 24 h after cell seeding to ensure that all the cells are adherent to the surface of the flask and are 60 – 80% confluent. Appropriate amounts of Lipofectamine® RNAiMAX reagent with Opti-MEM® medium and siRNA with Opti-MEM® medium were put in two separate tubes A and B (Table 3.14). The components from tube-B were transferred to tube-A in 1:1 ratio and vortexed for 5 seconds. The solution was incubated for 5 min at RT and added dropwise to the cells under constant and slow rotation of the dish. Cells were incubated at 37°C with 5% atmospheric CO_2 for 48 h after siRNA transfection until irradiation to ensure efficient depletion of the target protein.

Table 3.14: siRNA transfection solutions with Lipofectamine® RNAiMAX

Cell culture dish	Tube A		Tube B
35 mm (2.2 ml medium)	4.5 µl Lipofectamine®RNAiMAX + 150 µl Opti-MEM® medium		1.5 – 2.5 µl siRNA + 150 µl Opti-MEM® medium

Inhibitor treatments

The inhibitors listed in table 3.7 were added to the cell culture medium 1 h prior to irradiation and were maintained in the medium during the entire repair incubation time.

3.2.3. DNA damage induction

Cells were irradiated with X-Rays to induce DSBs. 30 min prior to irradiation, EdU (1 µl/ml) was added to the cell culture medium to label S phase cells. EdU is a thymidine analogue which incorporates into the DNA of replicating cells and thus marks S phase cells. Using EdU treatment, all the cells which were in S phase at the time of irradiation and all the cells which entered S phase during the repair incubation time were marked.

X-Ray irradiation

For irradiation with X-Rays, cells were seeded on sterile glass coverslips in cell culture dishes (Section 3.2.1.) at least 24 h prior to irradiation. Cells were irradiated using a Philips X-Ray tube equipped with a tungsten anode and a thin beryllium window. A 1 mm aluminum plate was used to filter soft (low energy) X-Rays and for holding samples. The setting of the equipment for irradiation was 19 mA and 90 kV. Irradiation was performed under consideration of the dose doubling effect of glass slides (Kegel, Riballo, Kühne, Jeggo, & Löbrich, 2007).

3.2.4. Immunofluorescence staining and microscopic analysis

Fixation and permeabilization

Once the repair incubation time was over, the cells were washed with PBS and fixed with 2.5% formaldehyde for 15 min at RT. After fixation, the cells were washed (3 times for 10 min) with PBS and incubated with 0.2% TritonX-100 for permeabilization. Following permeabilization, the cells were again washed (3 times for 10 min) with PBS/1% FCS and BSA blocking solution was added for a minimum of 30 min at RT.

Staining

Cells were incubated with appropriate primary antibodies (Table 3.8) diluted in BSA solution at 4°C over night. The following day, cells were washed with PBS/1%FCS/0.1% Tween (3 times for 10 min) and incubated with EdU-Click solution for 30 min at RT. Manufacturer's instructions were followed to prepare the EdU-Click solution. Next, the cells were washed again with PBS/1%FCS/0.1%Tween (3 times for 10 min) and incubated with the appropriated secondary antibodies (Table 3.9) diluted in BSA solution for 60 min at RT. Cells were subsequently washed 3 times for 5 min with PBS/1%FCS/0.1% Tween and incubated with DAPI solution for 5 min at RT to stain cell nuclei. Finally, the cells were washed with PBS for 5 min and the coverslip was transferred on to a microscopic slide with 2 µl of mounting medium and sealed with nail polish.

Microscopic analysis

IF staining was analyzed using a semi-automated microscopy approach. Metafer software was used to scan the cells for DAPI and EdU signal intensity which gave a horse-shoe shaped histogram depicting the different cell cycle phases (Figure 3.1). The cell population was gated according to the cell cycle phase of interest (G1, S or G2) and for each experiment and condition a minimum of 40 cells were analyzed.

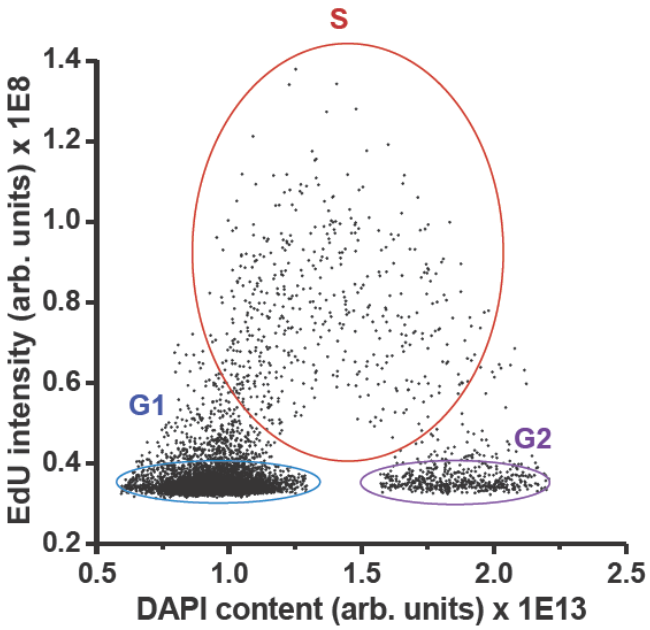

Figure 3.1. **Identification of various cell cycle phases**. HeLa cells were irradiated with 2 Gy and stained for EdU and DAPI. The cells were scanned using a semi-automated scanning system by Metafer software. The cell cycle phase of interest (G1, G2 or S phase) was gated and cell cycle specific analysis was performed. Taken from Biehs et al. 2017.

Statistical analysis

To obtain replicates, each experiment was repeated independently by seeding and treating cells on different days. For each individual experiment, cells with different passage numbers were used and all the solutions were freshly prepared. For all the data points with $n \geq 3$, the SEM between means of the independent experiments was calculated. A two-sample Students test was used to calculate the P values (* = $p<0.05$, ** = $p<0.01$, *** = $p<0.001$).

3.2.5. Western Blot

Western Blot was used to check the depletion efficiencies of siRNA treatments. Cells were seeded in 35 mm dishes and transfected with siRNAs as described in section 3.2.2.

Cell Harvest

Cells were washed with ice-cold PBS and scrapped off the surface of the dish by using a scrapper and 2 ml ice-cold PBS. The cell solution was transferred in a 15 ml falcon tube. For efficient removal of all remaining cells, the cell culture dish was washed with 2 ml ice-cold PBS and the cells were centrifuged for 3 min at 1500 rpm to form a cell pellet. This cell pellet was then transferred to the 15 ml falcon tube.

Cell lysis

Cells were resuspended in 50 – 200 µl lysis buffer (RIPA buffer + protease inhibitor + Phosphostop) depending on the size of the cell pellet. For complete and efficient cell lysis, the cell lysate was placed in an ultrasound bath (3 times for 1 min) and briefly vortexed in between. Following this, the cells were incubated for 30 min on ice and subsequently centrifuged at 4 °C and 13000 rpm for 30 min. The supernatant was transferred in a fresh 1.5 ml micro tube.

Bradford protein assay

Protein concentration in samples was determined by Bradford protein assay. For each sample, 1 µl protein was added to 800 µl MilliQ. 200 µl of Bradford reagent was added to each sample, briefly vortexed and incubated for 5 min. Absorption was measured immediately at 590 nm using a Nanophotometer.

Western Blot

The samples were mixed with 5x loading buffer (Laemmli) and boiled for 5 min at 95 °C to denature the proteins. Following this, the samples were loaded in gel pockets and electrophoresis buffer was added to the chamber. The gel was run for 10 min at 95 V for optimal accumulation of the proteins in the stacking gel. Once the proteins entered the running gel, the voltage was increased to 130 V. Consequently, the total running time varied depending on the size of the proteins. After SDS PAGE, the proteins were transferred (blotted) on to a PVDF membrane which was activated by incubation in methanol for at least 1 min. The gel and the membrane were sandwiched tightly between multiple layers of filter papers and sponges. Additionally, air bubbles were removed to ensure optimal transfer. The assembled gel holder cassette was placed inside the transfer chamber with the membrane facing the anode. Blotting buffer was added and an ice block was placed inside the chamber and a current of 310 mA was applied for approximately 3 h, depending on the size of the protein of interest. After protein transfer, the membrane was blocked with 5% non-fat milk in TBS-T for 1 h. After blocking, the membrane was incubated with appropriate primary antibodies (Table 3.8) at 4 °C for overnight. Following day, the membranes were washed (3 times for 10 min) with TBS-T and incubated with appropriate HRP-conjugated secondary antibodies (diluted in 1% non-fat milk, Table 3.9) for 1 h at RT. Finally, the membrane was washed in TBS-T (3 times for 5 min) before signal detection. An HRP

substrate was added to the membrane, resulting in a chemical reaction that releases luminal, which emits a chemiluminescent signal that was detected using ChemiSmart5000 or Fusion FX image acquisitions systems.

3.2.6. Establishment of EdU-BrdU double-labeling

The EdU-BrdU double-labeling was established to mark G2 phase cells and to analyze them in the consequent G1 phase. This method allowed strict analysis of those cells which were irradiated in G2 phase and entered the consequent G1 phase during the repair incubation time.

EdU-BrdU double-labeling

S-phase cells were pulse-labeled with EdU by treating the cells with 1 µM EdU (1 µl/ml) and storing them in an incubator for 1 h. After 1 h, the cells were washed thoroughly twice with PBS, fresh medium was added to the cells and again stored in an incubator for 1 h. This incubation time (a total of 2 h) allowed the EdU-marked mid- and late-S phase cells to enter the G2 phase. Consequently, a small G2 phase cell population was EdU-positive. Next, 10 mM BrdU (10 µl/ml) was added to the medium and the cells were stored for 1 h in an incubator. Like EdU, BrdU is a thymidine analog and gets incorporated in to the DNA of replicating cells. BrdU was kept in the medium during the entire repair incubation time. As a result, the S phase cells which did not traverse in to the G2 phase during the first 2 h of incubation time were double-labeled with EdU-BrdU and the G1 phase cells entering S phase were BrdU-labeled. A flowchart of EdU-BrdU double-labeling is shown in figure 3.2.

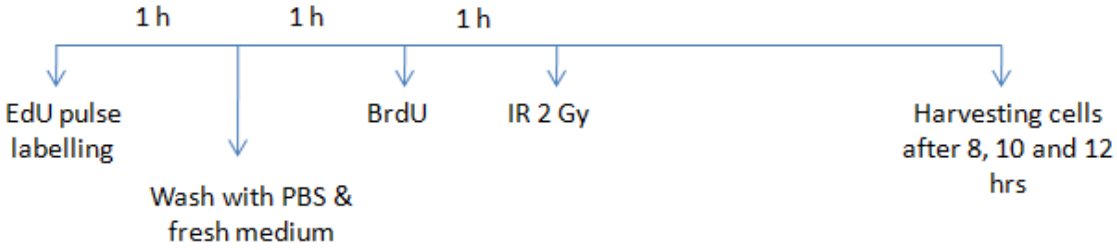

Figure 3.2. **Flowchart of EdU-BrdU double-labeling protocol**. The cells were pulse labeled with EdU and incubated for 2 h which allowed the mid- and late-S phase to traverse in to G2 phase. Later on, the cells were incubated with BrdU during the whole repair incubation time. This EdU-BrdU double-labeling allowed specific analysis of those cells that were irradiated in G2 phase and entered the consequent G1 phase during harvest.

Irradiation, fixation and staining

After double-labeling with EdU-BrdU, cells were irradiated with 2 Gy X-Rays and harvested at 8, 10 and 12 h post irradiation. For fixation, the cells were treated with 2.5% Formaldehyde for 15 min at RT and then washed (3 times for 10 min) with PBS. After fixation, cells were permeabilized with 0.5% Triton X-100 and blocked with 5% BSA solution for 30 min at RT. Next, the cells were incubated with

appropriate primary antibodies (diluted with BSA solution) at 4°C overnight. Next day, the cells were washed with PBS/1% FCS (3 times for 10 min) and the primary antibodies were cross linked by treating the cells with 2.5% Formaldehyde for 20 min at RT. Afterwards, the cells were washed with PBS and the DNA was denatured by incubating the cells with 2.5 M HCl for 20 min at RT. Next, the cells were washed with PBS for a minimum of 1 h. After denaturing the DNA, the cells were incubated for 2 h with fluorophor-conjugated primary antibody against BrdU to stain BrdU. Following this, the cells were washed (3 times for 10 min) with PBS/1%FCS and EdU-Click-IT staining, secondary antibody incubation and DAPI staining was performed as described in section 3.2.4. Finally, the cells were washed with PBS for 5 min and the coverslip was transferred on to a microscopic slide with 2 µl of mounting medium and sealed with nail polish.

Microscopic analysis

EdU-BrdU double-labeling and IF staining were analyzed using a semi-automated microscopy approach. Metafer software was used to scan cells for EdU vs DAPI and BrdU vs DAPI signal intensity which gave a horse-shoe shaped histogram depicting the different cell cycle phases. The cell cycle distribution and the exact position of the analyzed cells can be seen in figure 4.17 and 4.18. For foci quantification, only the EdU-positive-BrdU-negative G2 and G1 phase cells were analyzed. For each experiment and condition a minimum of 40 cells were analyzed. Statistical analysis was performed as described in section 3.2.4.

3.2.7. G2 phase Premature Chromosome Condensation (PCC) assay

Drug-induced G2 phase premature chromosome condensation was performed to yield chromosomes with two chromatids which are readily detected by preparing chromosome spreads on a microscopic slide. For PCC assay, cells were seeded in 65 mm culture dishes, treated with siRNA and/or inhibitors (section 3.2.2.), irradiated with 2 Gy of X-Rays (section 3.2.3.) and harvested at 8 – 10 h post irradiation.

Calyculin A-treatment and fixation

30 min before harvesting, 50 ng/ml of Calyculin A (1 µl/ml) was added to the cells. Calyculin A induces PCC by inhibiting serine/threonine protein phosphatases 1 and 2A (PP1 and PP2A). Treatment of cells with Calyculin A also detaches the cells from the surface of the dishes. After Calyculin A treatment, the cells were collected in 15 ml falcon tubes and centrifuged (4°C/400 g/5 min). The supernatant was discarded and the cell pellet was resuspended in 5 ml of pre-warmed KCl (75 mM) and incubated in a water bath (37°C) for 20 min. After KCl-treatment, the falcon tubes were centrifuged (4°C/400 g/5 min) and the supernatant was discarded. The cell pellet was fixed by adding 10 ml of ice-cold methanol-acetic acid solution (3:1) drop wise and with constant vortexing and incubated for 10 min at RT. The fixation step was repeated three times and the falcon tubes were stored at 4°C overnight.

Preparation of chromosome spreads

Next day, the cell-fixative solution was centrifuged (4°C/400 g/5 min) and, depending on the size of the cell pellet, 200-400 µl of the fixative (supernatant) was left in the falcon tubes and the rest was discarded. To prepare chromosome spreads, the cell pellet was resuspended in the fixative (200-400 µl) and approximately 20-30 µl of the cell solution was dropped on a moist microscopic slide from a height of 30-50 cm. The microscopic slides with the chromosome spreads were air dried and stored at RT until the staining step.

Giemsa staining and microscopic analysis

To stain the chromosome spreads, 6% of Giemsa stain was prepared with PBS. The microscopic slides were dipped in the Giemsa stain and incubated for 15 min at RT. After incubation with Giemsa stain, the slides were washed with MilliQ water to get rid of the extra stain and to ensure clean Giemsa-stained chromosome spreads. The slides were air dried and stored at RT until microscopic analysis. The chromosome spreads were scanned using Metafer software. Only the G2 phase chromosome spreads with two chromatids were taken in to account for analysis. For each experiment and condition a minimum of 40 chromosome spreads were analyzed. Statistical analysis was performed as described in section 3.2.4.

4. Results

Previous studies performed with mammalian cells in the group of Prof. M. Löbrich have shown that, following exposure to ionizing radiation, key HR proteins, such as Rad51 and Rad54, are withdrawn from the break site in late G2 phase and are also absent in the consequent M phase. On the other hand, Rad52 – the key HR protein in yeasts – is recruited in late G2 phase at the break sites and persists in the consequent M phase, indicating a function at the late steps of HR.

Further on, in response to induced DNA DSBs, the G2 – M checkpoint is activated. Nevertheless, earlier published data suggests that the G2 – M checkpoint is a leaky checkpoint and that the cells enter M phase with HR intermediate structures (DHJs) or unrepaired DSBs. These findings suggested another hypothesis where it was proposed that, during the transition from G2 to M phase, Rad52 might be providing protection to the unrepaired DSBs and/or keeping the HR intermediate structures intact and thus helping the cells to carry the unfinished HR business in M phase.

These interesting results led to the curiosity to understand the physiological function of Rad52 in the context of DSB repair mechanisms. Within the framework of this project, various experiments were performed to understand and characterize the role and function of Rad52 during ongoing, as well as, abrogated HR repair pathway following exposure to ionizing radiation.

4.1. Involvement of Rad52 during Homologous Recombination in G2 and M phase

4.1.1. Kinetics and quantification of Rad52-GFP foci in G2 and M phase

Initially, Rad52 was identified as the key HR protein in *Saccharomyces cerevisiae* where it performs the key steps of HR, such as assembling the Rad51 filaments, strand invasion and annealing of single stranded DNA. Moreover, Rad52 mutants are most IR-sensitive among all *S. cerevisiae* single mutants and display a severe DSB repair defect, significantly low HR frequency, impaired viability and deficiency in mating-type switching (Symington, 2002). Given the important role of Rad52 in yeast, it came as a surprise that in vertebrates Rad52 knock out show very little phenotype with no obvious effect on HR. Rad52 knockout mice exhibit normal growth and development and Rad52 deficient embryonic stem cells are not hypersensitive to agents inducing either simple or complex DNA DSBs (Feng et al., 2011).

As Rad52 knock-outs had no effect on HR in mice, Rad52's involvement in HR in mammalian cells was first investigated. To this end, HeLa tumor cells stably transfected with Rad52-GFP plasmid were used. HeLa-Rad52-GFP cells were grown on coverslips in a middle-sized Petridish and irradiated with 2 Gy of X – rays. As the HR repair pathway is active only in late S and G2 phase of the cell cycle, only those cells which were irradiated in G2 phase and remained in G2 phase during the entire repair incubation time were analyzed. In order to label and exclude S phase cells from analysis, EdU (a thymidine analogue which gets incorporated in the genome during replication) was added to the medium 30 min before irradiation and maintained throughout the entire repair incubation time. Post irradiation, cells

were fixed with formaldehyde (2.5 %) and harvested at various time points. Using Immunofluorescence (described in section 3.2.4.), the cells were stained with anti-GFP antibodies (to detect Rad52-GFP) and approximately 40 cells were analyzed to quantify Rad52-GFP foci. In addition, as a key HR marker, Rad51 was also stained to observe the ongoing HR process.

Figure 4.1.a shows the foci kinetic for Rad52-GFP and Rad51 in G2 phase cells post 2 Gy of IR. In this figure (figure 4.1.a) it can be seen that Rad51 accumulated at the break site and reached its maximum soon (2 h) after irradiation. The number of Rad51 foci gradually declined over time indicating ongoing repair. On the other hand, Rad52-GFP foci exhibited opposite kinetics as compared to Rad51 foci. Rad52-GFP foci number gradually increased over time and reached its maximum at late time points (7 h). This result indicates that Rad52 might be involved in the late steps of HR, i.e., post synaptic formation. This result is also in line with other publications where Rad52's function in late HR steps, such as second-end capture and strand annealing, has been discussed.

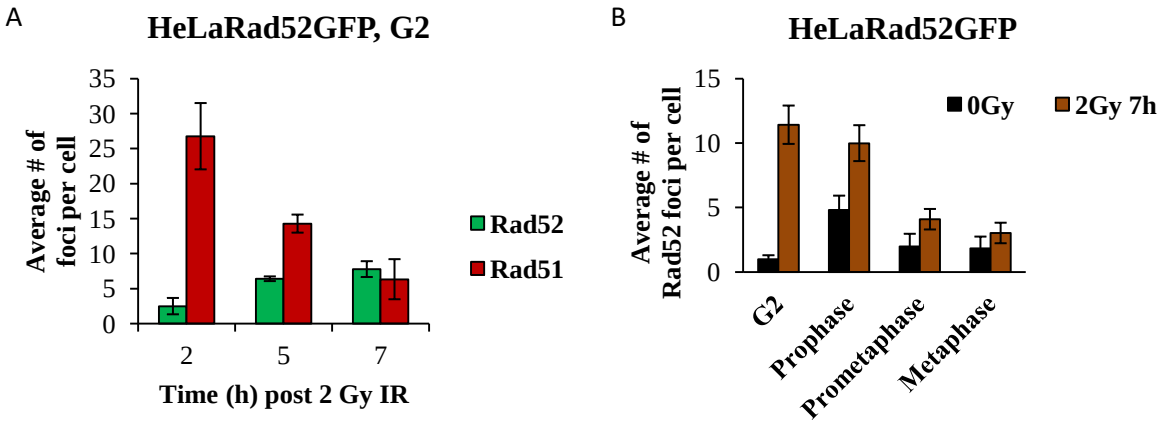

Figure 4.1. **Rad52-GFP and Rad51 foci kinetics in G2 and M phase**. HeLa-Rad52-GFP cells were treated with EdU 30 min before irradiation with 2 Gy X-rays. The cells were then harvested at various time points post irradiation and stained with anti-GFP (to detect Rad52-GFP), anti-Rad51 antibodies and DAPI. Samples were scanned using Metafer software and only EdU negative G2 or M phase cells were analyzed. For each individual experiment ≥ 40 cells were analyzed. (A) Rad52-GFP and Rad51 foci kinetics in G2 phase post 2 Gy irradiation. The error bars represent the SD of the mean values of two experiments. The foci number from unirradiated (0 Gy) samples were subtracted. (B) Rad52-GFP foci kinetics in G2 and M phase. The error bars represent the SEM of the mean values of three experiments. The foci number from unirradiated (0 Gy) samples were subtracted.

It has been previously shown that Rad51 dissociates from the chromatin before the cell enters M phase, whereas, Rad52 persists in M phase. In order to understand the behavior of Rad52 in M phase, Rad52-GFP foci kinetic in M phase was analyzed. In figure 4.1.b it can be seen that in early M phase (Prophase) the number of Rad52-GFP foci was very similar to the foci number in late G2 phase when Rad52 reached its maximum. Nevertheless, the number of Rad52-GFP foci declined as the cells progressed through M phase and reached its lowest shortly before chromatid segregation took place. If this gradual decrease in Rad52-GFP foci number in M phase represents actual repair events is still an open question. Additionally, earlier it was shown that in M phase, along with Rad52, Mus81 is also present at the break sites. Mus81 is a nuclease which is well known to carry out the resolution of HR intermediate structures (DHJs) to finalize repair events. This indicates that apart from being involved

in second end capture and strand annealing, Rad52 might be actively involved in or mediating the processing of HR intermediate structures together with other nucleases.

4.1.2. Kinetics of Rad52-GFP foci after hindering the early step (resection) of HR

DSB end resection represents a key process that commits the repair of DNA DSBs to HR. In eukaryotes, the process of resection is initiated and carried out by the Mre11-Rad50-NBS1 (MRN) complex and C-terminal binding protein-interacting protein (CtIP). A factor Mre11 of the MRN complex possesses endo- and exo-nuclease activity and functions in triggering DNA-damage checkpoints. Specifically, the endonuclease activity of Mre11 has been shown to initiate resection and to commit the repair of DSBs by HR repair pathway (Shibata et al., 2014). Further on, human CtIP is known to physically and functionally interact with the MRN complex to mediate the process of resection. During cell cycle, CtIP is regulated by the Cdks and phosphorylated by ATM and ATR in a damage dependent manner. Two Cdk sites on CtIP, S327 and T847, are known to regulate resection in the S and G2 phase (Sartori et al., 2007).

In order to understand if the appearance of Rad52-GFP foci is a resection-dependent process, HR was abrogated at an early step by inhibiting resection. To inhibit resection, CtIP protein was depleted and the nuclease activity of Mre11 was inhibited by using siRNA technology (siCtIP) and an inhibitor (Mirin) respectively. Mirin is an inhibitor which is known to specifically inhibit the exonuclease activity of Mre11 (Shibata et al., 2014). Before irradiation, HeLa-Rad52-GFP cells were treated with siCtIP and Mirin to inhibit resection and harvested 2 h and 7 h post irradiation. Using immunofluorescence, the cells were stained for anti-GFP antibodies (to detect Rad52-GFP). In addition, Rad51 was also stained to observe the efficiency of siCtIP and Mirin to inhibit resection.

Figure 4.2.a shows that, in G2 phase, the cells treated with siCtIP and Mirin had significantly low number of Rad51 foci compared to control cells at both time points (2 h and 7 h) post irradiation. This implies that by depleting CtIP and inhibiting the exonuclease activity of Mre11, there is a fall in the frequency of DSBs undergoing resection which is observed by the low Rad51 foci number. Further on, in figure 4.2.b it can be seen that siCtIP and Mirin-treatment (inhibited resection), and thus, abrogated HR, led to significantly low Rad52-GFP foci number at late time point (7 h) compared to control cells. This result indicates that appearance of Rad52-GFP foci in G2 phase is resection-dependent and that Rad52 has an active role in HR.

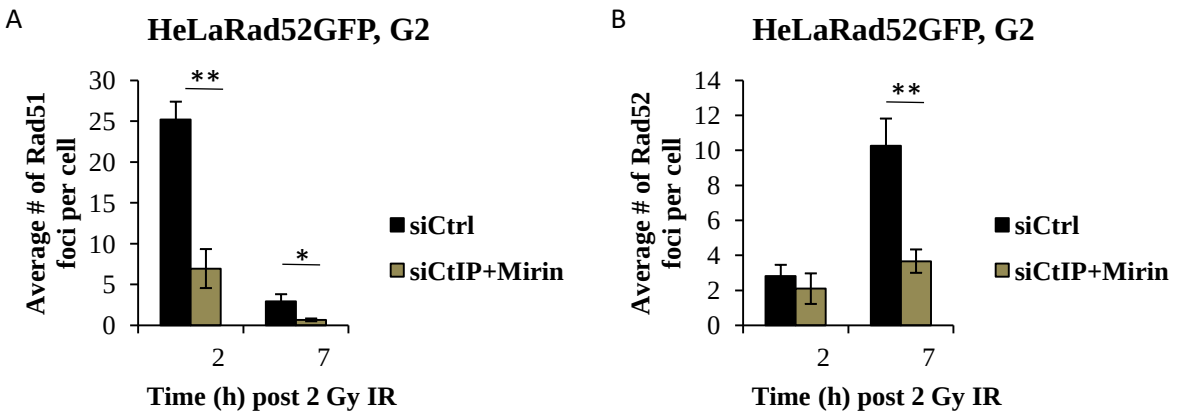

Figure 4.2. **Rad51 and Rad52-GFP foci kinetics in G2 phase after inhibition of resection**. HeLaRad52GFP cells were treated with siCtrl or siCtIP before irradiation with 2 Gy X-rays. Additionally, 30 min prior to irradiation EdU was added to the medium to label and exclude S phase cells. The cells were then harvested at various time points post irradiation and stained with anti-GFP (to detect Rad52-GFP), anti-Rad51 antibodies and DAPI. Samples were scanned using Metafer software and only EdU negative G2 phase cells were analyzed. For each individual experiment ≥ 40 cells were analyzed. (A) Rad51 foci kinetics in G2 phase post 2 Gy irradiation. (B) Rad52-GFP foci kinetics in G2 phase. The error bars represent the SEM of the mean values of three experiments. The foci number from unirradiated (0 Gy) samples were subtracted. Statistical significance was tested by Student's T-test (** = $p < 0.01$, * = $p < 0.05$). The siRNA efficiency was controlled by scoring Rad51 foci.

4.1.3. Kinetics of Rad52-GFP foci after abrogating the late step of HR

In HR repair pathway, the step of resection is followed by the loading of Rad51 nucleoprotein filaments on the 3'-ssDNA by BRCA2. Later on, the Rad51 nucleoprotein filaments carry out strand invasion in to the donor sister chromatid in order to copy the missing genetic information at the break site. Following strand invasion, homology search and DNA synthesis takes place and ultimately HR is finalized by the resolution or dissolution of the formed double Holliday junctions. However, after homology search and prior to resolution/dissolution, Rad51 needs to be removed from the ssDNA in order to allow DNA synthesis and the final steps of HR to take place (Heyer et al., 2010).

The process of removal of Rad51 from the ssDNA is carried out by a motor protein called Rad54. There has been multiple roles described for Rad54 in HR mediated repair pathway but the most critical role is thought to be the removal of Rad51 to finalize HR events. It has been shown that, in G2 phase, Rad54 is phosphorylated by a kinase known as Nek1 in a damage dependent manner. Absence of Rad54 confers a repair defect with increased *γ*H2AX and Rad51 foci in late G2 phase cells (Spies et al., 2016).

Next, the kinetics of Rad52 after depleting Rad54, and thus abrogating the late step of HR, was investigated. Before irradiation, HeLa-Rad52-GFP cells were treated with siRNA targeted against Rad54 (siRad54) and harvested 2 and 7 h post irradiation. Also, prior to irradiation, the cells were treated with EdU in order to label and exclude S phase cells from foci analysis. Rad52-GFP foci were quantified at 2 and 7 h post irradiation. Rad51 foci were additionally stained to check the efficiency of depletion of Rad54.

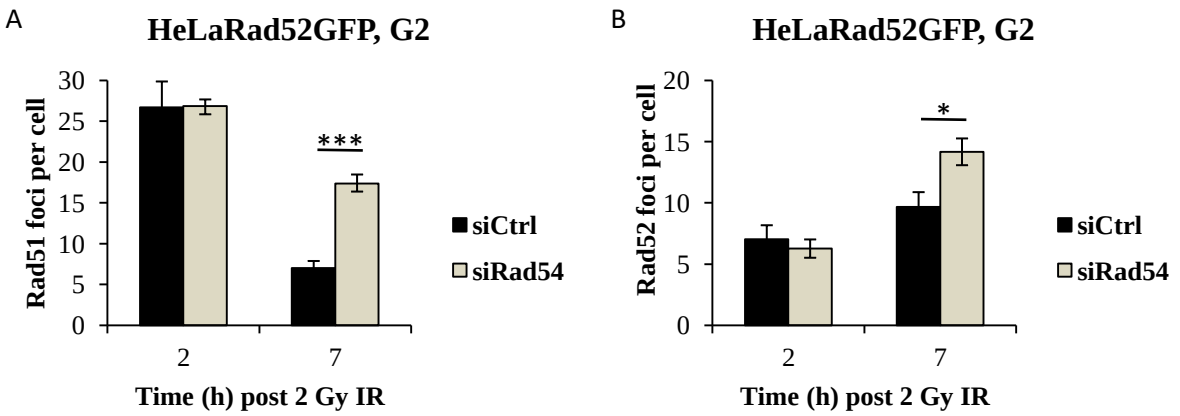

Figure 4.3. **Rad51 and Rad52-GFP foci kinetics in G2 phase after depletion of Rad54**. HeLa-Rad52-GFP cells were treated with siCtrl or siRad54 before irradiation. Additionally, 30 min prior to irradiation EdU was added to the medium to label and exclude S phase cells. The cells were then harvested at various time points post irradiation and stained with anti-GFP (to detect Rad52-GFP), anti-Rad51 antibodies and DAPI. Samples were scanned using Metafer software and only EdU negative G2 phase cells were analyzed. For each individual experiment ≥ 40 cells were analyzed. (A) Rad51 foci kinetics in G2 phase post 2 Gy irradiation. (B) Rad52-GFP foci kinetics in G2 phase. The error bars represent the SEM of the mean values of three experiments. The foci number from unirradiated (0 Gy) samples were subtracted. Statistical significance was tested by Student's T-test (*** = $p < 0.001$, * = $p < 0.05$). The siRNA efficiency was controlled by scoring Rad51 foci.

As shown in figure 4.3.a, in control cells (siCtrl) the number of Rad51 foci decreased at late time point (7 h) post irradiation. This decrease in Rad51 foci number represents its removal by Rad54 and, as such, the ongoing HR-mediated repair. Consistent with Rad54's function, depletion of Rad54 (siRad54) clearly showed much higher number of Rad51 foci at late time point post irradiation. This result shows that in the absence of Rad54, Rad51 cannot be removed from the ssDNA and that the cells are stuck with unprocessed HR intermediate structures (D-loop, DHJs). As a consequence, HR events cannot be finalized. This result is very much in line with other published data where it has been shown that, in the absence of Rad54, Rad51 foci persist in G2 phase cells. Figure 4.3.b shows that depletion of Rad54 resulted in significantly higher Rad52-GFP foci number at late time point (7 h) post irradiation as compared to control cells. This result suggests that Rad52 might bind to the ssDNA regions within the unprocessed HR intermediate structures and thus help to keep the structures intact until they are processed and repaired in the subsequent M phase or the next cell cycle phases.

4.2. Effect of depletion of Rad52 and other HR factors (Rad51 & BRCA2) on cell proliferation

From studies performed with *S. cerevisiae*, it is known that Rad52 is involved in the loading of Rad51 nucleoprotein filaments on 3'-ssDNA and that its depletion has a severe effect on cell proliferation. On the contrary, in mammalian cells, the loading of Rad51 nucleoprotein filaments on 3'-ssDNA is performed by BRCA2. Moreover, depletion of Rad51 or BRCA2 results in the accumulation of chromosomal aberrations and impaired cell proliferation in mammalian cells. Interestingly, inactivation of Rad52 in BRCA2-deficient cells is synthetically lethal (Feng et al., 2011). In order to understand if Rad52 has an important physiological role during spontaneous HR, its effect on cell proliferation was investigated. To this end, Rad52 was depleted alone or in combination with Rad51 or BRCA2.

First, optimal conditions were established to achieve efficient depletion of Rad52 protein by siRNA. HeLa wt cells were treated with different concentrations of siRNA (figure 4.4.a). The siRNA sequence information is provided in Table 3.5 and transfection of the cells was performed as explained in section 3.2.2. Cells were transfected twice with a gap of 24 h and harvested 24 h after the second transfection. In figure 4.4.a, it can be seen that the efficient depletion of Rad52 protein was achieved by transfecting the cells with an siRNA concentration of 50 nM. In addition, HeLa cells, stably transfected with a Rad52-GFP plasmid (HeLa-Rad52-GFP), were treated with 50 nM of siRNA and depletion of both endogenous (50 kDa) and exogenous (GFP-tagged, 80 kDa) Rad52 protein was observed (figure 4.4.b). Furthermore, depletion of Rad52 protein in fibroblast cells (82-6) was also achieved by transfecting the cells with an siRNA concentration of 50 nM (figure 4.4.b.).

To observe if the absence of Rad52 has a similar effect on cell proliferation in tumor as well as in healthy cell lines, HeLa tumor and 82-6 hTert fibroblast cell lines were used. Both cell lines were seeded separately in a 24-well plate and treated twice (with a gap of 24 h) with siRNA to deplete Rad52 either alone or in combination with Rad51 or BRCA2. 24 h post second siRNA transfection, the cells were trypsinized and the cell number was counted using a Neubauer cell counting chamber. As the cells in the control siRNA-treated well reached almost 80 – 90 % confluency on the 4th day, the cell counting was repeated consecutively for 4 days following second siRNA transfection.

Figure 4.4.c shows that in HeLa tumor cells, treatment with control siRNA showed normal cell growth and depletion of Rad52 had no effect on cell proliferation; as cell growth was very similar to control siRNA treated cells. Depletion of Rad51 had a negative impact on cell proliferation where the cell growth was clearly reduced as compared to the control cells. Moreover, depletion of Rad52 and Rad51 in combination had no additive effect. As Rad51 performs a key step of strand invasion during HR and is also known to provide protection to stalled and collapsed replication forks in S phase, it is not surprising to observe reduced cell growth in its absence. On the other hand, as Rad52 is a highly conserved protein and has almost 90 % similarity with its yeast homologue, it is highly surprising to observe that its absence has no impact on cell proliferation. Nevertheless, this data is consistent with previously published results where it has been shown that Rad52 deficient embryonic stem cells show normal cell growth and are not hypersensitive to agents that induce DSBs (Yamaguchi-Iwai, 1998). For 82-6 hTert fibroblast cell line (figure 4.4.d) identical results were obtained in comparison to the HeLa cell line (figure 4.4.c) upon depletion of Rad52 alone or together with Rad51.

Depletion of BRCA2 alone impaired cell growth for both the cell lines; however, this effect was more severe when Rad52 was additionally depleted along with BRCA2 (figure 4.4.e and f). Indeed, cell growth was severely reduced when BRCA2 and Rad52 were depleted in combination (figure 4.4.e and f). This data suggests that in the absence of BRCA2, Rad52 plays an important physiological role and renders viability to cells. These results are in line with earlier published data by Feng et al. and confirm the relationship of synthetic lethality between Rad52 and BRCA2. However, the exact function of Rad52 in BRCA2-deficient cells is unclear. Further on, we set out to investigate if, in the absence of

BRCA2, Rad52 provides a back-up function of loading of Rad51 and/or if Rad52 is involved in mediating an alternative recombination mediated repair pathway.

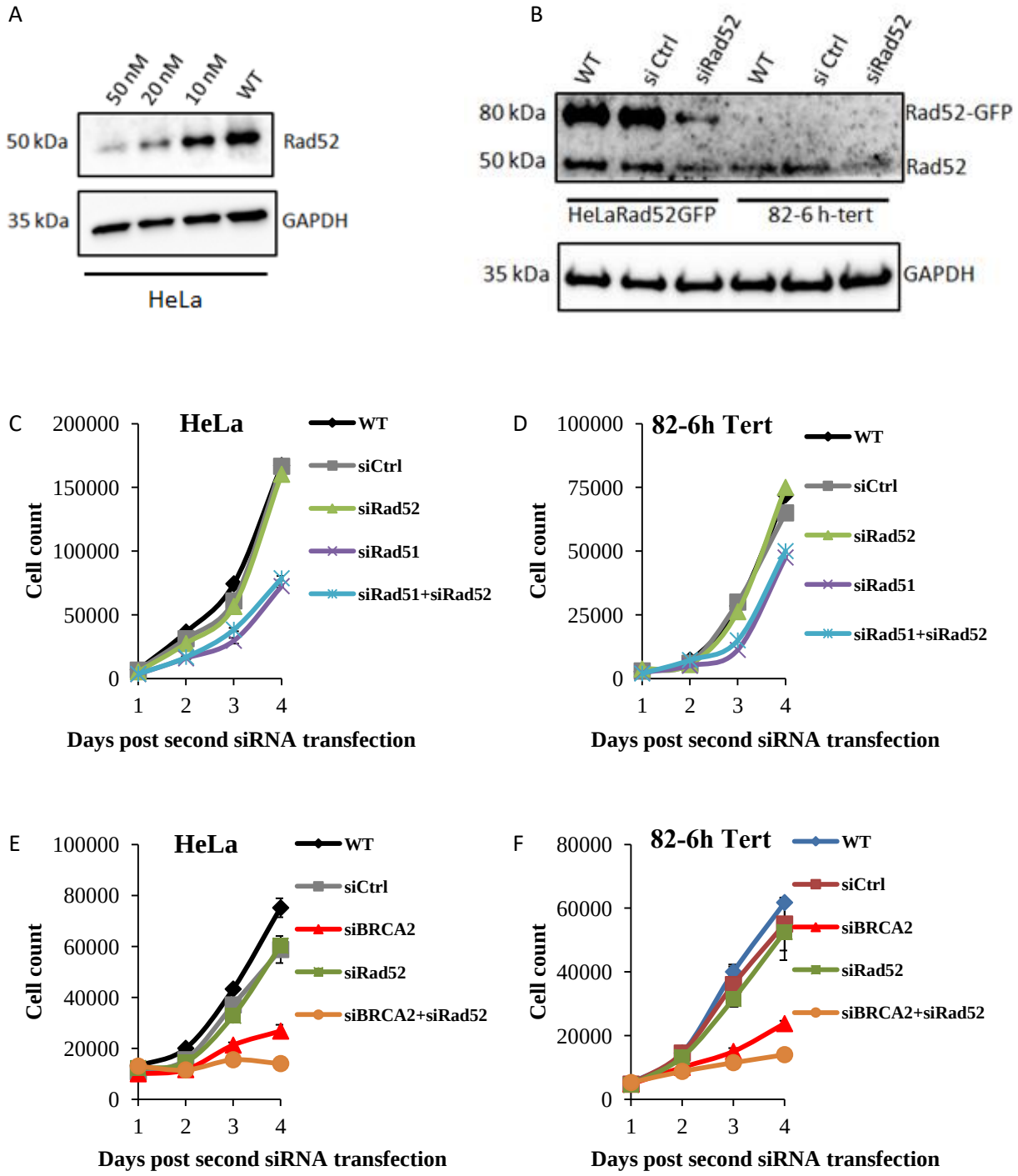

Figure 4.4. **WB analysis of depletion of Rad52 and cell count of HeLa tumor and 82-6 hTert fibroblast cell lines**. The cells were seeded, trypsinized each day and the cell number was counted using a Neubauer cell counting chamber.The cells were treated with various siRNA combinations.(A and B) Efficiency of depletion of Rad52 protein was controlled by Western Blot analysis. (C) Cell growth of HeLa cells after depletion of Rad52 and/or Rad51. (D) Cell growth of 82-6 hTert cells after depletion of Rad52 and/or Rad51. (E) Cell growth of HeLa cells after depletion of BRCA2 and/or Rad52. (F) Cell growth of 82-6 hTert cells after depletion of BRCA2 and/or Rad52. The error bars represent the SD of the mean values of two experiments.

4.3. Role of Rad52 in the formation of ionizing radiation induced Rad51 foci

As mentioned earlier, the loading of Rad51 on 3'-ssDNA is actively performed by BRCA2. BRCA2 interacts with Rad51 through its 8 BRC (Breast Cancer) repeats and a region located at its C terminus (Chatterjee, Jimenez-Sainz, Presti, Nguyen, & Jensen, 2016). Earlier it has been published that in HCC1937 cells, which harbor mutation of BRCA1 but not of BRCA2, IR-induced Rad51 foci were readily detected. Whereas, in Capan-1 cells, which do not express functional BRCA2, very little Rad51 foci formation was observed in response to a wide range of radiation dosages (Yuan et al., 1999).

In this study, the involvement of Rad52 in the formation of IR-induced Rad51 foci, in the presence or absence of BRCA2, was next investigated. In addition, by using image analysis software ImageJ, colocalization of Rad52-GFP and Rad51 foci was also investigated. To this end, HeLa cells were treated with siRNA to deplete Rad52 and BRCA2 either alone or in combination before exposure to IR. Additionally, an extra sample was treated with control siRNA. The cells were harvested at various time points post irradiation, stained with anti-Rad51 antibodies and only EdU-negative G2 phase cells were analyzed.

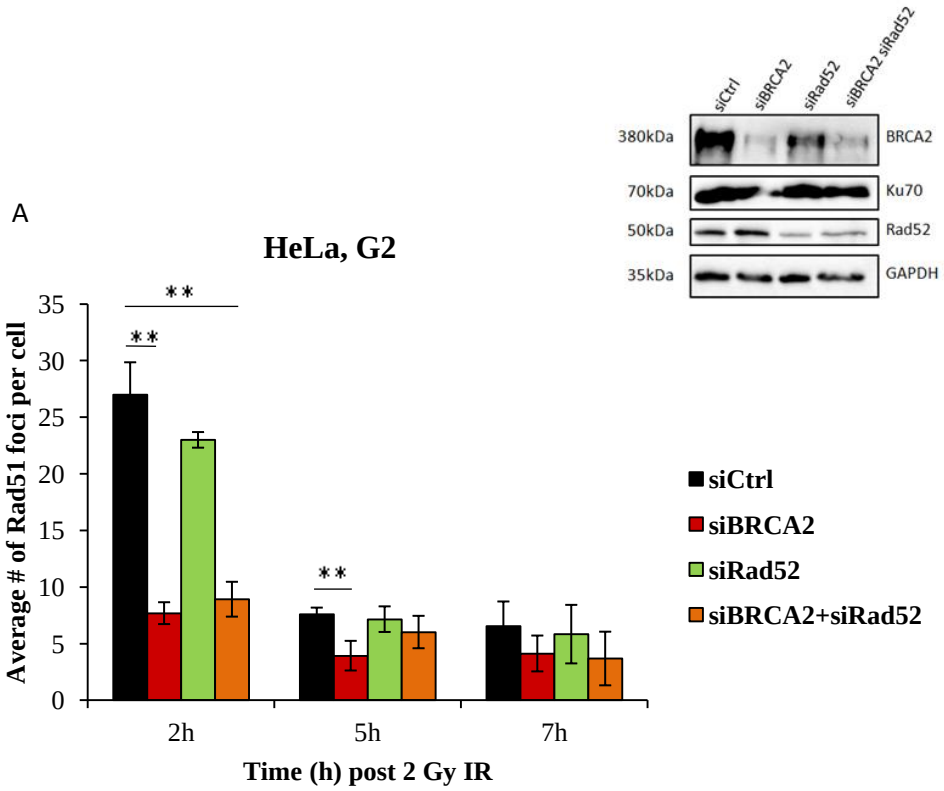

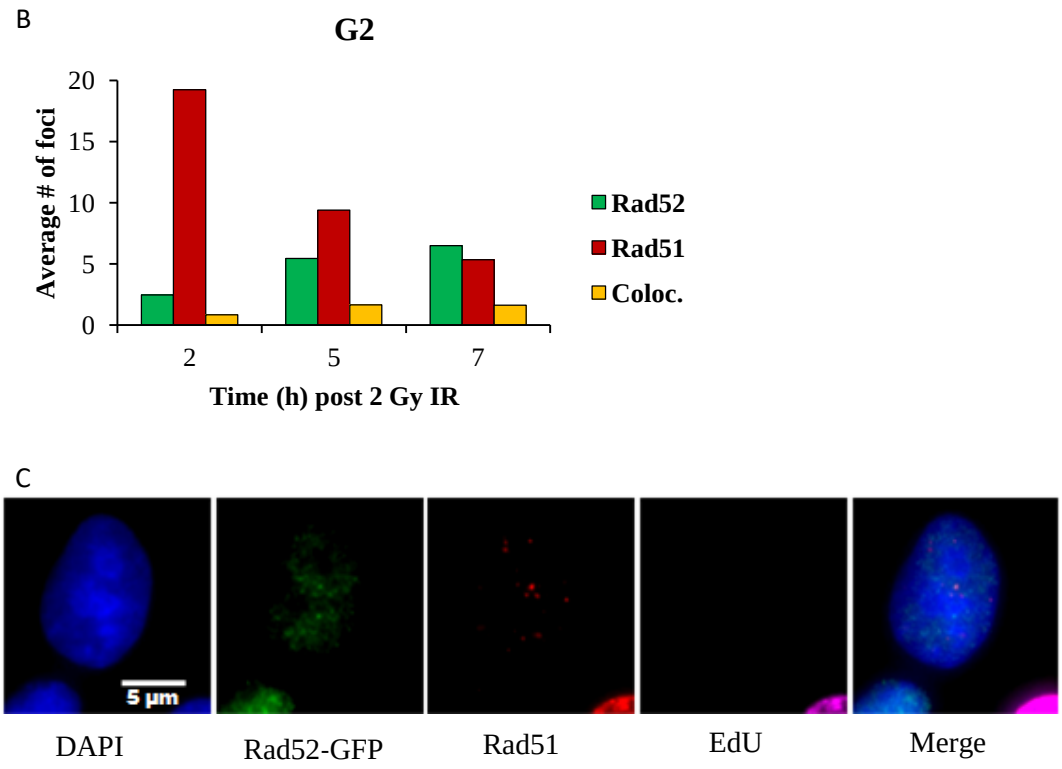

Figure 4.5. **Rad51 foci kinetics in G2 phase and co-localization analysis with Rad52-GFP foci**. (A) Rad51 foci kinetics in G2 phase HeLa cells. The cells were treated with BRCA2 and/or Rad52 before irradiation with 2 Gy X-rays. Additionally, 30 min prior to irradiation EdU was added to the medium to label and exclude S phase cells. The cells were then harvested at various time points post irradiation and stained with anti-Rad51 and anti-GFP antibodies and DAPI. Samples were scanned using Metafer software and only EdU negative G2 phase cells were analyzed. For each individual experiment ≥ 40 cells were analyzed. The error bars represent the SEM of the mean values of three experiments. The foci number from unirradiated (0 Gy) samples were subtracted. Statistical significance was tested by Student's T-test (** = $p < 0.01$, * = $p < 0.05$). (B) Co-localization analysis of Rad52-GFP and Rad51 foci. The cells were scanned using Metafer software and co-analysis was done using ImageJ software. (C) Representative images of Rad52-GFP and Rad51 foci in G2 phase cell. The images were acquired using Metafer software. The siRNA efficiency was controlled using Western blot by Marta Llorens Agost.

Post irradiation, Rad51 foci were readily detected in control cells, peaking at 2 h after IR. As time progressed, the number of Rad51 foci steadily decreased, corresponding to the ongoing HR mediated DSB repair (figure 4.5.a). As expected, in cells depleted for BRCA2, the number of Rad51 foci was substantially lower than in siCtrl-treated cells. On the other hand, in cells depleted for Rad52, Rad51 foci were readily formed and the kinetics of Rad51 foci was very similar to siCtrl-treated cells. Furthermore, depletion of BRCA2 and Rad52 together did not have any additive negative impact on the formation of Rad51 foci. Moreover, image analysis showed that there was hardly any colocalization between Rad52-GFP and Rad51 foci (figure 4.5.b and c) indicating no interaction between Rad52 and Rad51. Taken together, these results clearly indicate that in mammalian G2 phase cells, Rad52 is not involved in the loading and formation of Rad51 foci upon IR treatment.

Next, the function of Rad52 in providing a back-up alternative DSB repair pathway in the absence of BRCA2 was investigated.

4.4. Role of Rad52 in providing a back-up alternative DSB repair pathway in case of impaired Homologous Recombination

Feng et al. (2011) have proposed that in BRCA2 deficient cells, Rad52 mediates an independent and alternative repair pathway of HR. They show that in the presence or absence of BRCA2, IR-induced and S phase associated Rad52 and Rad51 foci were readily detected. Based on these results they claim that Rad52 can respond to DNA DSBs and replication stalling independently of BRCA2. Therefore, the function of Rad52 to provide an alternative back-up repair pathway in case of impaired HR (absence of BRCA2) was next investigated.

To this end, HeLa-Rad52-GFP cells were used and, before exposure to IR, treated with either control siRNA or siRNA targeted against BRCA2. Only those cells which were irradiated in G2 phase and stayed in G2 phase during the whole repair incubation time were taken into account for analysis. In order to label and exclude the S phase cells, half an hour prior to irradiation, EdU was added to the medium and left during the entire repair incubation time till harvest. Following irradiation, cells were harvested at different time points and stained with anti-Rad51, anti-GFP (to detect Rad52-GFP) and anti-*γ*H2AX antibodies.

As Rad51 is widely accepted as a key marker for HR, Rad51 was stained in order to observe the ongoing HR mechanism. As shown in figure 4.6.a, Rad51 foci were promptly detected in control siRNA treated samples with a steady decrease during the time course corresponding to the ongoing HR mediated DSB repair. As expected, depletion of BRCA2 (siBRCA2) resulted in a significant downfall in the number of Rad51 foci indicating an impaired HR repair process. Consequently, depletion of BRCA2 also resulted in a repair defect in G2 phase as observed by staining *γ*H2AX, a prominent DSB marker (figure 4.6.b). Interestingly, in comparison to control samples, a significantly increased numbers of Rad52-GFP foci were observed in BRCA2 depleted samples (figure 4.6.c and d). Moreover, at 2 h post irradiation, the number of Rad52-GFP foci in BRCA2 depleted samples was very similar to the number of Rad51 foci in control samples. This implies that in case of impaired HR (absence of BRCA2), the DSBs, which were supposed to undergo repair by classical Rad51-dependent HR, are decorated by Rad52. This result suggests that upon depletion of BRCA2, Rad52 might provide an alternative recombination mediated back-up repair pathway. Nevertheless, assuming that Rad52 provides a back-up repair pathway in a BRCA2 deficient background, a repair defect is still observed at 8 h post irradiation, suggesting an inefficient back-up pathway to repair DSBs (figure 4.6.b). In this case, the function to provide protection to unrepaired DSBs by Rad52 cannot be overlooked. In order to further understand the function of Rad52 in detail and to figure out if Rad52 mediates a back-up repair pathway or protects the unrepaired resected DSBs, DSB repair kinetic was next investigated.

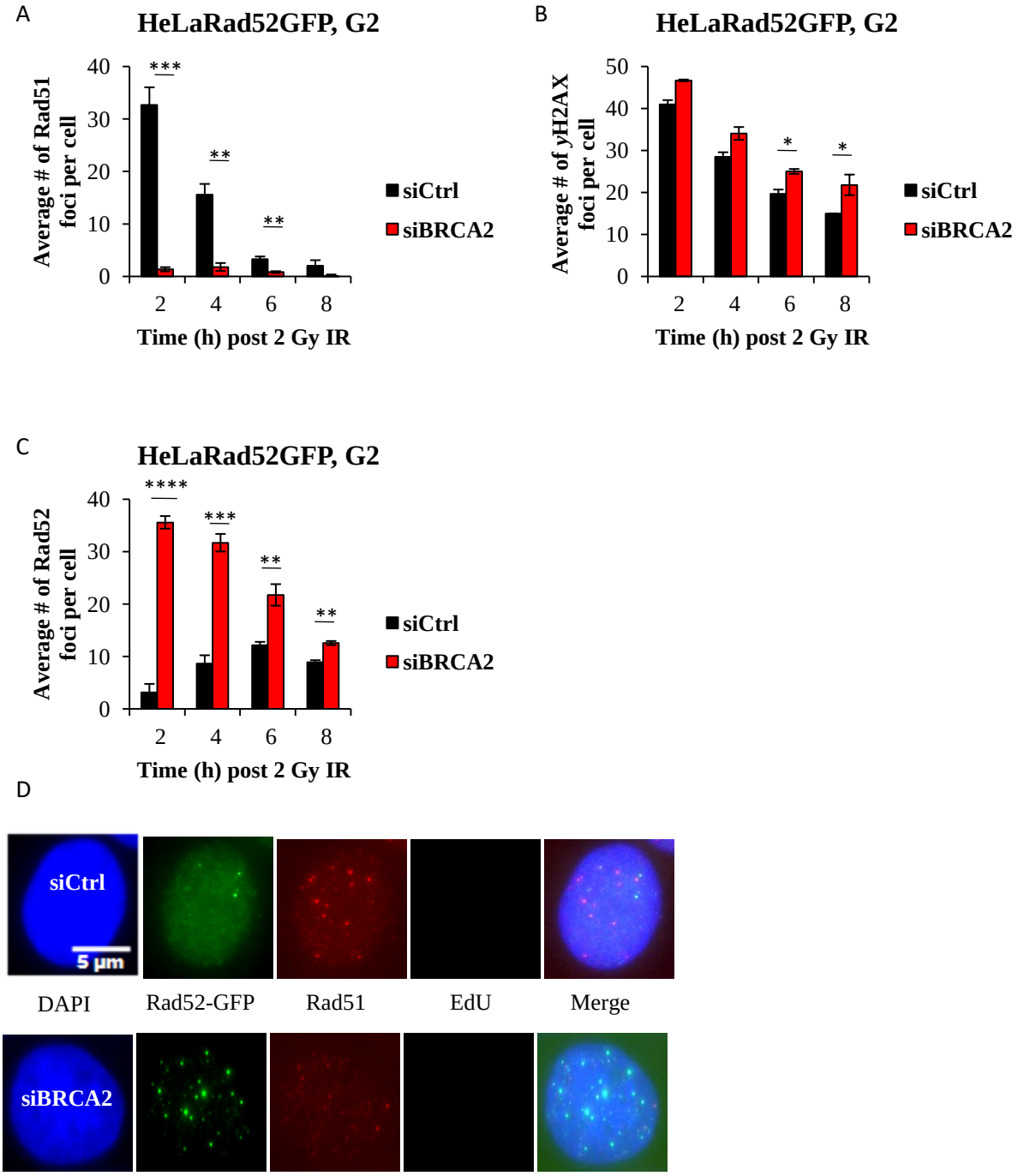

Figure 4.6. **Rad52 bind to the resected DSBs in the absence of BRCA2**. The cells were treated with siCtrl or siBRCA2 before irradiation with 2 Gy X-rays. Additionally, 30 min prior to irradiation EdU was added to the medium to label and exclude S phase cells. The cells were then harvested at various time points post irradiation, scanned using Metafer software and only EdU negative G2 phase cells were analyzed. For each individual experiment ≥ 40 cells were analyzed. (A) Rad51 foci kinetics in HeLaRad52GFP G2 phase cells. The cells were stained with anti-Rad51 antibodies and DAPI. (B) *γ*H2AX foci kinetics in HeLaRad52GFP G2 phase cells. The cells were stained with anti-*γ*H2AX antibodies and DAPI. (C) Rad52-GFP foci kinetics in HeLaRad52GFP G2 phase cells. The cells were stained with anti-GFP antibodies (to detect Rad52-GFP) and DAPI. The foci number from unirradiated (0 Gy) samples were subtracted. The error bars represent the SEM of the mean values of three experiments. Statistical significance was tested by Student's T-test (**** = $p < 0.0001$, *** = $p < 0.001$, ** = $p < 0.01$, * = $p < 0.05$). (D) Representative images of Rad52-GFP foci in siCtrl and siBRCA2-treated G2 phase cells at 2h post 2 Gy IR. The images were acquired using Metafer software. The siRNA efficiency was controlled by scoring Rad51 foci.

4.5. Double strand break repair kinetics

4.5.1. Double strand break repair kinetics in G2 phase

The *y*H2AX foci are widely accepted as a DSB marker and represent the DSBs in a 1:1 ratio. By using the *y*H2AX assay, the kinetics of DSB repair was analyzed. To this end, HeLa tumor cells, wt 82-6 hTert and BRCA2 mutant HSC-62 hTert fibroblast cell lines were used. Prior to irradiation, the cells were treated with siRNA against BRCA2 and Rad52. As in previous experiments, for this experiment also, only those cells, which were irradiated in G2 phase and stayed in G2 phase during the whole repair incubation time, were analyzed. The cells were stained with anti-*y*H2AX antibodies and approximately 40 cells were analyzed to quantify unrepaired DSBs.

Consistent with previous reports, in comparison to control siRNA (siCtrl) treated cells, depletion of BRCA2 (siBRCA2) in HeLa cells displayed impaired DSB repair, resulting in more residual *y*H2AX foci at 8 h post 2 Gy (figure 4.7). Depletion of Rad52 (siRad52) had no effect on DSB repair and the breaks were repaired efficiently as in siCtrl treated cells. Assuming that Rad52 mediates an alternative back-up repair pathway, one might expect an additive repair defect upon co-depletion of BRCA2 and Rad52 as both the repair pathways (classical HR and a back-up repair pathway) would be unavailable for the cell. Interestingly, upon depletion of BRCA2 and Rad52 together, no additive DSB repair defect was displayed. Instead, double depletion of BRCA2 and Rad52 led to the rescue of the BRCA2 repair defect and, as a consequence, an efficient repair was observed where the number of residual *y*H2AX foci was similar to siCtrl treated cells (figure 4.7).

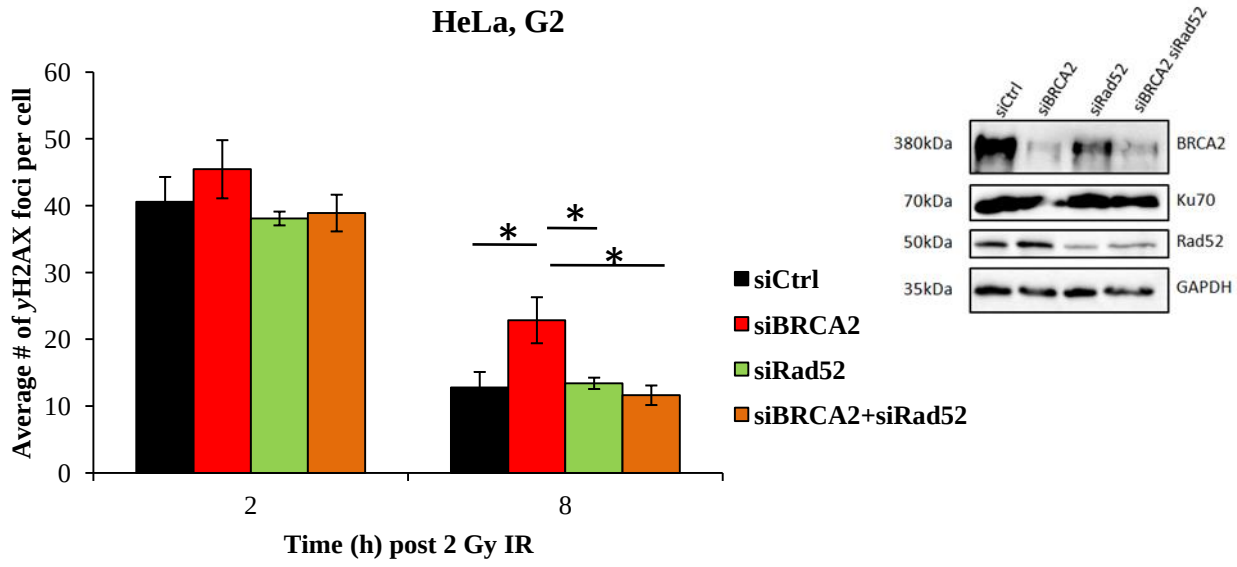

Figure 4.7. **Co-depletion of BRCA2 and Rad52 rescues the BRCA2 repair defect in HeLa cells**. The cells were treated with siCtrl or siBRCA2 and/or siRad52 before irradiation with 2 Gy X-rays.30 min prior to irradiation EdU was added to the medium to label and exclude S phase cells. The cells were then harvested at various time points post irradiation and stained with anti- *y*H2AX antibodies and DAPI. Samples were scanned using Metafer software and only EdU negative G2 phase cells were analyzed. For each individual experiment ≥ 40 cells were analyzed. The foci number from unirradiated (0 Gy) samples were subtracted. The error bars represent the

SEM of the mean values of three experiments. Statistical significance was tested by Student's T-test (* = $p < 0.05$).The siRNA efficiency was controlled by Western blot (performed by Marta Llorens Agost).

Similar results were observed when the experiment was conducted with wt 82-6 hTert and BRCA2 mutant HSC-62 hTert fibroblast cell lines (figure 4.8.a and b). As observed with HeLa cells, depletion of BRCA2 (siBRCA2) in wt 82-6 hTert cells displayed a repair defect, whereas, co-depletion of BRCA2 and Rad52 resulted in the rescue of the BRCA2 repair defect at 8 h post 2 Gy (figure 4.8.a). BRCA2 mutant HSC-62 hTert fibroblasts displayed an impaired repair at 8 h post irradiation compared to wt 82-6 hTert fibroblasts (figure 4.8.b). Importantly, upon depletion of Rad52 in HSC-62 fibroblasts, the BRCA2 repair defect was rescued (figure 4.8.b). In order to represent and explain the results in a more clear fashion, data only from fibroblast (82-6 & HSC-62) cell lines is shown until section 4.7.

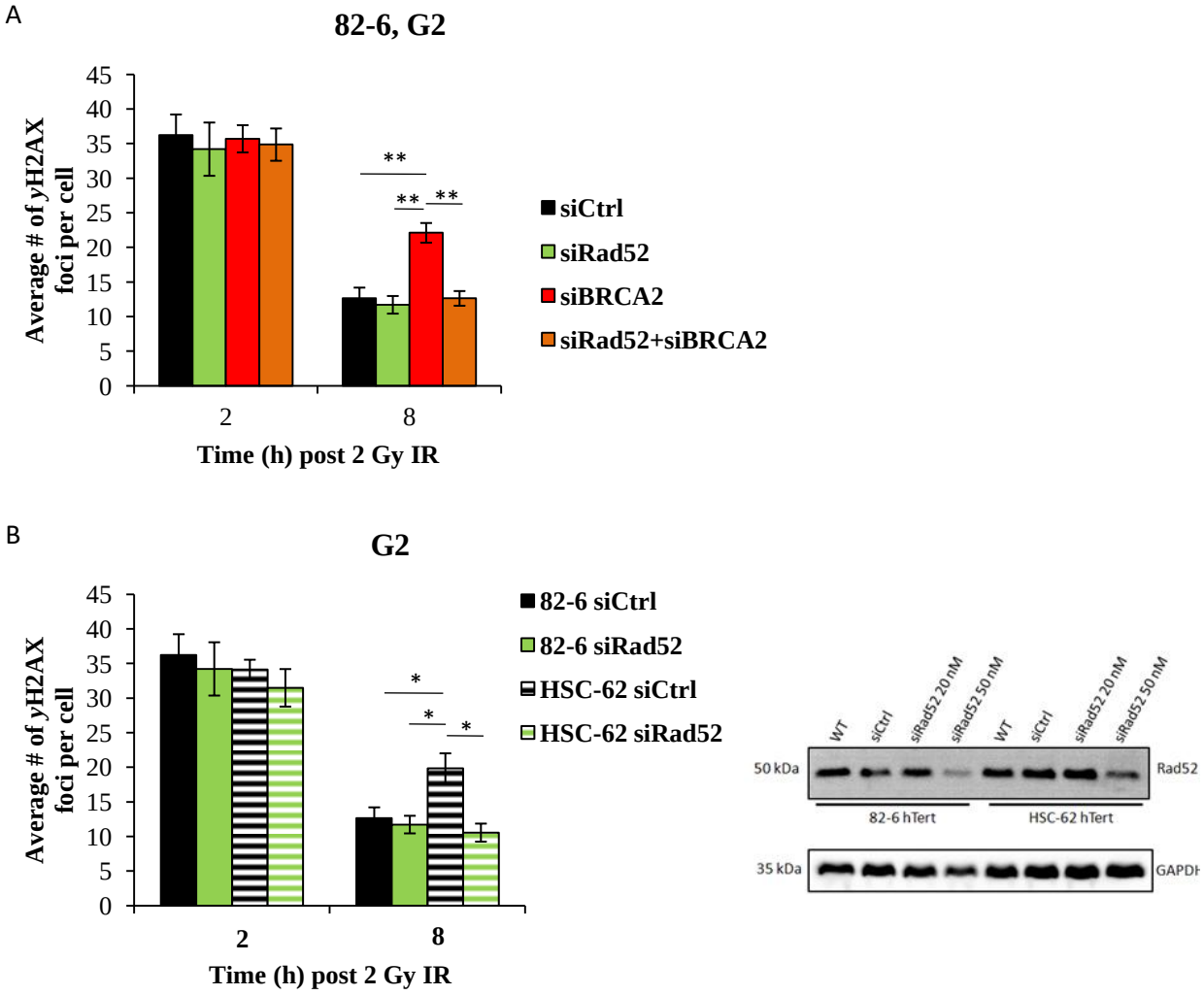

Figure 4.8. **Depletion of Rad52 in BRCA2-mutant cells rescues the BRCA2 repair defect**. 30 min prior to irradiation (2 Gy X-rays) EdU was added to the medium to label and exclude S phase cells. The cells were then harvested at various time points post irradiation and stained with anti-γH2AX antibodies and DAPI. Samples were scanned using Metafer software and only EdU negative G2 phase cells were analyzed. For each individual experiment ≥ 40 cells were analyzed. (A) γH2AX foci kinetics in 82-6 hTert G2 phase cells. The cells were treated with siCtrl or siBRCA2 and/or siRad52before irradiation. (B) γH2AX foci kinetics in 82-6 hTert and HSC-62 hTert G2 phase cells. The cells were treated with siCtrl or siRad52 before irradiation. The foci number from unirradiated (0 Gy) samples were subtracted. The error bars represent the SEM of the mean values of three experiments. Statistical significance was tested by Student's T-test (** = $p < 0.01$,* = $p < 0.05$). The siRNA efficiency was controlled by Western blot.

4.5.2. Double strand break repair kinetics in S phase

The shift from c-NHEJ to HR is gradual, with the highest proportion of DSBs being repaired by HR in mid-S phase where the amount of DNA replication is at its peak (Karanam, Kafri, Loewer, & Lahav, 2012). In G2 phase, approximately 20 % of the DSBs are repaired by HR. After ascertaining that in G2 phase, co-depletion of BRCA2 and Rad52 leads to the rescue of the BRCA2 repair defect, we next set out to investigate if this phenomenon is also true for S phase where the contribution of HR is much higher than in G2 phase. For this purpose, wt 82-6 hTert and BRCA2 mutant HSC-62 hTert fibroblast cell lines were used. DSBs were induced in the cells randomly by exposure to IR or specifically in S phase by treatment with camptothecin (CPT). CPT is a topoisomerase I inhibitor which forms a complex with topoisomerase I and ssDNA. Upon collision of this complex with a replication fork, S phase specific DSBs are generated.

Prior to exposure to IR or treatment with CPT, BRCA2 and Rad52 proteins were depleted either alone or in combination using the siRNA technology. For this experiment, only EdU labeled S phase cells were taken into account for foci quantification, whereas, G1 and G2 phase cells were excluded from the analysis. Using immunofluorescence, the cells were stained with anti-*γ*H2AX antibodies and approximately 40 S phase cells were analyzed to quantify unrepaired DSBs.

In wt 82-6 hTert fibroblasts, depletion of Rad52 (siRad52) had no effect on DSB repair in S phase at 8 h post 2 Gy irradiation or CPT treatment (figure 4.9.a and b). In BRCA2 mutant HSC-62 hTert cells, a repair defect was observed at 8 h post 2 Gy irradiation or CPT treatment, displayed by an increased number of residual *γ*H2AX foci compared to wt 82-6 hTert fibroblast cells (figure 4.9.c and d). Moreover, the repair defect observed in BRCA2 mutant HSC-62 hTert cells was rescued upon depletion of Rad52 (figure 4.9.c and d). This observation was true for both the cases: damage induced by exposure to IR or by CPT treatment (figure 4.9.c and d). Henceforth, consistent with the results obtained for G2 phase (figure 4.8.a and b), the phenomenon of rescue of the BRCA2 repair defect upon depletion of Rad52 was also observed and validated for S phase (figure 4.9.c and d).

These results taken together suggest that, in case of impaired HR during S and/or G2 phase, rather than mediating an alternative repair pathway, Rad52 provides some sort of protection to the unrepaired breaks. This function of Rad52 is very much likely to protect the resected 3'-ssDNA from being degraded by the action of some nucleases or to prevent an erroneous pathway from acting upon the resected DNA breaks. Further on, the repair pathway responsible for the repair of DSBs in the absence of BRCA2 and Rad52 was next investigated. To this end, G2 phase-specific experiments were performed where only those cells, which were in G2 phase at the time of harvest, were analyzed.

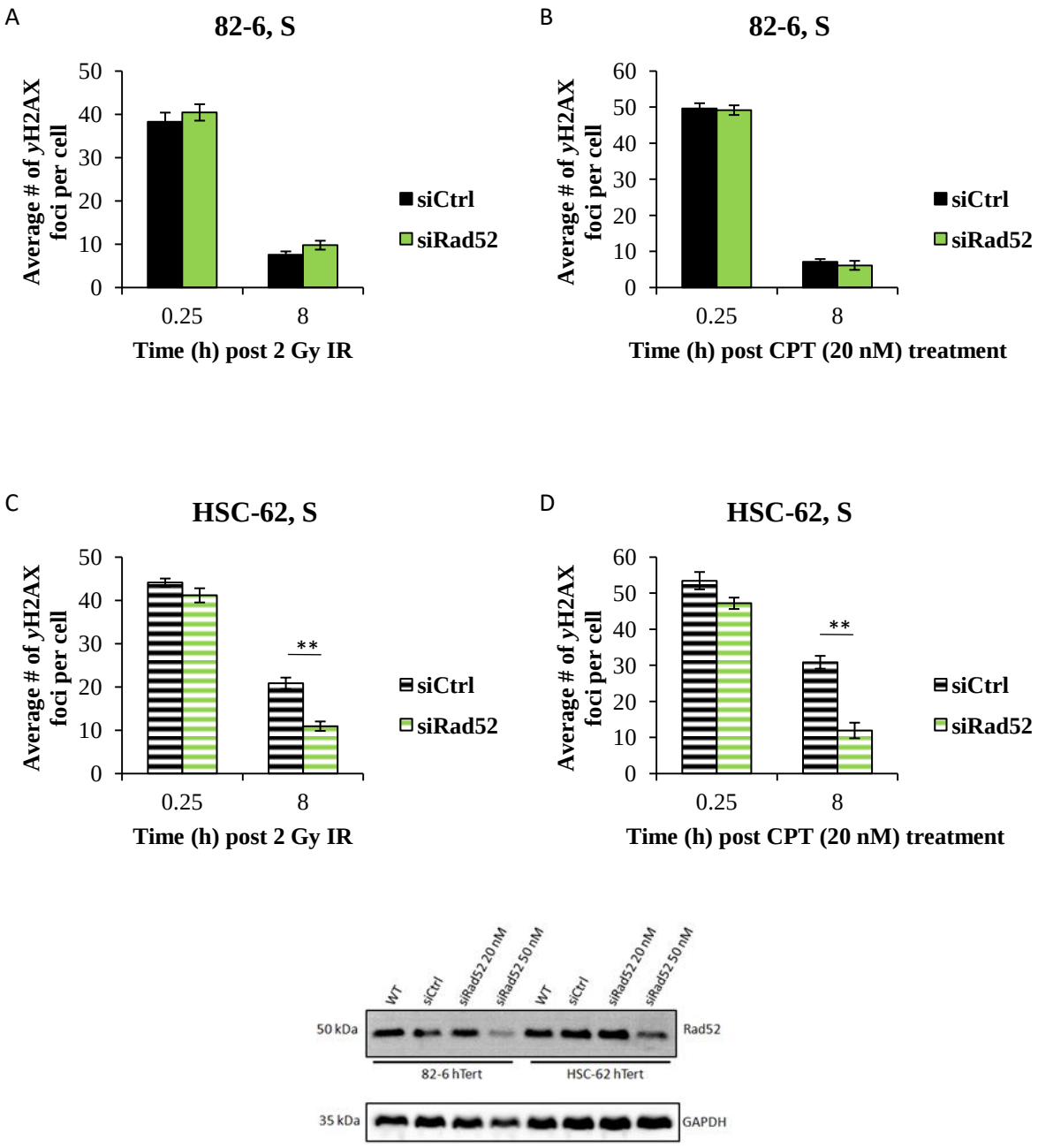

Figure 4.9. **Rescue of the BRCA2 repair defect in S phase**. Cells were treated with siCtrl or siRad52 and 30 min prior to irradiation (2 Gy X-rays) EdU was added to the medium to label S phase cells. The cells were then harvested at various time points post irradiation and stained with anti- *γ*H2AX antibodies and DAPI. Samples were scanned using Metafer software and only EdU positive S phase cells were analyzed. For each individual experiment ≥ 40 cells were analyzed. (A) *γ*H2AX foci kinetics in 82-6 hTert S phase cells after irradiation with 2 Gy X-rays. (B) *γ*H2AX foci kinetics in 82-6 hTert S phase cells after treatment with 20 nM CPT. (C) *γ*H2AX foci kinetics in HSC-62 hTert S phase cells after irradiation with 2 Gy X-rays. (D) *γ*H2AX foci kinetics in HSC-62 hTert S phase cells after treatment with 20 nM CPT. The foci number from unirradiated (0 Gy) samples were subtracted. The error bars represent the SEM of the mean values of three experiments. Statistical significance was tested by Student's T-test (** = $p < 0.01$). The siRNA efficiency was controlled by Western blot (supplement figure 6.3).

4.5.3. Involvement of theta-mediated end joining in the rescue of BRCA2 repair defect upon Rad52 depletion in G2 phase

Increasing evidence suggest that HR-deficient tumor cells are dependent on Polθ-mediated repair for their survival (Ceccaldi, Liu, et al., 2015). Polθ functions by annealing the microhomologies (MHs) present within the resected 3'-ssDNA and, thus, mediates TMEJ repair pathway (Kent et al., 2015). Molecular characterization has revealed that PARP1 and Ligase3 are also involved in TMEJ repair pathway (Sfeir & Symington, 2015).

To figure out if TMEJ is responsible for the repair of DSBs in the absence of BRCA2 and Rad52, DSB repair kinetic experiments were performed after inhibiting or depleting TMEJ factors (PARP & Polθ). To this end, primary fibroblast (wt 82-6 & BRCA2 mutant HSC-62) cell lines were used. Before irradiation, Rad52 or Polθ were depleted using siRNAs and PARP was inhibited using an inhibitor called Olaparib. 8 h post 2 Gy of IR, cells were harvested, fixed with 2.5 % formaldehyde, stained with anti-*y*H2AX antibodies and only EdU negative G2 phase cells were analyzed.

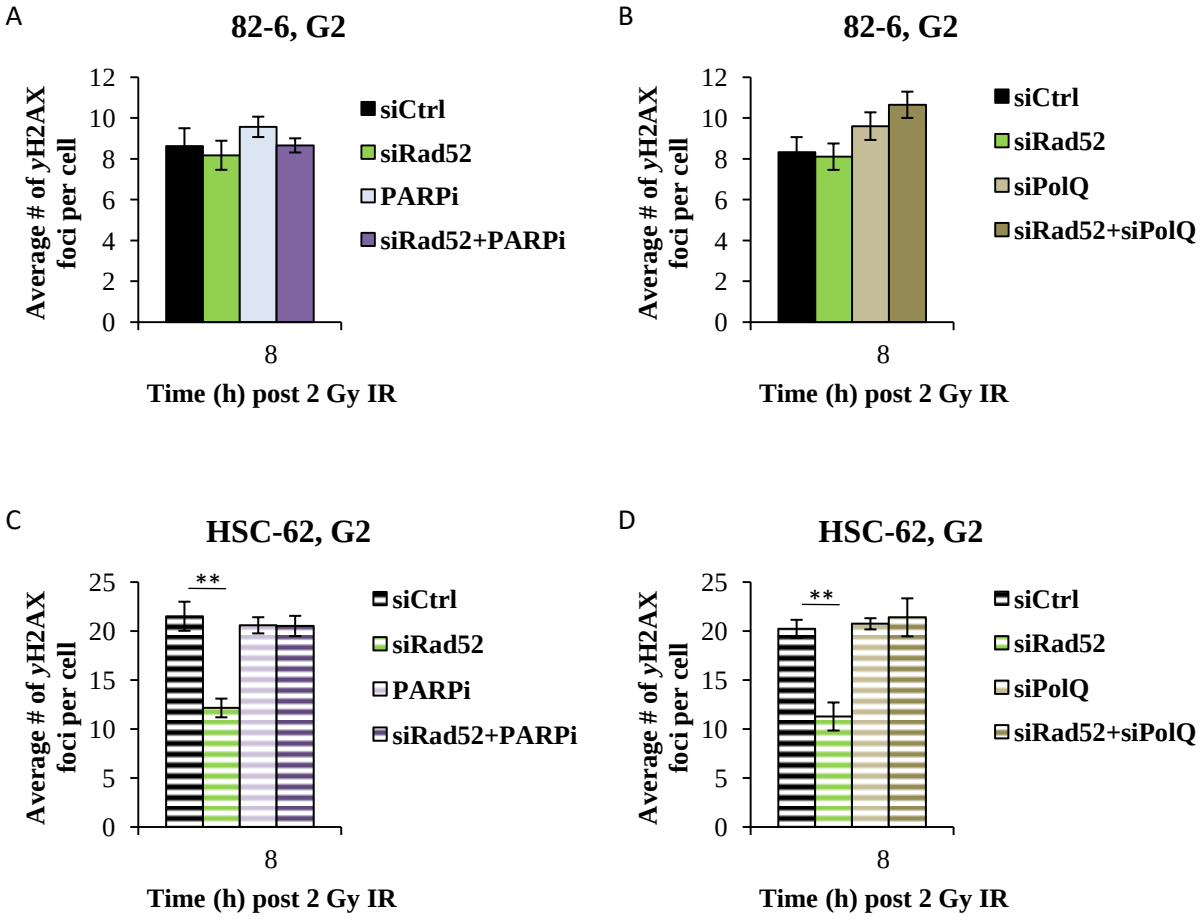

Figure 4.10. **BRCA2 repair defect is rescued by Polθ-dependent TMEJ**. 30 min prior to irradiation EdU was added to the medium to label and exclude S phase cells from analysis. The cells were then harvested at 8 h post irradiation and stained with anti- *y*H2AX antibodies and DAPI. Samples were scanned using Metafer software and only EdU negative G2 phase cells were analyzed. For each individual experiment ≥ 40 cells were analyzed. (A) *y*H2AX foci kinetics in 82-6 hTert G2 phase cells. Before irradiation, the cells were treated with siRad52 and/or PARPi (1 µM Olaparib). (B) *y*H2AX foci kinetics in 82-6 hTert G2 phase cells. Before irradiation, the cells were treated with siRad52 and/or siPolθ. (C) *y*H2AX foci kinetics in HSC-62 hTert G2 phase cells. Before irradiation, the cells were

treated with siRad52 and/or PARPi (1 µM Olaparib). (D) *γ*H2AX foci kinetics in HSC-62 hTert G2 phase cells. Before irradiation, the cells were treated with siRad52 and/or siPolθ. The foci number from unirradiated (0 Gy) samples were subtracted. The error bars represent the SEM of the mean values of three experiments. Statistical significance was tested by Student's T-test (** = $p < 0.01$).

As shown in figure 4.10.a and b, inhibition of PARP or depletion of Rad52 or Polθ had no impact on the repair of DSBs in wt 82-6 G2 phase cells. Also, inactivation of PARP or Polθ together with Rad52 displayed no impaired DSB repair kinetic. For all the above mentioned conditions, the residual *γ*H2AX foci number was similar to control-siRNA (siCtrl) treated cells (figure 4.10.a and b). Figure 4.10.c and d show that, at 8 h post irradiation, siCtrl treated BRCA2 mutant HSC-62 cells showed a repaired defect observed by substantial increase in number of residual *γ*H2AX foci compared to wt 82-6 cells. Indeed, this repair defect was rescued upon depletion of Rad52. Like in wt 82-6 cells, in BRCA2 mutant HSC-62 cells inactivation of PARP or Polθ had no impact on the repair of DSBs neither an additive repair defect was observed (figure 4.10.c and d). Importantly, depletion of Rad52 together with inactivation of PARP or Polθ did not result in the rescue of the BRCA2 repair defect (figure 4.10.c and d) which is displayed by an increased number of residual *γ*H2AX foci as compared to Rad52 depleted situation. These results indicate that, in BRCA2-deficient cells, absence of Rad52 leads to the repair of DSBs by TMEJ repair pathway mediated by PARP and Polθ, and, as such, rescues the BRCA2 repair defect. In other words, presence of Rad52 in BRCA2 deficient cells prevents TMEJ repair pathway from acting upon the unrepaired DSBs.

4.6. Kinetics of replication protein A in G2 phase during the rescue of BRCA2 repair defect

TMEJ and HR repair pathways share a common initial step of resection (Truong et al., 2013). Deng et al. (2014) showed that the process of resection exposes the MHs present along the stretch of 3'-ssDNA. Furthermore, the presence of RPA on the ssDNA prevents spontaneous annealing between MHs. Thus, RPA antagonizes TMEJ and channels the repair of DSBs from TMEJ to HR (Deng, Gibb, de Almeida, Greene, & Symington, 2014).

After establishing the fact that in G2 phase upon co-depletion of BRCA2 and Rad52 repair of DSBs is channeled to TMEJ, the presence of RPA bound to ssDNA and its effect on TMEJ-mediated repair pathway was next investigated. To this end, fibroblasts 82-6 and HSC-62 cells were used and depleted for BRCA2 and Rad52 before exposure to IR. Immunofluorescence staining of RPA phosphorylated at Threonine21 (pRPA pT21) can detect ssDNA bound RPA which is readily visible as foci in S/G2 phase. As such, the cells were stained with anti-pRPA (pT21) antibodies and only EdU negative G2 phase were analyzed for foci quantification.

As presented in figure 4.11.a, pRPA foci were readily detected in siCtrl-treated 82-6 G2 phase cells at 2 h post 2 Gy IR. In these cells, the number of pRPA foci clearly decreased at 6 h post 2 Gy IR corresponding to HR mediated repair of DSBs. After depleting Rad52, no effect on the kinetics of pRPA foci was observed. On the other hand, in siCtrl-treated HSC-62 cells, a clearly higher number of pRPA foci was observed at 2 h post 2 Gy IR compared to 82-6 cells. Additionally, instead of decreasing, this high pRPA foci number was maintained throughout the entire repair incubation time which refers to a

repair defect due to mutant BRCA2 in HSC-62 cells. Interestingly, the high amount of pRPA foci was significantly reduced upon depletion of Rad52 at both 2 and 6 h post irradiation in HSC-62 cells (figure 4.11.a). Furthermore, upon depletion of Rad52 together with Polθ, no reduction in pRPA was observed (figure 4.11.b). This observed pRPA kinetics corresponds well the DSB repair kinetic where no reduction of *γ*H2AX foci was observed upon co-depletion of Rad52 and Polθ (figure 4.10.d). These results suggest that in the absence of BRCA2 and Rad52, there is less RPA bound to ssDNA (shown by reduced pRPA foci number; figure 4.11.a), which exposes the MHs and allows TMEJ-mediated repair of DSBs. However, it is still an open question if the reduction in pRPA foci number is due to the absence of BRCA2 and Rad52 or due to repair itself (mediated by TMEJ).

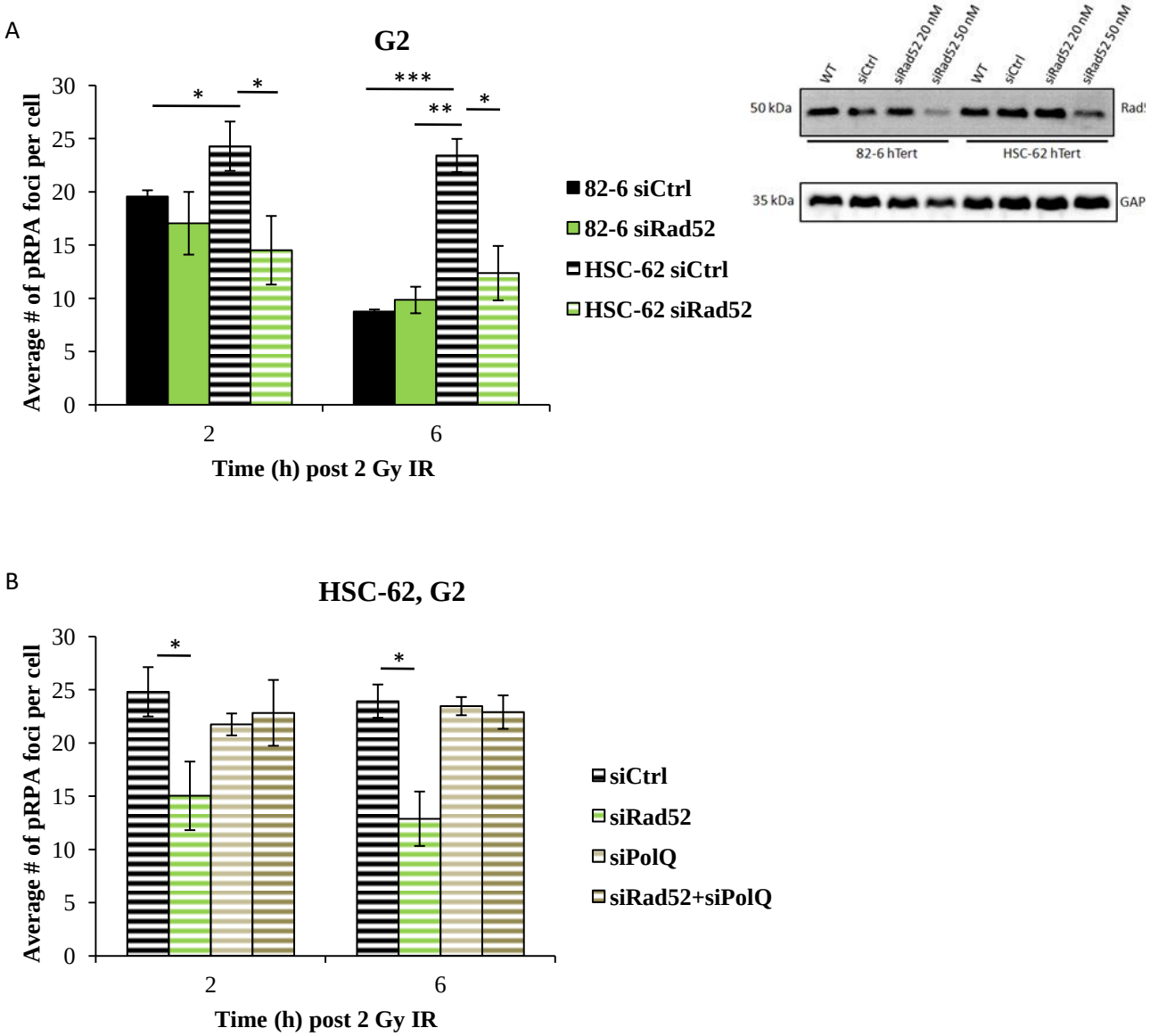

Figure 4.11. **Removal of RPA facilitates TMEJ.** 30 min prior to irradiation (2 Gy X-rays) EdU was added to the medium to label and exclude S phase cells from analysis. The cells were then harvested at various time points post irradiation and stained with anti-pRPA antibodies and DAPI. Samples were scanned using Metafer software and only EdU negative G2 phase cells were analyzed. For each individual experiment ≥ 40 cells were analyzed. (A) pRPA foci kinetics in 82-6 hTert and HSC-62 hTert G2 phase cells. Before irradiation, the cells were treated with siCtrl or siRad52. The error bars represent the SEM of the mean values of three experiments. (B) pRPA foci kinetics in HSC-62 hTert G2 phase cells. Before irradiation, the cells were treated with siCtrl or siRad52 and/or siPolθ. The error bars for siCtrl and siRad52 represent the SEM of the mean values of three experiments and for siPolQ and siRad52+siPolQ

represent the SD of the mean values of two experiments. The foci number from unirradiated (0 Gy) samples were subtracted. Statistical significance was tested by Student's T-test (*** = $p < 0.001$, ** = $p < 0.01$, * = $p < 0.05$). The siRNA efficiency for depletion of Rad52 protein was controlled by Western blot.

4.7. Chromosomal studies

4.7.1. Effect of Rad52 on chromosomal rearrangements

As presented in section 3.5., in wild type cells, presence or absence of Rad52 has no effect on the repair of DSBs. However, in a BRCA2-deficient background, availability of Rad52 does make a difference as its presence confers a repair defect, whereas, its absence leads to repair mediated by TMEJ (figure 4.8.b). Furthermore, it has been shown and discussed in many peer reviewed publications that TMEJ-mediated repair gives rise to chromosomal rearrangements and thus causes genomic instability (Ceccaldi, Liu, et al., 2015; Ceccaldi, Rondinelli, & D
Sfeir & Symington, 2015; D. W. Wyatt et al., 2016).Therefore, the effect of presence or absence of Rad52 on chromosomal rearrangements was next investigated. DSBs were induced either by exposure to IR or by treatment with CPT (S phase specific damage).

For this purpose, premature chromosome condensation assay (PCC) was performed. PCC is a widely used method which allows drug-induced premature condensation of interphase chromatin and makes them visible as mitotic chromosomes. Human fibroblast (wt 82-6 and BRCA2 mutant HSC-62) cell lines were used and depleted for Rad52 (siRad52) before 2 Gy irradiation or CPT treatment and harvested 8 – 10 h after irradiation. Calyculin A (50 ng / ml medium) was added to the medium 30 min before harvesting.

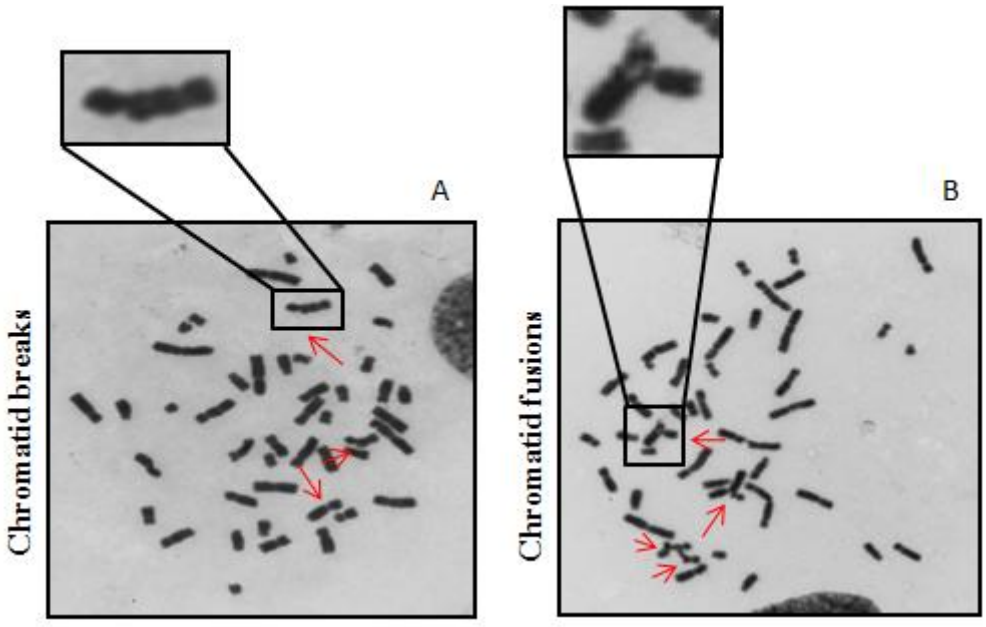

Figure 4.12. **Representative images of Calyculin A-induced G2 phase PCC spreads of 82-6 hTert cells showing chromatid breaks (A) and chromatid fusions (B).** The cells were irradiated with 2 Gy X-rays and harvested at 8 – 10 h post exposure to IR. 30 min prior to harvest, Calyculin A (50 ng / ml) was added to the medium to induce PCC. The cells were treated with 75 mM KCl and fixed with 3:1

methanol – acetic acid solution. Chromosome spreads were prepared by dropping the cells on a microscopic slide and staining the chromosomes with Giemsa stain. The chromosome spreads were scanned and the images were acquired using Metafer software.

Chromatid breaks represent unrepaired breaks, whereas, chromatid fusions represent mis-rejoining of chromosomal ends (chromosomal rearrangement; figure 4.12.a and b). For IR-treatment, in wt 82-6 cells, depletion of Rad52 had no effect on the repair of chromatid breaks as the number of unrepaired breaks at 8h post 2 Gy IR was similar to control-siRNA (siCtrl) treated cells. As expected, siCtrl-treated HSC-62 cells showed higher number of unrepaired chromatid breaks when compared to wt 82-6 cells, displaying a repair defect. Interestingly, this repair defect was rescued upon depletion of Rad52, displayed by similar number of residual chromatid breaks as compared to 82-6 cells (figure 4.13.a). The chromatid break analysis data is in line with the *γ*H2AX foci kinetic data, where a rescue of the BRCA2 repair defect was observed upon depleting Rad52 (figure 4.8.b). More importantly, in HSC-62 cells, a clear increase in the number of chromatid fusions was observed when Rad52 was depleted (figure 4.13.b). Similar results were observed for the cells treated with CPT (figure 4.13.c and d). This indicates that in a BRCA2-deficient background, absence of Rad52 results in a clear increase in chromatid fusions. In other words, the rescue of the BRCA2 repair defect by depleting Rad52 occurs at the cost of chromosomal fusions which are, most likely, the product of TMEJ-mediated repair.

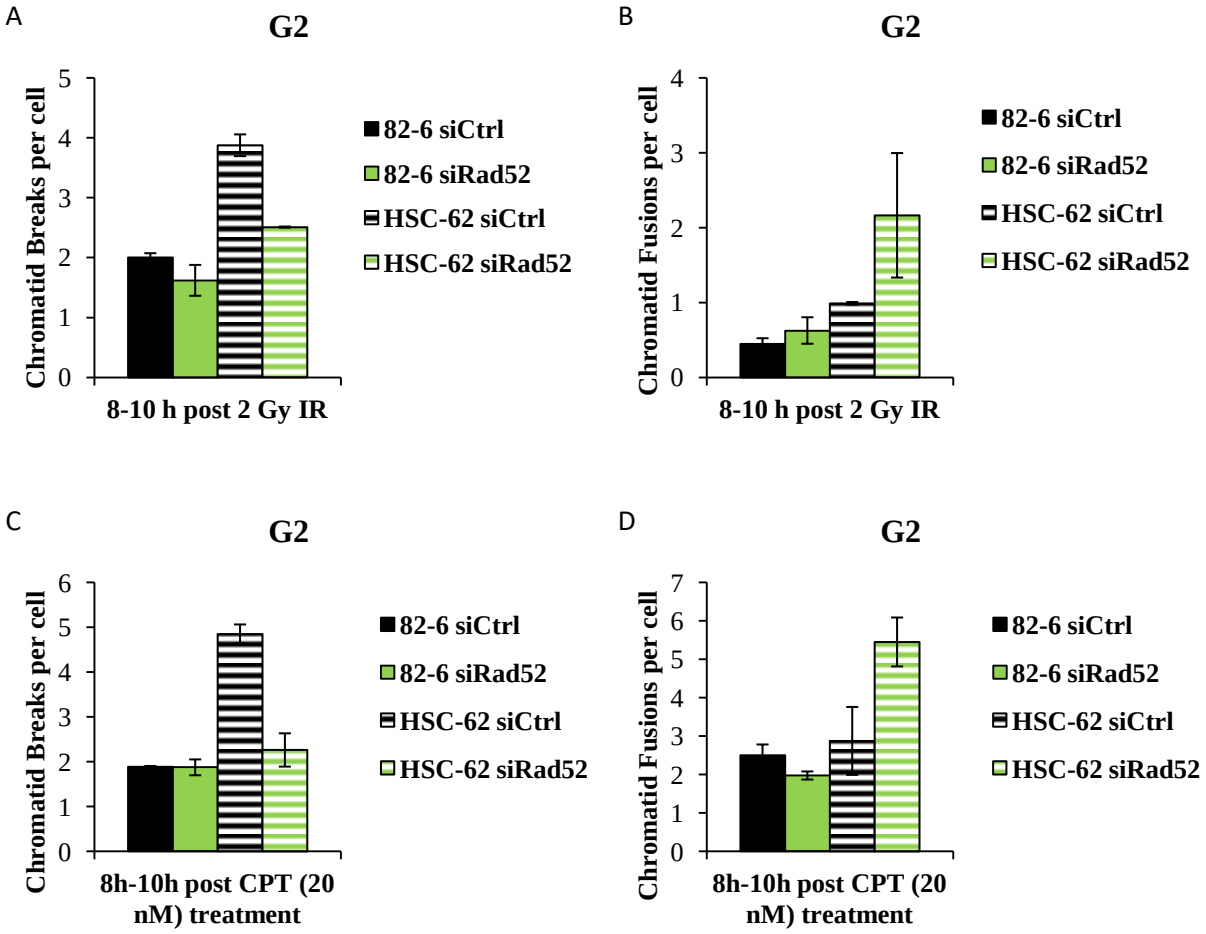

Figure 4.13. **Rescue of the BRCA2 repair defect increases chromosomal fusions**. Prior to exposure to IR or CPT treatment, the cells were treated with siCtrl or siRad52. 30 min prior to harvest, Calyculin A (50 ng / ml) was added to the medium to induce PCC. The cells were then treated with 75 mM KCl and fixed with 3:1 methanol – acetic acid solutionat 8 – 10 h post treatment. Chromosome spreads were prepared by dropping the cells on a microscopic slide and staining the chromosomes with Giemsa stain. The chromosome spreads

were scanned using Metafer software. For each individual experiment ≥ 40 chromosomal spreads were analyzed. (A) The average number of residual chromatid breaks post 2 Gy IR. (B) The average number of residual chromatid fusions post 2 Gy IR. (C) The average number of residual chromatid breaks post CPT treatment. (D) The average number of residual chromatid fusions post CPT treatment. The chromatid break and fusion numbers from unirradiated (0 Gy) samples were subtracted. The error bars represent the SD of the mean values of two experiments. The siRNA efficiency was controlled by Western blot (as shown in figure 4.11).

4.7.2. Effect of Rad52 and Polymerase-theta (Polθ) on chromosomal rearrangements

As learned from DSB repair kinetics data, in BRCA2 deficient cells, depletion of Polθ and Rad52 together does not lead to the activation of TMEJ repair pathway, and as a consequence, does not rescue the BRCA2 repair defect (figure 4.10.d). Hence, the effect of depletion of Polθ and Rad52 on chromosomal rearrangements in BRCA2 proficient and deficient cells was next investigated. To this end, human fibroblast (wt 82-6 and BRCA2 mutant HSC-62) cell lines were used and, prior to irradiation, the cells were depleted for Rad52 or Polθ or both in combination. Following this, PCC assay was performed using Calyculin A and G2 phase chromosome spreads were analyzed for chromatid breaks and fusions.

Similar to the DSB repair kinetic data (figure 4.10.b), no impact of depletion of Polθ or Rad52 or their co-depletion was observed on chromatid breaks or fusions in wt 82-6 cells (figure 4.14.a and b). Showing a repair defect, HSC-62 cells displayed more residual chromatid breaks compared to 82-6 cells and, as expected, this repair defect was rescued upon depletion of Rad52 (figure 4.14.c). Furthermore, co-depletion of Rad52 and Polθ did not lead to the rescue of the repair defect, displayed by a higher number of residual chromatid breaks when compared to Rad52 depleted situation (figure 4.14.c). This data is consistent with the DSB repair kinetic data (figure 4.10.d) and confirms the finding that, in the absence of BRCA2 and Rad52, the rescue of the repair defect is carried out by the Polθ-dependent TMEJ repair pathway.

Figure 4.14.d shows the chromatid fusion data in BRCA2 mutant HSC-62 cells upon depletion of Rad52 or Polθ or both together. As expected, depletion of Rad52 showed increased number of chromatid fusions as compared to siCtrl-treated cells, which is most likely due to the activation of TMEJ repair pathway. Interestingly, depletion of Polθ alone or together with Rad52 gave rise to significantly increased number of chromatid fusions as compared to siCtrl or siRad52-treated HSC-62 cells (figure 4.14.d). This finding was highly surprising because earlier (figure 4.13.b and d) it was observed that the formation of chromatid fusions was Polθ-dependent and, therefore, one might expect the number of chromatid fusions to decrease in the absence of Polθ. Nevertheless, this finding suggests that c-NHEJ might rejoin the chromosomal ends and form chromatid fusions when both the recombination mediated repair pathway – HR (BRCA2) & TMEJ (Polθ) – are unavailable for the cells.

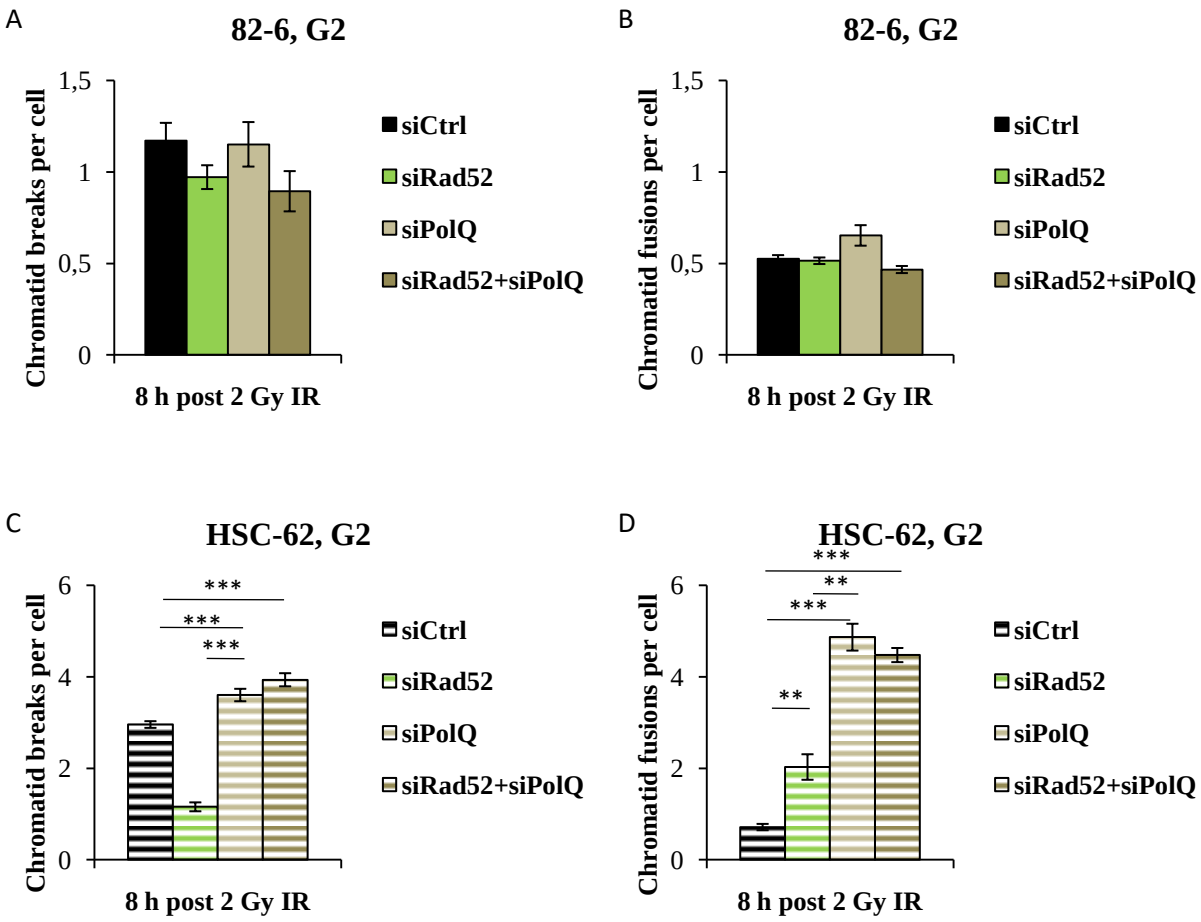

Figure 4.14. **Chromosomal fusions are formed in a Polθ-dependent manner**. Prior to exposure to 2 Gy IR, the cells were treated with siCtrl or siRad52 and/or siPolθ. 30 min prior to harvest, Calyculin A (50 ng / ml) was added to induce G2 phase PCC. The cells were then treated with 75 mM KCl and fixed with 3:1 methanol – acetic acid solution 8h post IR. Chromosome spreads were prepared by dropping the cells on a microscopic slide and staining the chromosomes with Giemsa stain. The chromosome spreads were scanned using Metafer software. For each individual experiment ≥ 40 chromosomal spreads were analyzed. (A) The average number of residual chromatid breaks in 82-6 hTert cells. (B) The average number of residual chromatid fusions in 82-6 hTert cells. (C) The average number of residual chromatid breaks in HSC-62 hTert cells. (D) The average number of residual chromatid fusions in HSC-62 hTert cells. The chromatid break and fusion numbers from unirradiated (0 Gy) samples were subtracted. The error bars represent the SEM of the mean values of three experiments. Statistical significance was tested by Student's T-test (*** = $p < 0.001$, ** = $p < 0.01$).

4.8. Interplay of Rad52, BRCA2 and Polymerase-theta in tumor cells

4.8.1. Impact of Rad52, BRCA2 and Polymerase-theta on DSB repair kinetics in tumor cells

Upon validating the result that, in BRCA2-deficient human fibroblast cell lines, depletion of Rad52 leads to the rescue of the BRCA2 repair defect by Polθ-dependent TMEJ repair pathway at the cost of chromosomal fusions, the impact of these factors (Rad52, BRCA2 &Polθ) on DSB repair kinetic in tumor cells was next investigated. For this purpose, HeLa tumor cells (cervix carcinoma) were used and depleted for Rad52, BRCA2 or Polθ in different combinations and *γ*H2AX foci were quantified.

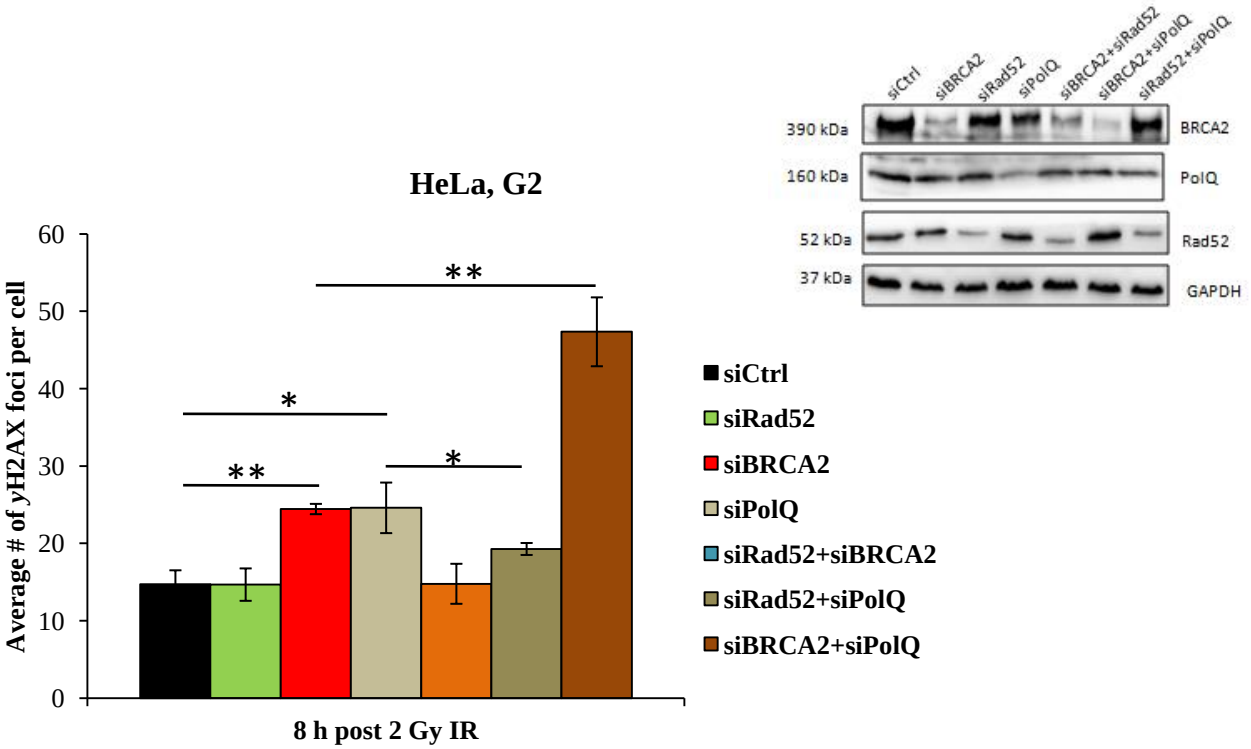

Figure 4.15. **HR and TMEJ are active simultaneously in G2 phase HeLa cells**. HeLa cells were treated with siCtrl, siRad52, siBRCA2 and siPolθ in various combinations before irradiation with 2 Gy X-rays. Only EdU-positive-BrdU-negative G2 phase cells were analyzed. The cells were stained with anti-γH2AX antibodies and DAPI. Samples were scanned using Metafer software. For each individual experiment ≥ 40 cells were analyzed. The foci numbers from unirradiated (0 Gy) samples were subtracted. The error bars represent the SEM of the mean values of three experiments. Statistical significance was tested by Student's T-test (** = $p < 0.01$, * = $p < 0.05$). The siRNA efficiency was controlled by Western blot (performed by Na Wei).

Figure 4.15 represents the average number of unrepaired DSBs (γH2AX foci) in HeLa G2 phase cells. As observed earlier (figure 4.7), in figure 4.15 it can be observed that in G2 phase HeLa cells depletion of Rad52 did not affect repair, depletion of BRCA2 displayed an impaired repair and, co-depletion of Rad52 and BRCA2 rescued the BRCA2 repair defect.

Interestingly, unlike fibroblast cell lines, depletion of Polθ in HeLa cells showed a repair defect in G2 phase cells (8 h post IR) and, moreover, a huge additive repair defect was observed upon co-depletion of BRCA2 and Polθ (figure 4.15). This result suggests that in G2 phase tumor cells, the two resection-dependent pathways (HR & TMEJ) are simultaneously active and, to most of the extent, can compensate for each other. However, even though the two pathways (HR & TMEJ) are available in G2 phase, depletion of a factor from either of the pathways results in a repair defect. Furthermore, an HR repair defect (due to the absence of BRCA2) is indeed rescued by Polθ-dependent TMEJ pathway upon depleting Rad52. This suggests that the presence of Rad52, in BRCA2-deficient tumor cells, makes sure that a "special sub-class" of DSBs (long resected DSBs) which are committed to HR do not undergo repair by the erroneous TMEJ repair pathway.

4.8.2. Impact of Rad52, BRCA2 and Polymerase-theta on chromosomal aberrations

After learning that in tumor cells both HR and TMEJ are distinctively active and that, in case of abrogated HR, presence of Rad52 prevents the repair of HR-committed DSBs by TMEJ repair pathway, the impact of Rad52 and Polθ on chromosomal aberrations in BRCA2 proficient and deficient tumor cells was next investigated. To this end, HeLa cells were used and, prior to irradiation, depleted for Rad52, BRCA2 or Polθ either alone or in combination with each other. Following exposure to 2 Gy IR, Calyculin A-induced PCC assay was performed and only G2 phase chromosome spreads were analyzed for chromatid breaks and fusions.

As observed for primary fibroblast cell lines, in HeLa cells as well, depletion of Rad52 had no effect on the repair of chromatid breaks, whereas, depletion of BRCA2 resulted in a repair defect displayed by an increased number of unrepaired chromatid breaks as compared to siCtrl-treated cells (figure 4.16.a). Indeed, the BRCA2 repair defect was rescued upon co-depletion of Rad52 and BRCA2 (figure 4.16.a). Additionally, it was observed that the rescue of the repair defect (BRCA2+Rad52 depleted situation) occurred at the expense of increased number of chromatid fusions (figure 4.16.b). These results support previous findings from fibroblast cell lines, where it was observed that absence of BRCA2 and Rad52 results in increased number of chromatid fusions, which are most likely the products of the TMEJ repair pathway (figure 4.13.b).

Consistent with the DSB repair (*γ*H2AX foci) kinetics data, depletion of Polθ alone showed a repair defect in G2 phase with increased number of unrepaired chromatid breaks compared to siCtrl-treated cells (figure 4.16.a). Co-depletion of Rad52 and Polθ did not have any additive effect on the number of unrepaired chromatid breaks (figure 4.16.a). Likewise, Rad52-depletion and Rad52+Polθ co-depletion had no impact on chromatid fusion numbers, however, a slight increase in chromatid fusion numbers was observed when Polθ was depleted alone (figure 4.16.b).

Furthermore, co-depletion of BRCA2 and Polθ resulted in an additive repair defect (figure 4.16.a). These results are in line with the *γ*H2AX foci kinetic data, where an additive repair defect was observed upon co-depletion of BRCA2 and Polθ (figure 4.15). Further on, as observed for fibroblast cell lines, co-depletion of BRCA2 and Polθ in Hela cells resulted in a significant increase in the number of chromatid fusions. This result suggests that, in case of impaired HR (BRCA2 deficiency) and TMEJ (Polθ deficiency), DNA break ends are joined and misrepaired leading to formation of chromosomal fusions. It is highly likely that, in this specific scenario (BRCA2+Polθ depletion), c-NHEJ repair pathway might be responsible for giving rise to chromosomal fusions. This finding is consistent with previously published data, where it has been shown that in BRCA2 deficient tumor cells, depletion of Polθ leads to an increase in chromosomal abnormalities in c-NHEJ-dependent manner (Mateos-Gomez et al., 2015).

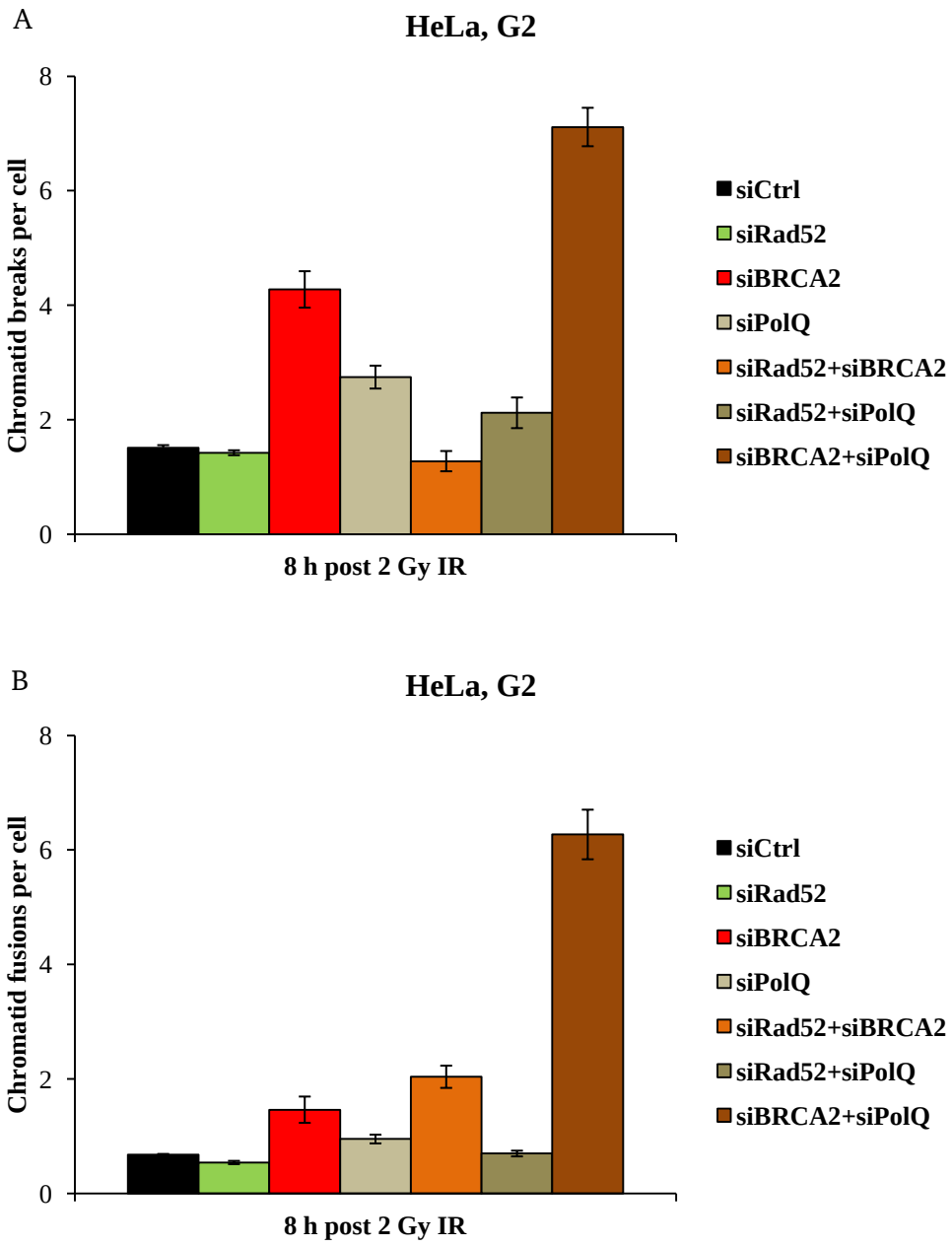

Figure 4.16. **In the absence of HR and TMEJ, c-NHEJ forms chromosomal fusions**. Before irradiation (2 Gy), HeLa cells were treated with siCtrl, siRad52, siBRCA2 and siPolQ in various combinations. 30 min prior to harvest, Calyculin A (50 ng / ml) was added to the medium to induce PCC. The cells were then treated with 75 mM KCl and fixed with 3:1 methanol – acetic acid solution at 8h post IR. Chromosome spreads were prepared by dropping the cells on a microscopic slide and staining the chromosomes with Giemsa stain and were scanned using Metafer software. For each individual experiment ≥ 40 chromosomal spreads were analyzed. (A) The average number of residual chromatid breaks in HeLa cells. (B) The average number of chromatid fusions at in HeLa cells. The error bars represent the SD of the mean values of two experiments. The chromatid break and fusion numbers from unirradiated (0 Gy) samples were subtracted. The siRNA efficiency was controlled by Western blot (shown in figure 4.15).

4.9. DSB repair kinetics in G1 phase cells following IR-treatment in the previous G2 phase

In section 4.8 it was observed that, in HeLa cells, the two resection-dependent pathways (HR & TMEJ) are active simultaneously in G2 phase. Nevertheless, presence of Rad52 in BRCA2-depleted cells prevents the repair of HR-committed breaks by the erroneous TMEJ repair pathway. Next, the effect of Rad52 on the fate of DSBs in BRCA2-proficient and deficient G1 phase cells was investigated. To this end, HeLa cells were used and depleted for Rad52, BRCA2 and Polθ in various combinations. The cells were irradiated in G2 phase and arrested in G2 and the consequent G1 phase. The cell cycle distribution and the position of the cells (G2 or G1 phase) during analysis is shown and explained in the following sections.

4.9.1. Cell cycle distribution

As explained in section 3.2.6, HeLa cells were double-labeled with EdU and BrdU and the G2 phase irradiated cells were arrested in the consequent G1 phase. In brief, the cells were pulse-labeled with EdU for 1 h and stored in an incubator for an additional 1 h. The total time of 2 h allowed a small population of late-S phase-EdU-positive cells to traverse in to G2 phase. Next, the cells were treated with BrdU for 1 h before irradiation and the BrdU was maintained in the medium throughout the repair incubation time. This allowed the S phase cells and the fresh S phase cell population coming from G1 phase to be labeled as either EdU+BrdU-positive or BrdU-positive respectively. By using semi-automated Metafer software, the cells were scanned for EdU and BrdU. Only EdU-positive-BrdU-negative cells (EdU-positive cells irradiated in G2 phase) were gated and analyzed. The cell cycle distribution and the gated cells can be seen in figure 4.17.

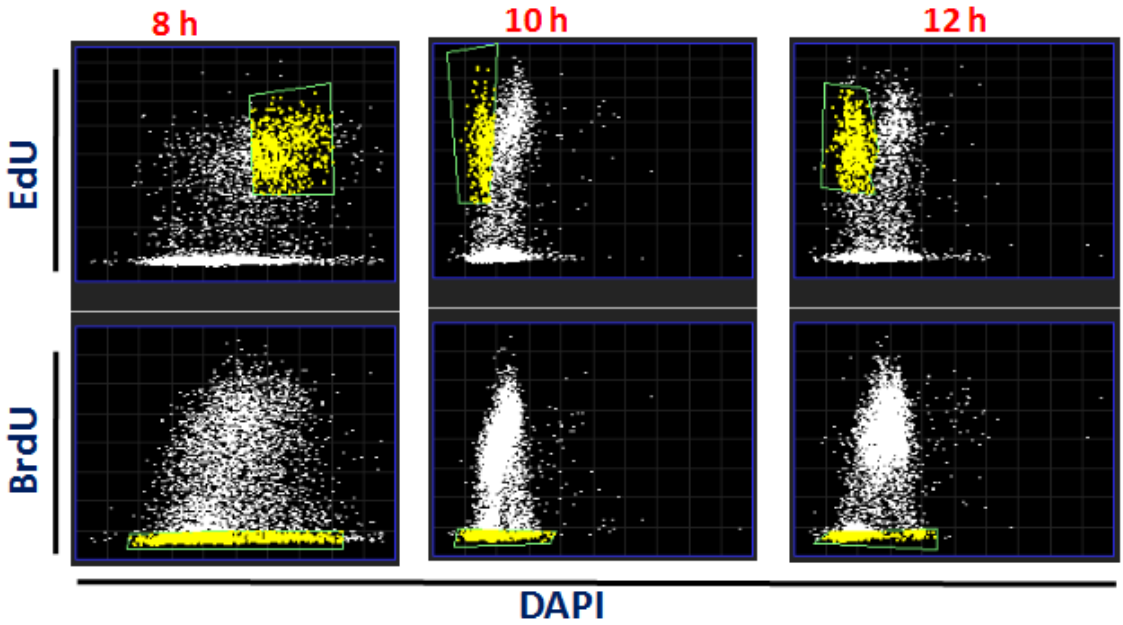

Figure 4.17. **Horse shoe-shaped diagram of EdU vs DAPI and BrdU vs DAPI**. HeLa cells were irradiated with 2 Gy IR, fixed with 2.5% formaldehyde and stained for EdU, BrdU and DAPI. At 10 and 12 h post IR, a small peak of EdU-positive G1 phase cells can be seen.

The exact position of each analyzed cell, present in the gated box, can be seen in figure 4.18.a-c. At 8 h post irradiation, the analyzed EdU-positive cells (shown in red) were in G2 phase, represented as a function of DAPI on the X-axis (figure 4.18.a). Later on, at 10 and 12 h post irradiation, an extra peak of EdU-positive cells was observed as shown in figure 4.17. The exact position of the analyzed EdU-positive cells (shown in red) at 10 and 12 h post irradiation is shown in figure 4.18.b and c, where it can be observed that the analyzed cells were in G1 phase, represented as a function of DAPI on the X-axis.

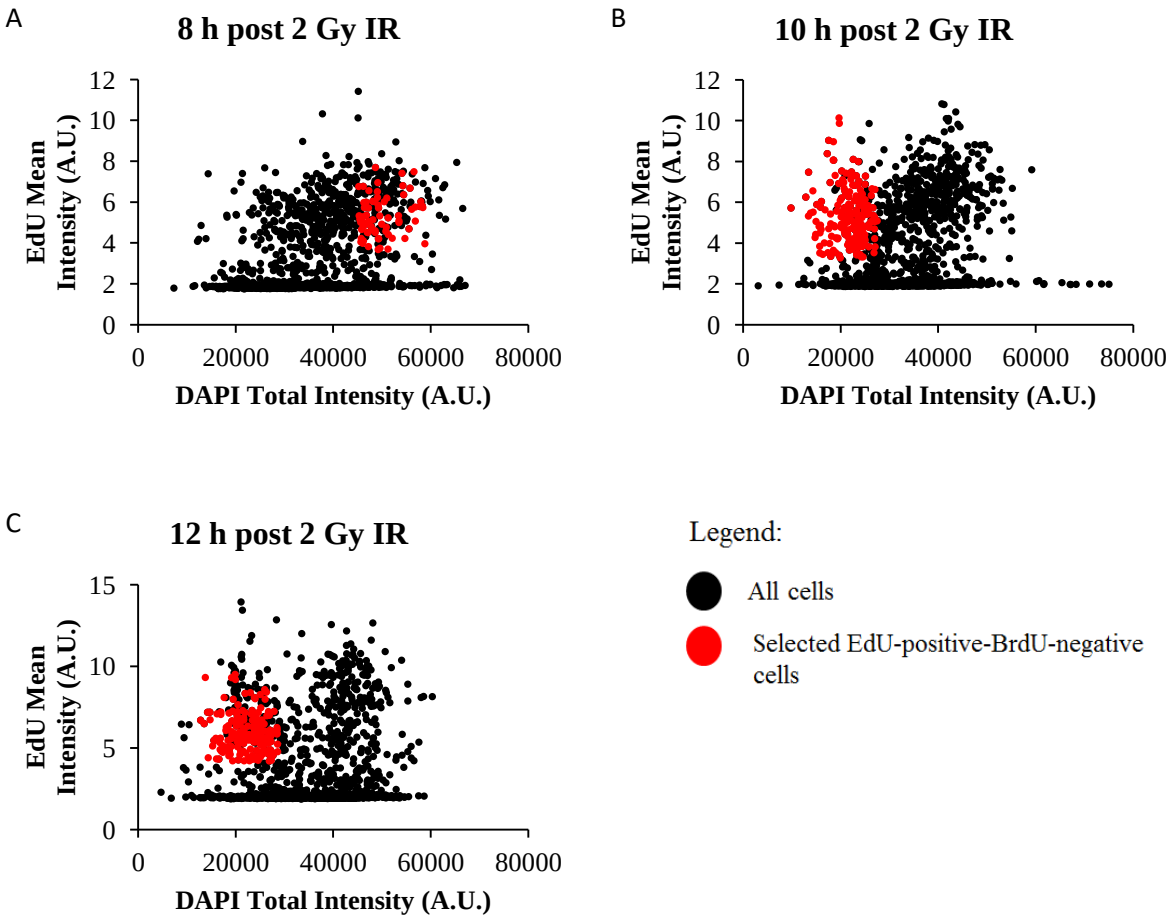

Figure 4.18. **Exact cell cycle phase position of selected EdU-positive-BrdU-negative cells**. The position of analyzed cells (shown in red) at 8 h post IR is in G2 phase, represented as a function of DAPI (A). Similarly, at 10 And 12 h post IR, it can be seen that the analyzed cells were in G1 phase (B and C).

4.9.2. DSB repair kinetics in G2 and consequent G1 phase cells

DSB repair kinetic in G2 phase after depletion of Rad52, BRCA2 and Polθ in various combinations is explained in section 4.8.1. In the consequent G1 phase cells (10 and 12 h post IR), it appears that the number of DSBs (*γ*H2AX foci) in siCtrl-treated cells were divided almost equally in the daughter cells. Like G2 phase cells, depletion of Rad52 did not affect the DSB repair in the G1 phase cells. The repair defect observed in G2 phase cells (8 h post IR) after depletion of BRCA2 was also detectable in the G1 phase cells (10 h post IR). However, as time progressed, the DSBs were repaired and no repair defect was detected for BRCA2-depleted situation at 12 h post IR as the number of residual *γ*H2AX foci was

similar to control cells. This data suggests that, presence of Rad52 in BRCA2-depleted cells prevents the repair of DSBs in G2 phase by erroneous TMEJ pathway and postpones the repair process to the consequent G1 phase, where DSBs can be repaired either by c-NHEJ or by resection-dependent c-NHEJ pathway. The huge additive repair defect observed in G2 phase cells (8 h post IR) due to the BRCA2+Polθ depleted situation was also observed in the consequent G1 phase cells. However, in G1 phase cells, a relatively slow repair of DSBs for BRCA2+Polθ depleted condition was observed.

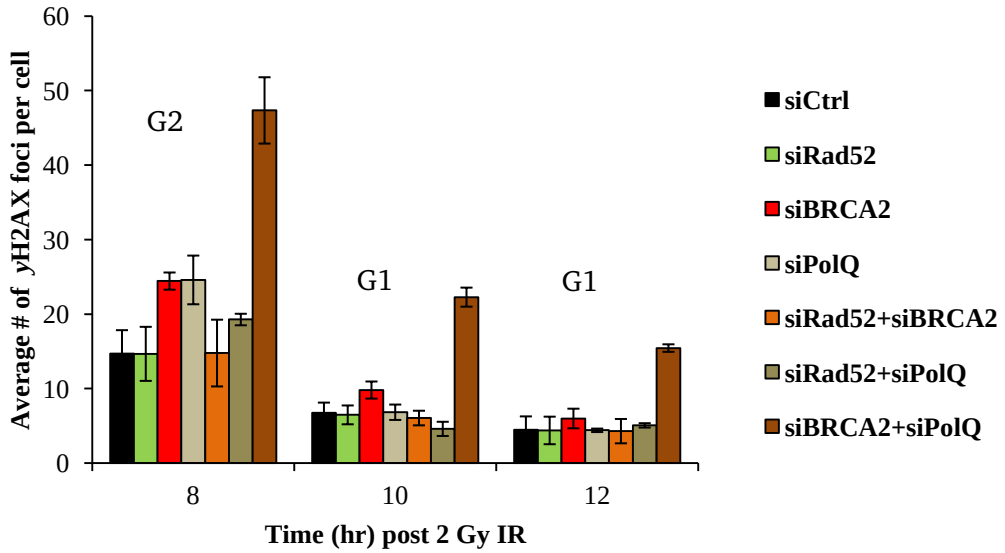

Figure 4.19. ***γ*H2AX foci kinetics in G2 and G1 phase**. The cells were treated with siCtrl, siRad52, siBRCA2 and siPolθ in various combinations. Prior to irradiation (2 Gy X-rays) EdU-BrdU double labeling was performed and only EdU positive G2 and G1 phase cells were analyzed. The cells were stained with anti-*γ*H2AX antibodies and DAPI. Samples were scanned using Metafer software. For each individual experiment ≥ 40 cells were analyzed. The foci numbers from unirradiated (0 Gy) samples were subtracted. The error bars represent the SEM of the mean values of three experiments. The siRNA efficiency was controlled by Western blot (shown in figure 4.15).

5. Discussion

5.1. Homologous Recombination and Rad52

Homologous Recombination is considered as one of the important biological mechanisms because of its active role in maintaining genomic stability and also because of its necessity for the faithful segregation of chromosomes during meiosis (Hanamshet, Mazina, & Mazin, 2016). HR constitutes a key repair pathway dedicated to faithfully repair complex DNA damages and is active mainly in the late S and G2 phases of the cell cycle when a sister chromatid is available as a template to repair DSBs (Heyer et al., 2010). In *S. Cerevisiae*, Rad52 is the key HR player as its inactivation is lethal for cells, whereas, in mammalian cells, loss of Rad52 exhibits normal DNA repair and HR phenotype. Nevertheless, increasing evidences from in vitro studies suggest that, in mammalian cells Rad52 might be involved in HR by mediating the formation of D-loops or by capturing the second end of a resected DSB (Kumar & Gupta, 2004; McIlwraith & West, 2008). As these functions (D-loop formation and second end capture) represent the late steps of HR, in this study also it was observed that the Rad52-GFP foci number in G2 phase HeLa cells showed a slow increase and reached its maximum at late time point (7 h) post exposure to 2 Gy X-rays (figure 1 a) suggesting a function for Rad52 in late steps of HR. On the other hand, the foci kinetic observed for Rad51 was totally opposite to Rad52-GFP foci kinetic with Rad51 foci number reaching their maximum at an early time point (2 h) suggesting an early Rad51 response to IR-induced DNA damage (figure 4.1.a). This finding is in line with earlier published data by Wray et al. (2008) where an early Rad51 response and a late Rad52 response to IR-induced DNA damage has been shown (Manuscript & Stress, 2009). However, in the above-mentioned publication, the authors conclude that Rad51 and Rad52 might be mediating different sub-pathways (DSBR/GC and SDSA, respectively) of HR.

The involvement of Rad52 in HR in mammalian cells was further investigated. HR was abrogated by inhibiting resection and the expression of Rad52-GFP foci in G2 phase cells was analyzed. Resection, the initial step of HR, involves the nucleolytic degradation of 5' DNA end and gives rise to a 3'-ssDNA overhang. This process is known to be initiated by the MRN complex and CtIP together. Mre11, a component of the MRN complex, possesses endo- as well as exo-nuclease activity and its exo-nuclease activity has been shown to commit the repair of DSBs to HR. Therefore, upon inhibition of the exo-nuclease activity of Mre11, no repair defect is observed in G2 phase as the cells still have the possibility to switch to c-NHEJ repair pathway (Shibata et al., 2014). Human CtIP is known to physically and functionally interact with MRN complex to mediate resection in mammalian G2 phase cells (Sartori et al., 2007). To impair resection, the cells were treated with Mirin, which inhibits the Mre11 exonuclease activity, and siCtIP to deplete CtIP. Significantly lower numbers of Rad51 foci were detected after inhibition of resection compared to control cells, indicating an abrogated HR process (figure 4.2.a). Importantly, the involvement of Rad52 in HR was confirmed by observing that inhibition of resection resulted in significantly reduced Rad52-GFP foci in G2 phase HeLa cells (figure 4.2 b).

Furthermore, HR was abrogated at a later step by depleting Rad54 and Rad52-GFP foci in G2 phase cells were analyzed. When Rad54 is depleted, Rad51 cannot be removed from the chromatin and the G2 phase cells are stuck with HR-intermediate structures, such as D-loops. In agreement with this notion, after depletion of Rad54, significantly increased Rad51 foci numbers were observed in G2 phase cells at 7 h post irradiation (figure 4.3.a). Interestingly, under the same conditions (siRad54, 2 Gy, 7 h), the number of Rad52-GFP foci significantly increased as well (figure 4.3.b). Previous work done in our laboratory has shown that Rad52-GFP foci are not only present in G2 phase, but also persist in the next M phase where they colocalize with Mus81 foci. Mus81 is a HR nuclease, which performs processing of HR-intermediate structures (D-loops, Holliday junctions) to finalize HR events. Therefore, it was hypothesized that Rad52 might play a role in keeping the HR-intermediate structures (D-loops, Holliday junctions) intact while the cell traverses from G2 to M phase. The significantly increased number of Rad52–GFP foci detected in the absence of Rad54 (figure 4.3 b) supports this hypothesis. Based on Rad52's activity to bind and wrap around ssDNA (Grimme et al., 2010), it is highly likely that when the cells get stuck with D-loops due to the absence of Rad54, Rad52 can bind to the ssDNA regions within the D-loops to keep these structures intact with the aim to finish repair in the consequent M or G1 phase. These results suggest that Rad52 is involved in the late steps of HR where it might be involved in mediating second end capture or in annealing complementary ssDNA strands post DNA repair synthesis. Additionally, in late G2 phase, Rad52 might also function to provide protection and keep the HR-intermediate structures intact while the cell traverses from G2 to M phase by binding to the ssDNA regions within the intermediate structures.

5.2. Rad52 and BRCA2

To understand the importance of Rad52 in BRCA2 proficient and deficient mammalian cells, both proteins were depleted either alone or in combination and the impact on cell growth was investigated. Additionally, Rad51 was also depleted (with or without Rad52) to understand if the association between Rad52 and Rad51 has any impact on cell growth. Cell proliferation experiments performed in this study showed that the absence of Rad52 had no impact on cell growth (figure 4.4.a and b). Given an important role for Rad51 during HR and in stabilizing stalled replication forks, its inactivation diminished cell growth, whereas, co-depletion of both Rad52 and Rad51 did not show any additive effect (figure 4 a and b). Like Rad51, inactivation of BRCA2 alone also resulted in diminished cell growth (figure 4 c and d). Interestingly, co-depletion of BRCA2 and Rad52 resulted in an additive negative impact and severely hindered cell proliferation (figure 4 c and d). These results are in line with the data published by Feng et al. (2011) and indicate that in the absence of BRCA2, Rad52 becomes indispensable. However, it is still unclear if Rad52 can compensate for the loss of BRCA2 in loading Rad51 in G2 phase cells. Thus, the exact function of Rad52 in the absence of BRCA2 is not yet clearly understood.

To address the aforementioned question, Rad52 and BRCA2 were depleted either alone or together and Rad51 foci were quantified in G2 phase cells. During HR in mammalian cells, BRCA2 interacts with Rad51 through its 8 BRC (Breast Cancer) repeats (Chatterjee et al., 2016) and actively loads Rad51 on the resected 3'-ssDNA. It has been shown that in Capan-1 cells, which do not express

functional BRCA2, very little Rad51 foci are formed in response to IR (Feng et al., 2011). In line with these observations, depletion of BRCA2 resulted in significantly low numbers of Rad51 foci in G2 phase cells (figure 4.5.a), suggesting that Rad52 cannot compensate for the absence of BRCA2 in loading Rad51. Moreover, co-depletion of BRCA2 and Rad52 did not display any additive effect (figure 4.5.a) indicating that the observed decrease in Rad51 foci number is a result of absence of BRCA2, and not Rad52. On the other hand, depletion of Rad52 alone had no impact on the formation of Rad51 foci and they were readily detected in G2 phase cells (figure 4.5.a). Also, there was hardly any co-localization observed between IR-induced Rad52-GFP and Rad51 foci (figure 4.5.b and c). Although human Rad52 contains a Rad51-interacting domain (amino acids 291 – 330), Rad51 foci are readily formed in the absence of Rad52. The interaction between human Rad52 and Rad51 is thought to modulate Rad51's catalytic activities such as homologous pairing and strand exchange. Further on, the Rad51-interacting domain of human Rad52 shows no homology with yeast Rad52 indicating that the interaction between Rad52 and Rad51 is species-specific (Shen et al., 1996). Taken together these results suggest that during HR in mammalian G2 phase cells, Rad52 is not involved in the loading of Rad51 and cannot compensate for the loss of BRCA2. However, Rad52 might interact with Rad51 to modulate its catalytic activity rather than mediating active loading of Rad51 filaments on resected 3'-ssDNA. Due to the synthetic lethality observed upon co-depletion of BRCA2 and Rad52, Rad52's function to mediate an alternative repair pathway was further investigated.

5.3. Interplay of Rad52 and BRCA2

HR is an error-free and a highly conserved mechanism for the repair of DNA DSBs. Moreover, HR plays an important role in restoring replication forks that have stalled or encountered a lesion and thus ensures a successful navigation through S phase. As such, HR is an essential biological mechanism required to maintain genome integrity and its dysfunction leads to diseases, cancer in particular (Negrini, Gorgoulis, & Halazonetis, 2010). One of the key factors of HR is BRCA2 and its importance is underlined by the fact that, individuals with BRCA2-mutations exhibit genomic instability and are predisposed to breast, ovarian and other cancers (Simon A. Gayther, Jonathan Mangion, 1997; Wooster et al., 1995). BRCA2-deficient cells are hypersensitive to genotoxic agents and replication stress (Heyer et al., 2010). Moreover, BRCA2 has been implicated in protecting perturbed replication forks against nucleolytic degradation (Schlacher et al., 2011).

Consolidating the defined functions for BRCA2, in this study it was observed that depletion of BRCA2 resulted in significantly decreased Rad51 foci numbers indicating inefficient Rad51 filament formation on the resected 3'-ssDNA (figure 4.6.a). As a consequence, a repair defect was observed in G2 phase cells displayed by high amounts of *γ*H2AX foci compared to control cells (figure 4.6.b). Interestingly, in comparison to control cells, significantly increased numbers of Rad52-GFP foci were observed in BRCA2 depleted samples (figure 4.6.c). Moreover, at 2 h post irradiation, in BRCA2 depleted samples the average number of Rad52-GFP foci was very similar to the number of Rad51 foci in control samples (figure 4.6.a and c).These results suggest that, when HR is impaired, Rad52 binds to almost all the resected DSBs which were supposed to undergo repair by HR. Previous studies showed that human Rad52 can interact with and bind to RPA. Thus, in the absence of BRCA2, Rad52 and RPA

might form a complex on the resected DNA breaks. However, depletion of both BRCA2 and Rad52 did not result in an additive repair defect (figure 4.7), suggesting that both proteins are involved in the same HR pathway. This suggests that, increased Rad52-GFP foci numbers in a BRCA2-deficient background do not imply activation of a Rad52-mediated alternative repair pathway. Instead, depletion of BRCA2 and Rad52 together resulted in the rescue of the BRCA2 repair defect (figure 4.7). This rescue of the BRCA2 repair defect by additionally depleting Rad52 was observed not only for tumor cells (HeLa, figure 4.7), but also for human fibroblast cell lines (figure 4.8.a and b). Moreover, in addition to G2 phase, rescue of the BRCA2 repair defect by depleting Rad52 was also observed in S phase where HR is most active (figure 4.8 and 4.9.c and d). Like G2 phase, depletion of Rad52 in BRCA2-proficient cells did not induce any DSB repair defect in S phase (figure 4.9.a and b). Recently, Sotiriou et al. (2016) showed that, in S phase, Rad52 promotes BIR repair pathway and facilitates restart of collapsed replication forks (Sotiriou et al., 2016). Additionally, they showed that, at 24 h after treatment with hydroxyurea (HU), *γ*H2AX phosphorylation levels increased much strongly in cells depleted for Rad52. In this study, however, no repair defect was observed in S phase after depleting Rad52.

Additionally, by scoring the number of unrepaired chromatid breaks in G2 phase (figure 4.13.a and c), the rescue of the BRCA2 repair defect after depleting Rad52 was further verified. In context of HR, these results suggest that in BRCA2-deficient cells, rather than mediating an alternative repair pathway, Rad52 accumulates on resected DSBs and prevents other, perhaps erroneous, repair pathways from acting upon the resected DNA breaks. Importantly, depletion of Rad52 in BRCA2-deficient cells results in the repair of DSBs by a pathway which acts independently of both BRCA2 and Rad52. Hence, this repair pathway was characterized next.

5.4. Contribution and fidelity of theta-mediated end joining repair pathway

5.4.1. Contribution of TMEJ

As mentioned in section 5.3, depletion of Rad52 in BRCA2-deficient cells resulted in the repair of DSBs by a pathway which acts independently of both BRCA2 and Rad52. As the absence of BRCA2 or Rad52 does not hinder the process of end resection and given that TMEJ and HR share the initial step of end resection, the contribution of TMEJ in BRCA2 and Rad52 deficient cells to repair DSBs was further investigated. By scoring the number of *γ*H2AX foci in G2 phase, it was observed that in BRCA2 deficient cells, depletion of Rad52 resulted in an efficient repair of DSBs and the BRCA2 repair defect was rescued. Importantly, when factors of TMEJ repair pathway (PARP or Polθ) were additionally inactivated along with Rad52, no rescue of the BRCA2 repair defect was observed, displayed by substantially higher amounts of *γ*H2AX foci compared to wild-type cells (figure 4.10.c and d). Furthermore, similar result was observed upon scoring the number of unrepaired chromatid breaks in G2 phase (figure 4.14.c). These results indicate that, in the absence of BRCA2 and Rad52, the resected DSBs are repaired by a PARP and Polθ-dependent pathway. Thus, due to the loss of BRCA2 and Rad52, the repair of the resected DSBs is channeled to TMEJ.

In support of the finding that Polθ-dependent TMEJ repair pathway rescues the BRCA2 repair defect, additional work from the group of Prof. Löbrich has shown that c-NHEJ repair pathway is not responsible for the rescue process. Experiments performed with c-NHEJ-deficient cell line have shown that the rescue of the BRCA2 repair defect takes place independent of c-NHEJ pathway (figure 5.1.a and b). By scoring *γ*H2AX foci a repair defect was observed in siCtrl-treated XLF-deficient hTert cells in comparison to wt 82-6 hTert cells at 8 h post IR (figure 5.1.a). By depleting BRCA2 in XLF-deficient cells, an additive repair defect was observed and, importantly, the additive repair defect was rescued when Rad52 was additionally depleted (figure 5.1.a). Further on, in HeLa cells, rescue of the BRCA2 repair defect was still observed when Ligase IV, a c-NHEJ factor, was depleted (figure 5.1.b). Therefore, these results further validate and support the notion that the rescue of the HR defect in G2 phase is a c-NHEJ-independent and TMEJ-dependent process.

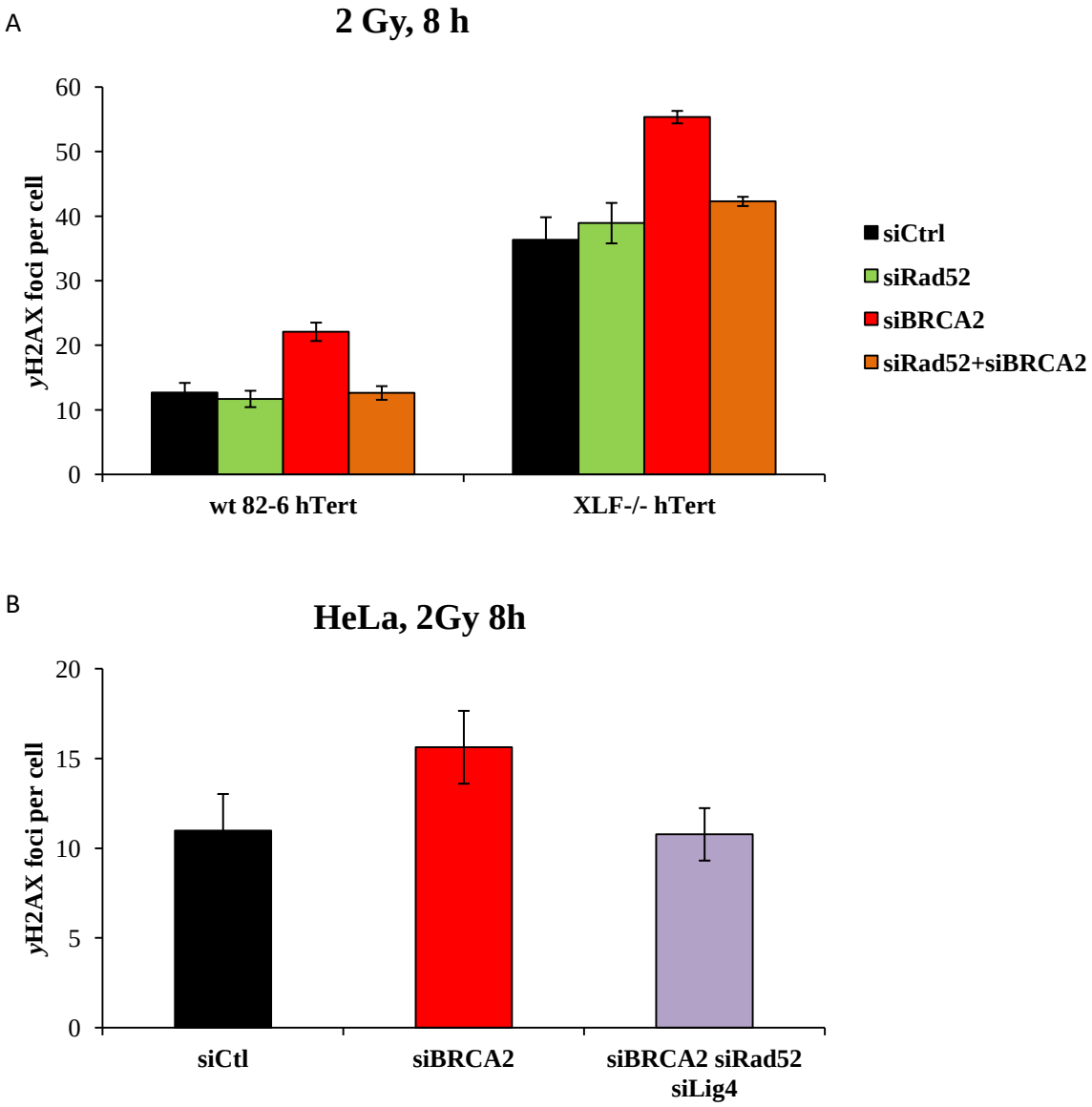

Figure 5.1. **Rescue of the BRCA2 repair defect in c-NHEJ-independent process**. 30 min prior to irradiation (2 Gy X-rays) HeLa cells were treated with EdU to label and exclude S phase cells from analysis. The cells were stained with anti-*γ*H2AX antibodies and DAPI. Samples were scanned using Metafer software. For each individual experiment ≥ 40 cells were analyzed. (A) yH2AX foci quantification

in G2 phase wt 82-6 and XLF-deficient hTert cell lines. Before irradiation, the cells were treated with siRad52 and/or siBRCA2. Additionally, the cells were treated with a control siRNA. (B) yH2AX foci quantification in G2 phase HeLa cells. Before irradiation, the cells were treated with siBRCA2 or siBRCA2+siRad52+siLigIV.The foci numbers from unirradiated (0 Gy) samples were subtracted. The error bars represent the SEM of the mean values of three experiments. Experiments were performed by Marta Llorens Agost.

It has been demonstrated that TMEJ is limited by RPA bound to ssDNA. Resection of DSB ends reveals microhomologies present internal to the break ends, however, these microhomologies are not accessible to the TMEJ machinery due to the presence of RPA. Only after the removal of RPA are these microhomologies exposed and made available to the TMEJ machinery to continue repair (Deng et al., 2014).

To further consolidate the contribution of TMEJ to repair DSBs in the absence of BRCA2 and Rad52, pRPA foci were quantified in G2 phase fibroblast cells. In comparison to WT 82-6 cells, BRCA2-deficient HSC-62 cells showed higher amounts of pRPA foci at 2 and 6 h post IR, representing a BRCA2 defect (figure 4.11.a). Interestingly, a significant decrease in the pRPA foci numbers was observed upon depleting Rad52 in HSC-62 cells (figure 4.11.a), indicating that less RPA is bound to ssDNA, thereby making the microhomologies available to the TMEJ machinery. Furthermore, in HSC-62 cells, upon additional depletion of Polθ together with Rad52, no decrease in pRPA foci numbers was observed (figure 4.11.b). This suggests that, in the absence of Polθ, RPA cannot be removed from the 3'-ssDNA overhang and TMEJ cannot be activated. These results, however, do not clearly explain if Polθ is actively involved in the removal of RPA from ssDNA to initiate repair by TMEJ pathway, or if RPA is removed by some other factors to activate repair by TMEJ. Nevertheless, these results suggest that, in cells deficient for BRCA2 and Rad52, less RPA is bound to the 3'-ssDNA overhang which facilitates repair by TMEJ.

5.4.2. Fidelity of TMEJ

TMEJ is a mutagenic repair pathway with potentially harmful consequences on genome integrity. It has been shown that TMEJ can result in the joining of different chromosomes, thereby generating chromosomal translocations and mutagenic rearrangements. In c-NHEJ deficient cells, increased amounts of chromosomal translocations have been observed, suggesting a role for TMEJ in giving rise to these translocation events. Furthermore, it recently became evident that TMEJ is triggered upon telomere de-protection to promote Polθ-dependent formation of chromosome end-to-end fusions (Ceccaldi, Rondinelli, et al., 2015; Mateos-Gomez et al., 2015).

In section 5.4.1 it was established that DSB repair in BRCA2 and Rad52-deficient cells is PARP and Polθ dependent. Next, the fidelity of the TMEJ repair pathway was examined. In G2 phase, after depletion of Rad52 in BRCA2-deficient cells, a substantial increase in the number of chromosomal fusions was observed (figure 4.13.b). The amount of chromosomal fusions was even higher when the cells were additionally treated with CPT to induce damages in S phase where HR is most active (figure 4.13.d). These results are consistent with the data published by Feng et al. (2011) where they showed that the absence of both BRCA2 and Rad52 results in extensive chromatid-type aberrations (Feng et

al., 2011). The high amounts of chromosomal fusions observed can be highly detrimental for cells and, thereby, might explain the reason why loss of BRCA2 and Rad52 is lethal for cells. Thus, presence of Rad52 in BRCA2 deficient cells prevents repair by the mutagenic TMEJ pathway and suppresses chromosomal aberrations and thus plays an important role in the survival of these cells. Consistent with this function of Rad52, a similar function to suppress TMEJ has also been shown for other HR factors – such as, BRCA2, BRCA1 and RPA. By using a sensitive HPRT assay to monitor DSB mis-repair, it was found that depletion of these HR proteins results in distinct mutational signatures associated with deletions and annealing of short regions of microhomologies. Furthermore, it was shown that these mutational signatures were PARP and Polθ-dependent and thus indicative of TMEJ (Ahrabi et al., 2016).

5.5. Distinct impacts of TMEJ in human fibroblast vs cancer cell lines

In this study, the impact of TMEJ on DSB repair and chromosomal aberrations and the function of Rad52 to suppress these mechanisms in human cancer cell lines was investigated. By scoring *γ*H2AX foci in G2 phase HeLa cells (cell line derived from epithelial cervical cancer), it was observed that BRCA2-depletion resulted in a repair defect, while additional depletion of Rad52 rescued the BRCA2 repair defect (figure 4.15). Importantly, an increased number of chromosomal fusions were observed under these conditions (figure 4.16.b). Hence, like fibroblast cells, Rad52's function to prevent formation of chromosomal fusions in HeLa cells was consolidated. However, depletion of Polθ in HeLa cells resulted in different consequences as compared to fibroblast cells and these differences are discussed in the following paragraph.

As mentioned earlier, in fibroblast cell lines, Polθ-dependent TMEJ repair pathway was activated only in the absence of BRCA2 and Rad52. Further on, no repair defect was observed in G2 phase after Polθ depletion in WT 82-6 or BRCA2-deficient HSC-62 fibroblast cells (figures 4.10.b and d). To our surprise, unlike fibroblast cell lines, single depletion of Polθ resulted in a repair defect in G2 phase HeLa cells at 8 h post IR (figure 4.15). Furthermore, a huge additive repair defect was observed upon co-depletion of BRCA2 and Polθ in HeLa cells, showing that these two factors are not epistatic (figure 4.15). These results indicate that in HeLa cells, BRCA2-dependent HR and Polθ-dependent TMEJ are active simultaneously. This implies that, in comparison to fibroblast cell lines, cancer cells deploy both resection-dependent pathways (HR and TMEJ) to repair DSBs. Although TMEJ is active alongside HR in HeLa cells, a repair defect is observed by depleting BRCA2 which is rescued upon depletion of Rad52. This observation raises the question, what makes a sub-class of HR-committed breaks so special that, in case of impaired HR, Rad52 prevents the repair of these DSBs by TMEJ.

As discussed earlier, HR and TMEJ share the initial step of DSB end resection and diverge post resection (Truong et al., 2013). Therefore, it is likely that end resection dictates repair pathway choice. It has been shown that the first phase of resection, called end clipping, is carried out by the structure-specific nucleases Mre11 and CtIP and relatively small number of base pairs are processed (i.e., 20 bp in mammalian cells or 100-300 bp in yeast). This makes the DNA ends available for joining by TMEJ (Huertas & Jackson, 2009; Truong et al., 2013). In the second phase of end resection, called extensive

resection, helicases and exonucleases (DNA2, BLM, WRN and EXO1) generate long stretches of ssDNA, thereby committing the cells to HR (Sturzenegger et al., 2014; Symington & Gautier, 2011). It is possible that repair of extensively resected DSBs by TMEJ can result in large deletions and other chromosomal aberrations. Therefore, it is likely that in case of impaired HR in HeLa cells, Rad52 binds to a sub-class of DSBs which underwent extensive resection and generated long stretches of 3'-ssDNA overhangs. As Rad52 can interact with and bind to RPA, it is possible that Rad52 and RPA form a complex on these long stretches of 3'-ssDNA overhangs. This Rad52-RPA complex prevents repair by TMEJ at these HR-committed breaks and consequently avoids formation of chromosomal fusions, which can be lethal for cells. A hypothesized model, explaining the function of Rad52 in G2 phase HeLa cells, is shown in figure 5.2.

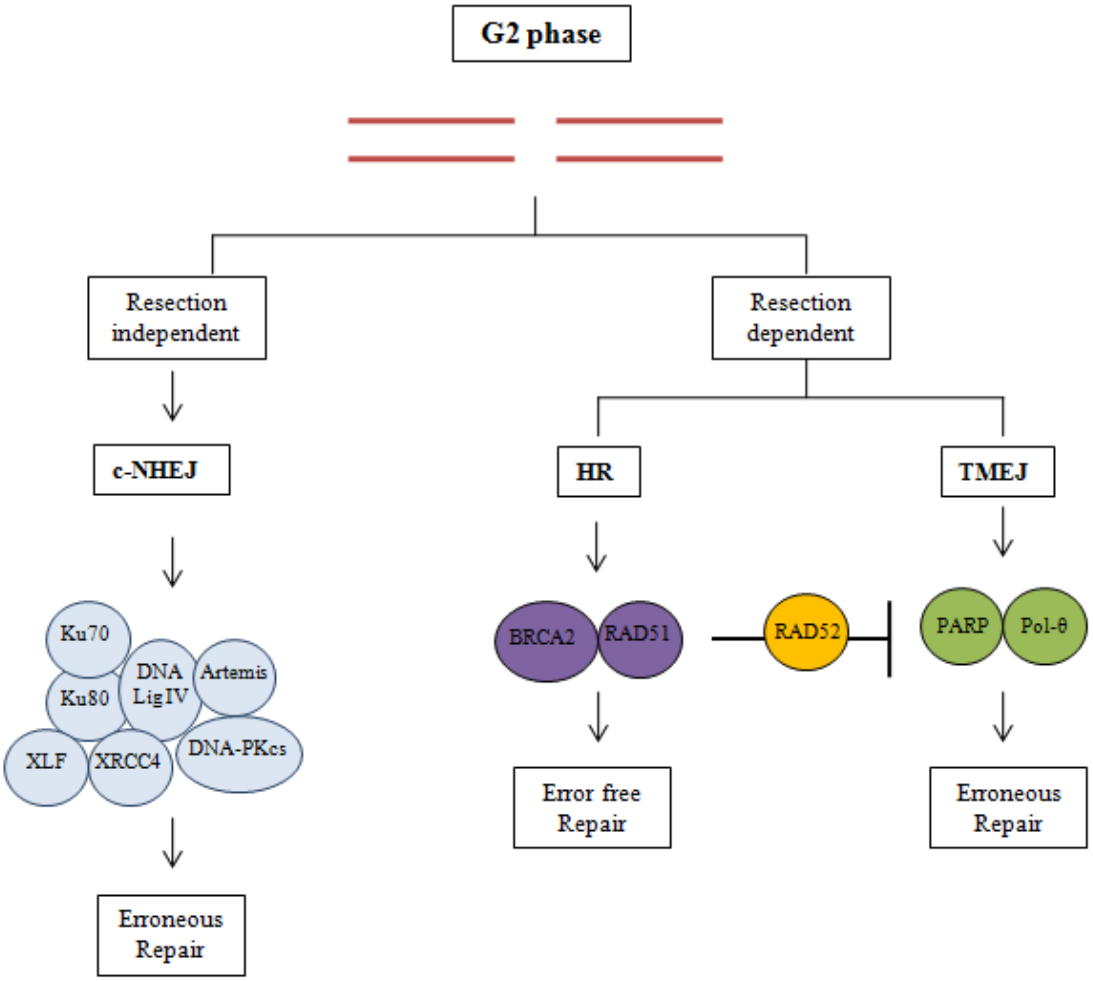

Figure 5.2. **Speculative model for the function of Rad52**. Depending on the extent of resection, in G2 phase mammalian cancer cells, extensively resected DSBs undergo repair by HR, whereas, shortly resected DSBs can be repaired by TMEJ. In case of impaired HR, Rad52 binds to the long stretches of 3'-ssDNA overhangs and prevent their repair by the erroneous TMEJ pathway. Activation of TMEJ pathway in the absence of BRCA2 and Rad52 results in the formation of chromosomal fusions. Thus, by inhibiting TMEJ and preventing the formation of chromosomal fusions, Rad52 maintains genomic stability in BRCA2-deficient cells.

By using EdU-BrdU double labeling, damage-induced G2 phase cells were analyzed in the consequent G1 phase and DSB repair kinetic was performed. It was observed that the repair defect, incurred in G2

phase (8 h post IR) due to the absence of BRCA2, was absent in the consequent G1 phase, indicating ongoing repair in G1 phase (figure 4.19). This data suggests that, in BRCA2 deficient G2 phase cells, Rad52 prevents the repair by TMEJ (an erroneous pathway) and postpones the repair to the next G1 phase. A huge repair defect was still detectable in G1 phase for BRCA2 and Polθ depleted situation and the DSBs were repaired relatively slowly. However, more control experiments are needed to be performed to confirm and validate the results obtained from G1 phase cells.

5.6. Chromosomal analysis in HeLa cells

Genomic instability refers to an increased tendency of alterations in the genome during the life cycle of cells. It is one of the hallmarks of cancer and is present in all stages of cancer, from initiation to advanced cancer (Nowell, 1950). Recently it became evident that the HR-deficient tumors are dependent on Polθ-mediated repair and, moreover, a synthetically lethal relationship between HR and Polθ-mediated repair has been revealed (Ceccaldi, Liu, et al., 2015). Additionally, it has been shown that HR-deficient tumor cells (U2OS) expressing high levels of Polθ, harbor more somatic point mutations compared to tumors with lower Polθ levels (Alexandrov et al., 2013). These results suggest that Polθ contributes to a certain extent in maintaining genomic instability in HR-deficient tumors.

Chromosomal analysis in G2 phase HeLa cells showed that the rescue of the BRCA2 repair defect by depleting Rad52 occurred at the cost of chromosomal fusions (figure 4.16.a and b). Thus, Rad52's function to prevent chromosomal fusions was observed in HeLa cells. Further on, consistent with the *γ*H2AX foci data, depletion of Polθ or BRCA2 showed higher numbers of unrepaired chromatid breaks compared to the siCtrl-treated cells (figure 4.16.a). However, no substantial increase in chromosomal fusions was observed after depleting Polθ or BRCA2 (figure 4.16.b). Importantly, co-depletion of BRCA2 and Polθ resulted in significantly higher number of chromatid breaks and fusions (figure 4.16.a and b). This observation confirms the earlier finding that HR and TMEJ both are simultaneously active in the G2 phase HeLa cells. In line with this notion, increasing evidence suggest that TMEJ is an important repair pathway in cancer cells. It has been shown that HR-deficient tumors rely heavily on Polθ-mediated repair for their survival. Additionally, it was shown that inactivation of Polθ in Fancd2-deficient (an HR gene) cells increased cell killing (Ceccaldi, Liu, et al., 2015). Furthermore, a substantial increase in chromosomal aberrations was observed after inactivation of Polθ in BRCA2 mutant cells (Mateos-Gomez et al., 2015). The increased numbers of chromosomal fusions observed in BRCA2+Polθ depleted cells suggest that, in the absence of HR and TMEJ, c-NHEJ can mis-rejoin DSBs and induce chromosomal fusions. Consistent with this finding Mateos-Gomez et al. (2015) showed that, inhibition of Polθ in BRCA-mutant cells leads to increased chromosomal aberrancies, especially radial chromosomal structures which are characteristic of Lig4-mediated processing via the c-NHEJ pathway (Mateos-Gomez et al., 2015).

Taken together, the results obtained in this study provide a novel insight to understand the role of Rad52 in the absence of BRCA2 in mammalian cells. Rad52 plays an important role in the survival of BRCA2-mutant cells by avoiding chromosomal fusions. This makes Rad52 a potential drug target to specifically kill BRCA2-mutant tumors without any adverse effects on healthy cells and tissue. As loss

of Polθ in BRCA2-deficient cells is also detrimental, inactivation of both Rad52 and Polθ in BRCA2-mutant tumors might provide an alternative strategy to treat cancer.

5.7. Outlook

Rad52 is an evolutionary conserved protein. In *S. Cerevisiae*, Rad52 is the key player of HR-mediated DNA repair and other recombination events. Importantly, absence of Rad52 in *S. Cerevisiae* is lethal. On the contrary, in mammalian cells, inactivation of Rad52 has no significant effect on HR or DNA repair in general. Recent studies have shown that, in BRCA-deficient mammalian cells, Rad52 is an indispensable factor and its presence renders viability to the cells. Furthermore, loss of Rad52 in BRCA-deficient cells is synthetically lethal. However, the exact functions of Rad52 which render viability to BRCA-deficient cells are yet unknown.

In this study, it was shown that in HeLa cells, Rad52-GFP foci peak at late times (8 h) in G2 phase after exposure to IR and persist in the consequent M phase, indicating a function for Rad52 at the late steps of HR. Importantly, it was shown for the first time that in G2 phase of BRCA2-depleted HeLa cells, significantly increased numbers of Rad52-GFP foci are present at early time point (2 h) after IR, suggesting that Rad52 binds to the resected break ends. Furthermore, it was observed that depletion of Rad52 in BRCA2-deficient cells rescued the BRCA2 repair defect in a TMEJ-dependent manner. Moreover, the rescue process mediated by TMEJ-repair pathway gave rise to chromosomal fusions, thereby compromising genomic stability. Thus, it was shown that, in G2 phase, Rad52 prevents the formation of chromosomal fusions and helps to maintain genomic stability.

In response to IR, unlike other HR factors (Rad51 and Rad54), Rad52-GFP foci are present in M phase. Moreover, in M phase, Mus81 foci are present along with Rad52-GFP foci. This data indicates that Rad52 might be mediating the Mus81-Eme1 complex-dependent resolution pathway to process the DHJs. In vitro experiments have shown that Rad52 captures the second-end of DSBs and, thus, helps in the formation of HR-intermediate structures (DHJs) (Nimonkar, Sica, & Kowalczykowski, 2009). Therefore, analysis of M phase cells will be helpful in understanding if Rad52 mediates formation or processing of DHJs. Furthermore, sister chromatid exchange analysis can provide additional information regarding the function of Rad52 in the formation of cross-over products.

By detecting the formation of EdU foci in M phase, Bhowmick et al. (2016) showed that mitotic DNA synthesis (MiDAS) takes place in a Rad52-dependent manner. Importantly, this function of Rad52 is independent of Rad51 and BRCA2. Furthermore, they showed that no DNA synthesis occurs in M phase in the absence of Rad52 and this gives rise to increased numbers of 53BP1 nuclear bodies in the consequent G1 phase (Bhowmick, Minocherhomji, & Hickson, 2016). In this publication, however, DNA damage originates from S phase at common fragile site (CFS) loci which, upon inducing replication stress, appear as DAPI-negative gaps on metaphase chromosomes. Therefore, it is highly interesting to investigate if Rad52 can promote repair of DSBs induced in G2 phase by mediating MiDAS, especially in HR-defective cells. This information is important and can help to understand how

HR-defective cancer cells repair endogenous DSBs and maintain their genomic stability when an error-free repair pathway in unavailable.

In addition to M phase, the function of Rad52 in S phase to repair one-ended DSBs is not yet fully understood. Recently, Sotiriou et al. (2016) showed that, in S phase, Rad52 mediates the strand invasion step to promote break-induced replication repair (BIR) and, thus, facilitates restart and repair of collapsed replication forks in cancer cells (Sotiriou et al., 2016). However, like Rad51, a recombinase activity for Rad52 has not yet been described. Biochemical analysis of Rad52 protein can provide important insight to understand Rad52's function of strand invasion. Furthermore, it would be interesting to understand if, in HR-defective cells, Rad52 can promote strand invasion in G2 phase and, thereby, facilitate MiDAS to repair IR-induced DSBs.

Recently, a direct role of RNA in the repair of DSBs has been revealed (Keskin et al., 2014). Interestingly, Mazina et al. (2017) showed that, in eukaryotes, inverse strand exchange between homologous dsDNA and RNA is a distinct activity of Rad52 (Mazina et al., 2017). In addition, recent investigations from the group of Prof. Löbrich have revealed that, in response to IR, RNA-DNA hybrids are formed that are involved in DSB repair by mediating resection and consequent formation of pRPA foci in G1 phase mouse embryonic stem cells (mESCs) (Dissertation, Amir Mofidi, 2017). Therefore, it would be highly interesting to understand if Rad52 is involved in the formation of RNA-DNA hybrids and, thus, plays a role in RNA-mediated DSB repair. This information will also be helpful to understand the repair of DSBs in G1 phase where limited end resection of DSBs has been shown (Biehs et al., 2017).

In this study, it was shown that the absence of Rad52 in BRCA2-deficient cells leads to the formation of chromosomal fusions and severely hinders cell growth. Consistent with these findings, other studies have shown that inactivation of Rad52 in BRCA2-deficient cells induces chromosomal aberrations and is synthetically lethal (Feng et al., 2011). In recent years, the synthetic lethal relationship between Rad52 and BRCA2 has been exploited to selectively kill BRCA-deficient cancer cells (Chandramouly et al., 2015; Huang et al., 2016). In context to cancer therapy, screening of inhibitors to disrupt the activity of Rad52 is highly important as this strategy holds a lot of potential to specifically treat BRCA-deficient cancers.

6. References

Adzuma, K., Ogawa, T., & Ogawa, H. (1984). Primary structure of the RAD52 gene in Saccharomyces cerevisiae. *Molecular and Cellular Biology*, *4*(12), 2735–2744.

Ahrabi, S., Sarkar, S., Pfister, S. X., Pirovano, G., Higgins, G. S., Porter, A. C. G., & Humphrey, T. C. (2016). A role for human homologous recombination factors in suppressing microhomology-mediated end joining. *Nucleic Acids Research*, gkw326. http://doi.org/10.1093/nar/gkw326

Alexandrov, L. B., Nik-Zainal, S., Wedge, D. C., Aparicio, S. A. J. R., Behjati, S., Biankin, A. V., … Stratton, M. R. (2013). Signatures of mutational processes in human cancer. *Nature*, *500*(7463), 415–421. http://doi.org/10.1038/nature12477

Audebert, M., Salles, B., & Calsou, P. (2008). Effect of double-strand break DNA sequence on the PARP-1 NHEJ pathway. *Biochemical and Biophysical Research Communications*, *369*(3), 982–988. http://doi.org/10.1016/j.bbrc.2007.11.132

Baumann, P., Benson, F. E., & West, S. C. (1996). Human Rad51 protein promotes ATP-dependent homologous pairing and strand transfer reactions in vitro. *Cell*, *87*(4), 757–766. http://doi.org/10.1016/S0092-8674(00)81394-X

Baumann, P., & West, S. C. (1998). Role of the human RAD51 protein in homologous recombination and double-stranded-break repair. *Trends in Biochemical Sciences*, *23*(7), 247–251. http://doi.org/10.1016/S0968-0004(98)01232-8

Bellini, A., Girard, P.-M., Lambert, S., Tessier, L., Sage, E., & Francesconi, S. (2012). Stress activated protein kinase pathway modulates homologous recombination in fission yeast. *PloS One*, *7*(10), e47987. http://doi.org/10.1371/journal.pone.0047987

Bezzubova, O. Y., Schmidt, H., Ostermann, K., Heyer, W. dietrich, & Buerstedde, J. marie. (1993). Identification of a chicken RAD52 homologue suggests conservation of the RAD52 recombination pathway throughout the evolution of higher eukaryotes. *Nucleic Acids Research*, *21*(25), 5945–5949. http://doi.org/10.1093/nar/21.25.5945

Bhowmick, R., Minocherhomji, S., & Hickson, I. D. (2016). RAD52 Facilitates Mitotic DNA Synthesis Following Replication Stress. *Molecular Cell*, *64*(6), 1117–1126. http://doi.org/10.1016/j.molcel.2016.10.037

Biehs, R., Shibata, A., Steinlage, M., Barton, O., Juhász, S., Künzel, J., … Löbrich, M. (2017). DNA Double-Strand Break Resection Occurs during Non-homologous End Joining in G1 but Is Distinct from Resection during Homologous Recombination. *Molecular Cell*, *65*(4), 671–684.e5. http://doi.org/10.1016/j.molcel.2016.12.016

Binz, S. K., Sheehan, A. M., & Wold, M. S. (2004). Replication Protein A phosphorylation and the cellular response to DNA damage. *DNA Repair*, *3*(8–9), 1015–1024. http://doi.org/10.1016/j.dnarep.2004.03.028

Ceccaldi, R., Liu, J. C., Amunugama, R., Hajdu, I., Primack, B., Petalcorin, M. I. R., … D'Andrea, A. D. (2015). Homologous-recombination-deficient tumours are dependent on Polθ-mediated repair. *Nature*, *518*(7538), 258–262. http://doi.org/10.1038/nature14184

Ceccaldi, R., Rondinelli, B., & D'Andrea, A. D. (2015). Repair Pathway Choices and Consequences at the Double-Strand Break. *Trends in Cell Biology*, *26*(1), 52–64. http://doi.org/10.1016/j.tcb.2015.07.009

Cells, H., Costantino, L., Sotiriou, S. K., Rantala, J. K., Magin, S., Mladenov, E., … Halazonetis, T. D. (2014). Break-Induced Replication Repair of. *Science*, *3*(January), 1–5. http://doi.org/10.1126/science.1243211

Chaganti, R. S., Schonberg, S., & German, J. (1974). A manyfold increase in sister chromatid exchanges in Bloom's syndrome lymphocytes. *Proceedings of the National Academy of Sciences of the United States of America*, *71*(11), 4508–12. http://doi.org/10.1073/pnas.71.11.4508

Chandramouly, G., McDevitt, S., Sullivan, K., Kent, T., Luz, A., Glickman, J. F., … Pomerantz, R. T. (2015). Small-Molecule Disruption of RAD52 Rings as a Mechanism for Precision Medicine in

BRCA-Deficient Cancers. *Chemistry and Biology*, *22*(11), 1491–1504. http://doi.org/10.1016/j.chembiol.2015.10.003

Chatterjee, G., Jimenez-Sainz, J., Presti, T., Nguyen, T., & Jensen, R. B. (2016). Distinct binding of BRCA2 BRC repeats to RAD51 generates differential DNA damage sensitivity. *Nucleic Acids Research*, *44*(11), 5256–5270. http://doi.org/10.1093/nar/gkw242

Choi, B. H., Chen, Y., & Dai, W. (2013). Chromatin PTEN is involved in DNA damage response partly through regulating Rad52 sumoylation. *Cell Cycle (Georgetown, Tex.)*, *12*(21), 3442–7. http://doi.org/10.4161/cc.26465

Corneo, B., Wendland, R. L., Deriano, L., Cui, X., Klein, I. A., Wong, S.-Y., … Roth, D. B. (2007). Rag mutations reveal robust alternative end joining. *Nature*, *449*(7161), 483–486. http://doi.org/10.1038/nature06168

Cramer-Morales, K., Nieborowska-Skorska, M., Scheibner, K., Padget, M., Irvine, D. A., Sliwinski, T., … Skorski, T. (2013). Personalized synthetic lethality induced by targeting RAD52 in leukemias identified by gene mutation and expression profile. *Blood*, *122*(7), 1293–1304. http://doi.org/10.1182/blood-2013-05-501072

de Mayolo, A. A., Lisby, M., Erdeniz, N., Thybo, T., Mortensen, U. H., & Rothstein, R. (2006). Multiple start codons and phosphorylation result in discrete Rad52 protein species. *Nucleic Acids Research*, *34*(9), 2587–2597. http://doi.org/10.1093/nar/gkl280

Deckbar, D., Jeggo, P. a, & Löbrich, M. (2011). Understanding the limitations of radiation-induced cell cycle checkpoints. *Critical Reviews in Biochemistry and Molecular Biology*, *46*(4), 271–83. http://doi.org/10.3109/10409238.2011.575764

Deng, S. K., Gibb, B., de Almeida, M. J., Greene, E. C., & Symington, L. S. (2014). RPA antagonizes microhomology-mediated repair of DNA double-strand breaks. *Nature Structural & Molecular Biology*, *21*(4), 405–412. http://doi.org/10.1038/nsmb.2786

Desouky, O., Ding, N., & Zhou, G. (2015). Targeted and non-targeted effects of ionizing radiation. *Journal of Radiation Research and Applied Sciences*, *8*(2), 247–254. http://doi.org/10.1016/j.jrras.2015.03.003

Dilley, R. L., Verma, P., Cho, N. W., Winters, H. D., Wondisford, A. R., & Greenberg, R. A. (2016). Break-induced telomere synthesis underlies alternative telomere maintenance. *Nature*, *539*(7627), 54–58. http://doi.org/10.1038/nature20099

Donnianni, R. A., & Symington, L. S. (2013). Break-induced replication occurs by conservative DNA synthesis. *Proceedings of the National Academy of Sciences*, *110*(33), 13475–13480. http://doi.org/10.1073/pnas.1309800110

Environmental Sciences Training Center. (1996). What Are the Sources of Ionizing Radiation? *The State University of New Jersey - RUTGERS*, 1–3.

Feng, Z., Scott, S. P., Bussen, W., Sharma, G. G., Guo, G., Pandita, T. K., & Powell, S. N. (2011). Rad52 inactivation is synthetically lethal with BRCA2 deficiency. *Proceedings of the National Academy of Sciences of the United States of America*, *108*(2), 686–91. http://doi.org/10.1073/pnas.1010959107

Fujimori, A., Tachiiri, S., Sonoda, E., Thompson, L. H., Dhar, P. K., Hiraoka, M., … Takata, M. (2001). Rad52 partially substitutes for the Rad51 paralog XRCC3 in maintaining chromosomal integrity in vertebrate cells. *EMBO Journal*, *20*(19), 5513–5520. http://doi.org/10.1093/emboj/20.19.5513

Game, J. C., & Mortimer, R. K. (1974). A genetic study of X-ray sensitive mutants in yeast. *Mutation Research - Fundamental and Molecular Mechanisms of Mutagenesis*, *24*(3), 281–292. http://doi.org/10.1016/0027-5107(74)90176-6

Grimme, J. M., Honda, M., Wright, R., Okuno, Y., Rothenberg, E., Mazin, A. V, … Spies, M. (2010). Human Rad52 binds and wraps single-stranded DNA and mediates annealing via two hRad52-ssDNA complexes. *Nucleic Acids Research*, *38*(9), 2917–30. http://doi.org/10.1093/nar/gkp1249

Hanamshet, K., Mazina, O., & Mazin, A. (2016). Reappearance from Obscurity: Mammalian Rad52 in Homologous Recombination. *Genes*, *7*(9), 63. http://doi.org/10.3390/genes7090063

Heyer, W.-D., Ehmsen, K. T., & Liu, J. (2010). Regulation of homologous recombination in eukaryotes. *Annual Review of Genetics*, *44*, 113–39. http://doi.org/10.1146/annurev-genet-051710-150955

Huang, F., Goyal, N., Sullivan, K., Hanamshet, K., Patel, M., Mazina, O. M., … Mazin, A. V. (2016). Targeting BRCA1- and BRCA2-deficient cells with RAD52 small molecule inhibitors. *Nucleic Acids Research*, *44*(9), gkw087-. http://doi.org/10.1093/nar/gkw087

Huertas, P., & Jackson, S. P. (2009). Human CtIP Mediates Cell Cycle Control of DNA End Resection and Double Strand Break Repair. *Journal of Biological Chemistry*, *284*(14), 9558–9565. http://doi.org/10.1074/jbc.M808906200

Iliakis, G., Murmann, T., & Soni, A. (2015). Alternative end-joining repair pathways are the ultimate backup for abrogated classical non-homologous end-joining and homologous recombination repair: Implications for the formation of chromosome translocations. *Mutation Research - Genetic Toxicology and Environmental Mutagenesis*, *793*, 166–175. http://doi.org/10.1016/j.mrgentox.2015.07.001

Jackson, S. P., & Bartek, J. (2009). The DNA-damage response in human biology and disease. *Nature*, *461*(7267), 1071–1078. http://doi.org/10.1038/nature08467

Jensen, R. B., Carreira, A., & Kowalczykowski, S. C. (2010). Purified human BRCA2 stimulates RAD51-mediated recombination. *Nature*, *467*(7316), 678–683. http://doi.org/10.1038/nature09399

Jette, N., & Lees-Miller, S. P. (2015). The DNA-dependent protein kinase: a multifunctional protein kinase with roles in DNA double strand break repair and mitosis. *Prog Biophys Mol Biol.*, *117*(0), 1–29. http://doi.org/10.1016/j.pbiomolbio.2014.12.003

Kagawa, W., Kurumizaka, H., Ikawa, S., Yokoyama, S., & Shibata, T. (2001). Homologous Pairing Promoted by the Human, Rad52 Protein. *Journal of Biological Chemistry*, *276*(37), 35201–35208. http://doi.org/10.1074/jbc.M104938200

Karanam, K., Kafri, R., Loewer, A., & Lahav, G. (2012). Quantitative Live Cell Imaging Reveals a Gradual Shift between DNA Repair Mechanisms and a Maximal Use of HR in Mid S Phase. *Molecular Cell*, *47*(2), 320–329. http://doi.org/10.1016/j.molcel.2012.05.052

Kegel, P., Riballo, E., Kühne, M., Jeggo, P. A., & Löbrich, M. (2007). X-irradiation of cells on glass slides has a dose doubling impact. *DNA Repair*, *6*(11), 1692–1697. http://doi.org/10.1016/j.dnarep.2007.05.013

Kent, T., Chandramouly, G., McDevitt, S. M., Ozdemir, A. Y., & Pomerantz, R. T. (2015). Mechanism of microhomology-mediated end-joining promoted by human DNA polymerase θ. *Nature Structural & Molecular Biology*, *22*(3), 230–237. http://doi.org/10.1038/nsmb.2961

Keskin, H., Shen, Y., Huang, F., Patel, M., Yang, T., Ashley, K., … Storici, F. (2014). Transcript-RNA-templated DNA recombination and repair. *Nature*, *515*(7527), 436–439. http://doi.org/10.1038/nature13682

Kitao, H., & Yuan, Z.-M. (2002). Regulation of ionizing radiation-induced Rad52 nuclear foci formation by c-Abl-mediated phosphorylation. *The Journal of Biological Chemistry*, *277*(50), 48944–8. http://doi.org/10.1074/jbc.M208151200

Koike, M., Yutoku, Y., & Koike, A. (2013). The C-terminal region of Rad52 is essential for Rad52 nuclear and nucleolar localization, and accumulation at DNA damage sites immediately after irradiation. *Biochemical and Biophysical Research Communications*, *435*(2), 260–6. http://doi.org/10.1016/j.bbrc.2013.04.067

Kojic, M., Mao, N., Zhou, Q., Lisby, M., & Holloman, W. K. (2008). Compensatory role for Rad52 during recombinational repair in Ustilago maydis. *Molecular Microbiology*, *67*(5), 1156–1168. http://doi.org/10.1111/j.1365-2958.2008.06116.x

Kumar, J. K., & Gupta, R. C. (2004). Strand exchange activity of human recombination protein Rad52. *Proceedings of the National Academy of Sciences of the United States of America*, *101*(26), 9562–7. http://doi.org/10.1073/pnas.0403416101

Li, X., Stith, C. M., Burgers, P. M., & Heyer, W. D. (2009). PCNA Is Required for Initiation of

Recombination-Associated DNA Synthesis by DNA Polymerase ?? *Molecular Cell*, *36*(4), 704–713. http://doi.org/10.1016/j.molcel.2009.09.036
Lloyd, J. A., Forget, A. L., & Knight, K. L. (2002). Correlation of biochemical properties with the oligomeric state of human Rad52 protein. *Journal of Biological Chemistry*, *277*(48), 46172–46178. http://doi.org/10.1074/jbc.M207262200
Lloyd, J. A., McGrew, D. A., & Knight, K. L. (2005). Identification of residues important for DNA binding in the full-length human Rad52 protein. *Journal of Molecular Biology*, *345*(2), 239–249. http://doi.org/10.1016/j.jmb.2004.10.065
Lok, B. H., & Powell, S. N. (2012). Molecular pathways: Understanding the role of Rad52 in homologous recombination for therapeutic advancement. *Clinical Cancer Research*, *18*(23), 6400–6406. http://doi.org/10.1158/1078-0432.CCR-11-3150
Malone, R. E., & Esposito, R. E. (1980). The RAD52 gene is required for homothallic interconversion of mating types and spontaneous mitotic recombination in yeast. *Proceedings of the National Academy of Sciences*, *77*(1), 503–507. http://doi.org/10.1073/pnas.77.1.503
Mao, Z., Bozzella, M., Seluanov, A., & Gorbunova, V. (2008). DNA repair by nonhomologous end joining and homologous recombination during cell cycle in human cells. *Cell Cycle*, *7*(18), 2902–2906. http://doi.org/10.4161/cc.7.18.6679
Mateos-Gomez, P. A., Gong, F., Nair, N., Miller, K. M., Lazzerini-Denchi, E., & Sfeir, A. (2015). Mammalian polymerase θ promotes alternative NHEJ and suppresses recombination. *Nature*, *518*(7538), 254–257. http://doi.org/10.1038/nature14157
Mazina, O. M., Keskin, H., Hanamshet, K., Storici, F., & Mazin, A. V. (2017). Rad52 Inverse Strand Exchange Drives RNA-Templated DNA Double-Strand Break Repair. *Molecular Cell*, *67*(1), 19–29.e3. http://doi.org/10.1016/j.molcel.2017.05.019
McCarthy, J. (2004). Science and society: Tackling the challenges of interdisciplinary bioscience. *Nature Reviews Molecular Cell Biology*, *5*(11), 933–937. http://doi.org/10.1038/nrm1501
McIlwraith, M. J., & West, S. C. (2008). DNA repair synthesis facilitates RAD52-mediated second-end capture during DSB repair. *Molecular Cell*, *29*(4), 510–6. http://doi.org/10.1016/j.molcel.2007.11.037
Mcllwraith, M. J., Vaisman, A., Liu, Y., Fanning, E., Woodgate, R., & West, S. C. (2005). Human DNA polymerase η promotes DNA synthesis from strand invasion intermediates of homologous recombination. *Molecular Cell*, *20*(5), 783–792. http://doi.org/10.1016/j.molcel.2005.10.001
Minocherhomji, S., Ying, S., Bjerregaard, V. A., Bursomanno, S., Aleliunaite, A., Wu, W., … Hickson, I. D. (2015). Replication stress activates DNA repair synthesis in mitosis. *Nature*, *528*(7581), 286–290. http://doi.org/10.1038/nature16139
Motycka, T. a, Bessho, T., Post, S. M., Sung, P., & Tomkinson, A. E. (2004). Physical and functional interaction between the XPF/ERCC1 endonuclease and hRad52. *The Journal of Biological Chemistry*, *279*(14), 13634–9. http://doi.org/10.1074/jbc.M313779200
Namsaraev, E. A., & Berg, P. (1998). Interaction of Rad51 with ATP and Mg2+ induces a conformational change in Rad51. *Biochemistry*, *37*(34), 11932–11939. http://doi.org/10.1021/bi9810297
Nasmyth, K., & Haering, C. H. (2009). Cohesin: Its Roles and Mechanisms. *Annual Review of Genetics*, *43*(1), 525–558. http://doi.org/10.1146/annurev-genet-102108-134233
Negrini, S., Gorgoulis, V. G., & Halazonetis, T. D. (2010). Genomic instability — an evolving hallmark of cancer. *Nature Reviews Molecular Cell Biology*, *11*(3), 220–228. http://doi.org/10.1038/nrm2858
Nimonkar, A. V, Sica, R. A., & Kowalczykowski, S. C. (2009). Rad52 promotes second-end DNA capture in double-stranded break repair to form complement-stabilized joint molecules. *Proceedings of the National Academy of Sciences of the United States of America*, *106*(9), 3077–82. http://doi.org/10.1073/pnas.0813247106
Nowell, P. C. (1950). The Clonal Evolution of Tumor Cell Populations. *Science, New Series*, *194*(4260), 23–28. http://doi.org/10.1098/rstb.2004.1522

Ochi, T., Blackford, A. N., Coates, J., Jhujh, S., Mehmood, S., Tamura, N., … Jackson, S. P. (2015). PAXX, a paralog of XRCC4 and XLF, interacts with Ku to promote DNA double-strand break repair. *Science*, *347*(6218), 185–188. http://doi.org/10.1126/science.1261971

Park, M. S., Ludwig, D. L., Stigger, E., & Lee, S.-H. (1996). Physical Interaction between Human RAD52 and RPA Is Required for Homologous Recombination in Mammalian Cells. *Journal of Biological Chemistry*, *271*(31), 18996–19000. http://doi.org/10.1074/jbc.271.31.18996

Rahman, N., & Stratton, M. R. (1998). the Genetics of Breast Cancer Susceptibility. *Annual Review of Genetics*, *32*(1), 95–121. http://doi.org/10.1146/annurev.genet.32.1.95

Renkawitz, J., Lademann, C. A., & Jentsch, S. (2014). Mechanisms and principles of homology search during recombination. *Nature Reviews Molecular Cell Biology*, *15*(6), 369–383. http://doi.org/10.1038/nrm3805

Riballo, E., Kühne, M., Rief, N., Doherty, A., Smith, G. C. M., Recio, M. J., … Löbrich, M. (2004). A pathway of double-strand break rejoining dependent upon ATM, Artemis, and proteins locating to γH2AX foci. *Molecular Cell*, *16*(5), 715–724. http://doi.org/10.1016/j.molcel.2004.10.029

Rijkers, T., Van Den Ouweland, J., Morolli, B., Rolink, A. G., Baarends, W. M., Van Sloun, P. P. H., … Pastink, A. (1998). Targeted Inactivation of Mouse *RAD52* Reduces Homologous Recombination but Not Resistance to Ionizing Radiation. *Molecular and Cellular Biology*, *18*(11), 6423–6429. http://doi.org/10.1128/MCB.18.11.6423

Rogakou, E. P., Pilch, D. R., Orr, A. H., Ivanova, V. S., & Bonner, W. M. (1998). Double-stranded Brekas Induce Histone H2AX phosphorylation on Serine 139. *The Journal of Biological Chemistry*, *273*(10), 5858–5868. http://doi.org/10.1074/jbc.273.10.5858

Sacher, M., Pfander, B., Hoege, C., & Jentsch, S. (2006). Control of Rad52 recombination activity by double-strand break-induced SUMO modification. *Nature Cell Biology*, *8*(11), 1284–1290. http://doi.org/10.1038/ncb1488

Saito, K., Kagawa, W., Suzuki, T., Suzuki, H., Yokoyama, S., Saitoh, H., … Kurumizaka, H. (2010). The putative nuclear localization signal of the human RAD52 protein is a potential sumoylation site. *Journal of Biochemistry*, *147*(6), 833–842. http://doi.org/10.1093/jb/mvq020

San Filippo, J., Sung, P., & Klein, H. (2008). Mechanism of Eukaryotic Homologous Recombination. *Annual Review of Biochemistry*, *77*(1), 229–257. http://doi.org/10.1146/annurev.biochem.77.061306.125255

Sarbajna, S., Davies, D., & West, S. C. (2014). Roles of SLX1-SLX4, MUS81-EME1, and GEN1 in avoiding genome instability and mitotic catastrophe. *Genes and Development*, *28*(10), 1124–1136. http://doi.org/10.1101/gad.238303.114

Sarbajna, S., & West, S. C. (2014). Holliday junction processing enzymes as guardians of genome stability. *Trends in Biochemical Sciences*, *39*(9), 409–419. http://doi.org/10.1016/j.tibs.2014.07.003

Sartori, A. A., Lukas, C., Coates, J., Mistrik, M., Fu, S., Bartek, J., … Jackson, S. P. (2007). Human CtIP promotes DNA end resection. *Nature*, *450*(7169), 509–514. http://doi.org/10.1038/nature06337

Schiestl, R. H., Dominska, M., & Petes, T. D. (1993). Transformation of Saccharomyces cerevisiae with nonhomologous DNA: illegitimate integration of transforming DNA into yeast chromosomes and in vivo ligation of transforming DNA to mitochondrial DNA sequences. *Molecular and Cellular Biology*, *13*(5), 2697–2705. http://doi.org/10.1128/MCB.13.5.2697

Schlacher, K., Christ, N., Siaud, N., Egashira, A., Wu, H., & Jasin, M. (2011). Double-strand break repair-independent role for BRCA2 in blocking stalled replication fork degradation by MRE11. *Cell*, *145*(4), 529–542. http://doi.org/10.1016/j.cell.2011.03.041

Sfeir, A., & Symington, L. S. (2015). Microhomology-Mediated End Joining: A Back-up Survival Mechanism or Dedicated Pathway? *Trends in Biochemical Sciences*, *40*(11), 701–714. http://doi.org/10.1016/j.tibs.2015.08.006

Shen, Z., Cloud, K. G., David, J., Park, M. S., & Chen, D. J. (1996). Protein Chemistry and Structure : Specific Interactions between the Human RAD51 and RAD52 Proteins Specific Interactions

between the Human RAD51 and RAD52 Proteins *, *271*(1), 148–152. http://doi.org/10.1074/jbc.271.1.148
Shibata, A., Moiani, D., Arvai, A. S., Perry, J., Harding, S. M., Genois, M.-M., … Tainer, J. a. (2014). DNA double-strand break repair pathway choice is directed by distinct MRE11 nuclease activities. *Molecular Cell*, *53*(1), 7–18. http://doi.org/10.1016/j.molcel.2013.11.003
Shiotani, B., & Zou, L. (2009). Single-Stranded DNA Orchestrates an ATM-to-ATR Switch at DNA Breaks. *Molecular Cell*, *33*(5), 547–558. http://doi.org/10.1016/j.molcel.2009.01.024
Simon A. Gayther, Jonathan Mangion, et al. (1997). Variation of risk of breast and ovarian cancer associated with different germline mutations of the BRCA2 gene. *Nature Genetics*, *15*, 103–105.
Sørensen, C. S., Hansen, L. T., Dziegielewski, J., Syljuåsen, R. G., Lundin, C., Bartek, J., & Helleday, T. (2005). The cell-cycle checkpoint kinase Chk1 is required for mammalian homologous recombination repair. *Nature Cell Biology*, *7*(2), 195–201. http://doi.org/10.1038/ncb1212
Sotiriou, S. K., Kamileri, I., Lugli, N., Evangelou, K., Da-Ré, C., Huber, F., … Halazonetis, T. D. (2016). Mammalian RAD52 Functions in Break-Induced Replication Repair of Collapsed DNA Replication Forks. *Molecular Cell*, *64*(6), 1127–1134. http://doi.org/10.1016/j.molcel.2016.10.038
Spies, J., Waizenegger, A., Barton, O., Sürder, M., Wright, W. D., Heyer, W. D., & Löbrich, M. (2016). Nek1 Regulates Rad54 to Orchestrate Homologous Recombination and Replication Fork Stability. *Molecular Cell*, *62*(6), 903–917. http://doi.org/10.1016/j.molcel.2016.04.032
Stark, J. M., Pierce, A. J., Oh, J., Pastink, A., & Jasin, M. (2004). Genetic Steps of Mammalian Homologous Repair with Distinct Mutagenic Consequences. *Molecular and Cellular Biology*, *24*(21), 9305–9316. http://doi.org/10.1128/MCB.24.21.9305-9316.2004
Sturzenegger, A., Burdova, K., Kanagaraj, R., Levikova, M., Pinto, C., Cejka, P., & Janscak, P. (2014). DNA2 cooperates with the WRN and BLM RecQ helicases to mediate long-range DNA end resection in human cells. *Journal of Biological Chemistry*, *289*(39), 27314–27326. http://doi.org/10.1074/jbc.M114.578823
Sugiyama, T., New, J. H., & Kowalczykowski, S. C. (1998). DNA annealing by Rad52 Protein is stimulated by specific interaction with the complex of replication protein A and single-stranded DNA. *Proceedings of the National Academy of Sciences*, *95*(11), 6049–6054. http://doi.org/10.1073/pnas.95.11.6049
Sullivan, K., Cramer-Morales, K., McElroy, D. L., Ostrov, D. A., Haas, K., Childers, W., … Skorski, T. (2016). Identification of a Small Molecule Inhibitor of RAD52 by Structure-Based Selection. *PLoS ONE*, *11*(1), 1–11. http://doi.org/10.1371/journal.pone.0147230
Symington, L. S. (2002). Role of RAD52 epistasis group genes in homologous recombination and double-strand break repair. *Microbiology and Molecular Biology Reviews : MMBR*, *66*(4), 630–70, table of contents. http://doi.org/10.1128/MMBR.66.4.630
Symington, L. S., & Gautier, J. (2011). Double-Strand Break End Resection and Repair Pathway Choice. *Annual Review of Genetics*, *45*(1), 247–271. http://doi.org/10.1146/annurev-genet-110410-132435
Truong, L. N., Li, Y., Shi, L. Z., Hwang, P. Y.-H., He, J., Wang, H., … Wu, X. (2013). Microhomology-mediated End Joining and Homologous Recombination share the initial end resection step to repair DNA double-strand breaks in mammalian cells. *Proceedings of the National Academy of Sciences*, *110*(19), 7720–7725. http://doi.org/10.1073/pnas.1213431110
Van Dyck, E., Hajibagheri, N. M., Stasiak, a, & West, S. C. (1998). Visualisation of human rad52 protein and its complexes with hRad51 and DNA. *Journal of Molecular Biology*, *284*(4), 1027–38. http://doi.org/10.1006/jmbi.1998.2203
Vignard, J., Mirey, G., & Salles, B. (2013). Ionizing-radiation induced DNA double-strand breaks: A direct and indirect lighting up. *Radiotherapy and Oncology*, *108*(3), 362–369. http://doi.org/10.1016/j.radonc.2013.06.013
Wiesmüller, L., Ford, J. M., & Schiestl, R. H. (2002). DNA Damage, Repair, and Diseases. *Journal of Biomedicine and Biotechnology*, *2*(2), 45–45. http://doi.org/10.1155/S1110724302001985

Wooster, R., Bignell, G., Lancaster, J., Swift, S., Seal, S., Mangion, J., … Micklem, G. (1995). Identification of the breast cancer susceptibility gene BRCA2. *Nature*, *378*(6559), 789–92. http://doi.org/10.1038/378789a0

Wyatt, D. W., Feng, W., Conlin, M. P., Yousefzadeh, M. J., Roberts, S. A., Mieczkowski, P., … Doublié, S. (2016). Essential Roles for Polymerase θ-Mediated End Joining in the Repair of Chromosome Breaks. *Molecular Cell*, *63*(4), 662–673. http://doi.org/10.1016/j.molcel.2016.06.020

Wyatt, H. D. M., Sarbajna, S., Matos, J., & West, S. C. (2013). Coordinated actions of SLX1-SLX4 and MUS81-EME1 for Holliday junction resolution in human cells. *Molecular Cell*, *52*(2), 234–47. http://doi.org/10.1016/j.molcel.2013.08.035

Yamaguchi-Iwai, Y. (1998). Homologous recombination, but not DNA repair, is reduced in vertebrate cells deficient in RAD52. *Molecular and Cellular Biology*, *18*(11), 6430–6435. http://mcb.asm.org/content/18/11/6430.short

Yuan, S. S. F., Lee, S. Y., Chen, G., Song, M., Tomlinson, G. E., & Lee, E. Y. H. P. (1999). BRCA2 is required for ionizing radiation-induced assembly of Rad51 complex in vivo. *Cancer Research*, *59*(15), 3547–3551.

Zhao, W., Vaithiyalingam, S., San Filippo, J., Maranon, D. G., Jimenez-Sainz, J., Fontenay, G. V., … Sung, P. (2015). Promotion of BRCA2-Dependent Homologous Recombination by DSS1 via RPA Targeting and DNA Mimicry. *Molecular Cell*, *59*(2), 176–187. http://doi.org/10.1016/j.molcel.2015.05.032

7. Appendix

7.1. Ehrenwörtliche Erklärung

Ich erkläre hiermit ehrenwörtlich, dass ich die vorliegende Arbeit entsprechend den Regeln guter wissenschaftlicher Praxis selbstständig und ohne unzulässige Hilfe Dritter angefertigt habe.

Sämtliche aus fremden Quellen direkt oder indirekt übernommenen Gedanken sowie sämtliche von Anderen direkt oder indirekt übernommenen Daten, Techniken und Materialien sind als solche kenntlich gemacht. Die Arbeit wurde bisher bei keiner anderen Hochschule zu Prüfungszwecken eingereicht.

Darmstadt, den 27.10.2017

.....

Anugrah Gawai

7.2. Curriculum Vitae

Personal Information

Name:	Anugrah Gawai
Date of Birth:	27th January 1986
Place of Birth:	Padhar, India

Doctoral thesis

04/2014 – 09/2017	Technical University of Darmstadt *Radiation Biology and DNA Repair* AG Prof. Dr. Markus Löbrich

Education

10/2011 – 11/2013	University of Duisburg-Essen Master of Science, Environmental Toxicology
07/2004 – 08/2007	Bengaluru University, India Bachelor of Science, Biotechnology
08/2001 – 02/2003	Higher secondary school certificated examination Maharashtra state board, Nagpur, India
07/1990 – 04/2000	Secondary school examination Central board of secondary education, Chhindwara, India

7.3. Acknowledgements

First and foremost, I would like to thank Prof. Dr. Markus Löbrich for giving me the opportunity to work in his group and for his continuous supervision, support and motivation throughout the project.
I would also like to thank Prof. Cristina M. Cardoso for being my second supervisor and for providing her expertise whenever needed. I thank her also for being a member of my thesis committee in the framework of GRK-1657.

I thank Prof. Alexander Löwer for kindly accepting my request to be my examiner. I thank him also for being a member of my thesis committee and for his help in organizing workshops in the framework of GRK-1657. I also thank Prof. Franz Rödel for kindly accepting my request to be my examiner at a short notice and for conducting an interesting lecture series on “Clinical impacts of Radiation Biology” at the university hospital, Frankfurt.

I would like to thank Marta Llorens Agost for helping me with experiments, for all the interesting scientific and non-scientific discussions and for correcting my thesis. I would also like to thank Monika Steinlage for correcting my thesis, for positive criticism and for teaching me many new English words (especially their pronunciation). I thank all the technical assistants in our group (Mrs. Christel Braun, Mrs. Bettina Basso and Mrs. Cornelia Schmidt) for providing their support with the laboratory work all throughout these years. A big thank you goes also to Na Wei for helping me with the Western Blot experiments.

I thank all the members (former and current), with whom I have worked in the last 4 years, for making the lab a fun place to be. And at difficult times, thank you for constantly reminding me that every cloud has a silver lining. Amir Mofidi, thank you for all the good times in the lab, at the GRK retreats and at the gym. Michael Ensminger, thank you for your constant support to solve problems with the microscope and especially for your delicious Tiramisu and Himbeertraum. Silvia Juhász, although our projects were different, thank you for constantly motivating me to reach the end.

A very special thanks goes to Monika. It would have not been possible without her unending support during good as well as during very good times.

Last but (for sure) not the least, I thank my parents and my brothers with all my heart for believing in me. All this was just a dream without you all.